STUDY OF PATTERNED, MULTILAYERED, COLLAGEN-BASED SCAFFOLDS DESIGNED TO SERVE AS A CORNEA STROMA

A THESIS SUBMITTED TO
THE GRADUATE SCHOOL OF NATURAL AND APPLIED SCIENCES
OF
MIDDLE EAST TECHNICAL UNIVERSITY

BY

CEMİLE KILIÇ

IN PARTIAL FULFILLMENT OF THE REQUIREMENTS
FOR
THE DEGREE OF MASTER OF SCIENCE
IN
BIOLOGY

FEBRUARY 2013

Approval of the thesis:

STUDY OF PATTERNED, MULTILAYERED, COLLAGEN-BASED SCAFFOLDS DESIGNED TO SERVE AS A CORNEA STROMA

submitted by **CEMİLE KILIÇ** in partial fulfillment of the requirements for the degree of **Master of Science in Biological Sciences Department, Middle East Technical University** by,

Prof. Dr. Canan Özgen _____
Dean, Graduate School of **Natural and Applied Sciences**

Prof. Dr. Gülay Özcengiz _____
Head of Department, **Biological Sciences**

Prof. Dr. Vasıf Hasırcı _____
Supervisor, **Biological Sciences Dept., METU**

Prof. Dr. J. Carlos Rodriquez Cabello _____
Co-Supervisor, **Condensed Material Dept., Uni. of Valladolid, Spain**

Examining Committee Members:

Prof. Dr. Orhan Adalı _____
Biological Sciences Dept., METU

Prof. Dr. Vasıf Hasırcı _____
Biological Sciences Dept., METU

Assoc. Prof. Dr. İhsan Gürsel _____
Molecular Biology and Genetics Dept., Bilkent University

Assoc. Prof. Dr. Mesut Muyan _____
Biological Sciences Dept., METU

Assist. Prof. Dr. Can Özen _____
Biotechnology Dept., METU

Date: 01.02.2013

I hereby declare that all information in this document has been obtained and presented in accordance with academic rules and ethical conduct. I also declare that, as required by these rules and conduct, I have fully cited and referenced all material and results that are not original to this work.

Name, Last Name: Cemile Kılıç

Signature :

ABSTRACT

STUDY OF PATTERNED, MULTILAYERED, COLLAGEN-BASED SCAFFOLDS DESIGNED TO SERVE AS A CORNEA STROMA

Kılıç, Cemile
M.Sc., Department of Biological Sciences
Supervisor: Prof. Dr. Vasıf Hasırcı
Co-Supervisor: Prof. Dr. J. Carlos Rodriguez Cabello

February 2013, 73 pages

Cornea is the most exterior, avascular and transparent layer of the eye and is about 500 μm in thick. It protects the eye from external objects and it is the main optical element of the eye refracting 70 % of the incoming light. After cataract, corneal diseases and wounds are the second leading cause of the blindness that affects more than 4 million people worldwide. For the highly damaged corneas where the corrections with spectacles or contact lenses cannot be achieved, tissue replacement is the only choice, and is done by cornea transplantation or keratoprostheses. However, due to limited number of donor corneas and the risk of infections during transplantation, and development of glaucoma, necrosis and other complications caused by the keratoprostheses, prevent them from meeting expectations.

Tissue engineering is a promising field which emerged from biomaterials science and aims to replace, restore or improve the function of the diseased or injured tissues. In this method, after the production of an ideal scaffold that mimics the natural human tissue, cells of the host are isolated, increased in number, and seeded on the scaffold developed to serve as the microenvironment of the cells.

In the current study a 3D corneal stroma replacement was designed to mimic the native stroma. It consisted of 4 films of patterned collagen or collagen blended with Elastin Like Recombinamer (ELR) stacked on top of each other and then crosslinked by dehydrothermal (DHT) treatment.

The characterization of the films showed that the pattern fidelity was good and they did not deteriorate after crosslinking. Enzymatic and in situ degradation studies showed that the DHT treatment at 150 ^{o}C for 24 h (DHT150) was the optimum condition. The transparency of all the films was quite high where uncrosslinked (UXL) films and DHT150 Col:ELR films yielded the best results.

The individual films and 3D construct of 4 stacked films were seeded with isolated human corneal keratocytes (HK) and cultured for 21 days. Cells attached and proliferated well on the single Col and Col:ELR films. However, the proliferation was higher on Col multilayer constructs than their Col:ELR counterparts. Cells were aligned along the patterns of the films while no significant alignment was observed for the cells on unpatterned films. Ultimate tensile strength (UTS) and Young's Modulus (E) of Col and Col:ELR films were significantly lower after a 30 day culture than that of unseeded films of Day 1. Transparency of the seeded Col:ELR films was superior to Col films over a 30 days test and quite close to the transmittance of the native human cornea.

It was concluded that the Col and Col:ELR patterned films and their 3D constructs have a significant potential for use as a corneal stroma equivalent.

Keywords: Cornea, Stroma, Tissue Engineering, Micropatterning, Elastin Like Recombinamers, Collagen

ÖZ

KORNEA STROMASI YAPIMI İÇİN ÇOK KATMANLI DESENLİ KOLLAJEN TEMELLİ DOKU İSKELELERİNİN ARAŞTIRILMASI

Kılıç, Cemile
Yüksek Lisans, Biyolojik Bilimler Bölümü
Tez Yöneticisi: Prof. Dr. Vasıf Hasırcı
Ortak Tez Yöneticisi: Prof. Dr. J. Carlos Rodriquez Cabello

Şubat 2013, 73 sayfa

Damarsız, saydam ve gözün en dış kısmını oluşturan kornea yaklaşık 500 μm kalınlığındadır. Gözü dış objelerden korur ve gelen ışığın %70 ini odaklamasından dolayı gözün temel optik elementidir. Kornea hastalıkları ve yaralanmaları kataraktan sonra en önemli ikinci körlük sebebidir ve dünya çapında yaklaşık 4 milyon kişiyi etkiler. Önemli ölçüde zarar görmüş kornealar için eğer gözlük ya da lensler tedavi olarak kullanılamıyorsa tek tedavi yöntemi donör korneası ya da yapay kornea (keratoprotez) ile dokunun değiştirilmesidir. Ancak donör korneasının sınırlı sayıda olması ve transplantasyon sırasında hastalık bulaştırma riskinin bulunması ve glokom, doku kaybı ya da diğer komplikasyonların keratoprotezlerden kaynaklı oluşması bu yöntemlerin istekleri karşılamasını engellemektedir.

Doku mühendisliği yaralanmış ya da hastalıklı dokunun değiştirilmesi, düzeltilmesi ya da fonksiyonlarının geliştirilmesini amaçlayan, biyomalzeme biliminden ortaya çıkmış umut vaat eden bir alandır. Bu yöntemde doğal insan dokusunu taklit eden ideal doku iskelesi oluşturulduktan sonra hastanın hücreleri izole edilir, çoğaltılır ve hücrelerin mikro çevresini oluşturması için tasarlanan iskelelere ekilir.

Bu çalışmada doğal kornea stroması yapısını taklit edebilecek 3 boyutlu bir stroma eşleniği tasarlanmıştır. 4 adet desenli kollajen (Kol) ya da elastin benzeri proteinlerle (ELR) karıştırılmış filmler (Kol:ELR) üstüste gelecek şekilde birbirine yapıştırılmış ve dehidrotermal çapraz bağlama yöntemi kullanılarak sağlamlaştırılmıştır.

Film karakterizasyonu filmlerin desenlerinin sürekli olduğunu ve bu sürekliliğin çapraz bağlama sonrasında bozulmadığını göstermiştir. Enzimatik ve in situ bozunma testleri optimal dehidrotermal parametresinin 150 ^{o}C'de 24 saat bekletmek olduğunu göstermiştir. Bütün filmlerin, özellikle çapraz bağlanmamış ve çapraz bağlanmış Kol:ELR filmlerin, ışık geçirgenliği oldukça yüksektir.

Tek katmanlı filmlere ya da 4 tane yapıştırılmış filmden oluşan 3 boyutlu yapılara izole edilmiş insan kornea keratositleri ekilmiş ve 21 gün boyunca hücre kültüründe bekletilmiştir. Tek katmanlı Kol ve Kol:ELR filmlerindeki hücre yapışması ve büyümesi aynıyken çok katmanlı yapılarda Kol filmlerinde Kol:ELR filmlerine gore daha fazla hücre büyümesi saptanmıştır. Desenli filmlerdeki hücreler desen doğrultusunda büyürken desensiz filmlerde belirgin bir yönelme görülmemiştir. 30 gün kültür süresinin sonunda Kol ve Kol:ELR filmlerin gerilme direnci ve Young katsayısı hücresiz ilk gün verisiyle karşılaştırınca oldukça düşmüştür. Hücre ekilmiş Kol:ELR filmlerin ışık geçirgenliği Kol filmlere göre belirgin biçimde yükselmiştir ve doğal kornea ışık geçirgenliğine önemli ölçüde yaklaşmıştır.

Bu çalışmalara dayanarak, Kol ve Kol:ELR desenli filmlerin ve 3 boyutlu yapılarının kornea stroması eşleniği olarak kullanılma belirgin bir potansiyeli olduğu sonucuna varılmıştır.

Anahtar Kelimeler: Kornea, Stroma, Doku Mühendisliği, Mikrodesen, Elastin Benzeri Proteinler, Kollajen

Dedicated to my lovely families, in Mersin and in Ankara…

ACKNOWLEDGEMENTS

I would like to express my special endless thanks and gratitude to my supervisor, Prof. Dr. Vasıf Hasırcı for his continues advice, support, motivation and encouragement during all the stages of my research. I feel very lucky to have had opportunity to do my thesis under his guidance.

I also thank to my co-supervisor Prof. Dr. J. Carlos Rodriguez Cabello for his support and contribution to this work by kindly providing me a research area at University of Valladolid, Spain to be able synthesize ELR. I also would like to thank to his research group who made the life very easy and enjoyable during my studies there.

I am also deeply thankful to Dr. Engin Vrana for his comments, suggestions and continuous support during my studies at France and here. I also owe special thanks to his wife Alix Vrana who helped me and made me enjoy very much during my stay at France.

I wish to extend my thanks to Dr. Ahmed El-Sheikh who provided us mechanical test results in a very short time.

I would also like to thank to my best labmate Selcen Alagöz for her comments, support and especially for her great friendship.

I am very grateful to my labmates especially Arda Büyüksungur, Dr. Hayriye Özçelik, Damla Arslantunalı, Tuğba Dursun, and Gökhan Bahçecioğlu for their contribution to this work by spending long hours for microscopical studies.

I would like to thank to all members of BIOMATEN especially Aylin Acun, Ezgi Antmen, Aysu Küçükturhan, Damla Arslantunalı, Senem Heper, Gözde Eke, Bilgenur Kandemir, Sepren Öncü, Menekşe Ermiş, Büşra Günay, Esen Sayın, Dr. Türker Baran, Deniz Sezlev, and our technician Zeynel Akın.

I am also deeply grateful to my lovely friends especially Emine Kurt, Sadiye Kılçuval, Fatma Demir, Songül Köse, Derya Özhava, Cansu Evcin, Bahar Arslan, Chinare Ahmadova, Sona Khaneh Shenas, and Deniz Çakal for their presence in my life.

I would like to express my deepest thanks and loves to my big family in Ankara especially my fiance Özgür Bektaş and his family Elif Bektaş, Veysel Bektaş, and Seyfi family who made life easier, and very enjoyable in Ankara. Without them this work would not have any meaning.

Finally, I would like to express my deepest gratitude to my perfect, lovely family Ali İhsan Kılıç, Arzı Kılıç, Cennet Kılıç, Ahmet Kılıç and my little sister Eylül Kılıç for their love, understanding, friendship, patience, and trust in me.

I would like to thank to METU International Cooperations Office for giving me a chance to visit University of Valladolid, Spain and Strasbourg University, France through Erasmus Summer Internship Program Scholarship.

I would like to acknowledge to TÜBİTAK for their support through BİDEP 2228 Scholarship.

TABLE OF CONTENTS

LIST OF FIGURES

FIGURES

LIST OF TABLES

TABLES

LIST OF ABBREVIATIONS

3D	Three Dimensional
ALK	Anterior Lamellar Keratoplasty
ATP	Adenosine triphosphate
BSA	Bovine Serum Albumin
b-FGF	Basic Fibroblast Growth Factor
CO2	Carbon Dioxide
Col	Collagen
Da	Dalton
DALK	Deep Anterior Lamellar Keratoplasty
DAPI	4', 6-diamidino-2-phenylindole
DNA	Deoxyribonucleic acid
DHT	Dehydrothermal
DMEM/F12	Dulbecco's Modified Eagle Medium/Ham's F12 Nutrient Mixture
DMSO	Dimethyl Sulfoxide
E	Young's Modulus (upon tension)
ECM	Extracellular Matrix
E.coli	*Escherichia coli*
EDTA	Ethylenediaminetetraacetic Acid
ELP	Elastin Like Polymer
ELR	Elastin Like Recombinamer
FBS	Fetal Bovine Serum
FITC	Fluorescein Isothiocyanate
g	gram
GAG	Glucosaminoglycan
Gly	Glycine
h	hour
ITT	Inverse Transition Temperature
HAc	Acetic Acid
HSV	Herpes Simplex Virus
MALDI-TOF	Matrix-Assisted Laser Desorption/ Ionization Time-of-Flight
min	minute
Mg	Magnesium
mg	milligram
mm	millimeter
mL	milliliter
nm	nanometer
K	Potassium
kDa	kilo Dalton
KPro	Keratoprostheses
LK	Lamellar Keratoplasty
M	Molarity
mM	millimolar
Na	Sodium
NaCl	Sodium Chloride
NaH2PO4	Sodium phosphate monobasic
Na2HPO4	Sodium phosphate dibasic
OOKP	Osteo Odonto Keratoprostheses
PBS	Phosphate Buffer Saline

PCL	Poly(ε-caprolactone)
PDMS	Poly(dimethylsiloxane)
PEG	Polyethylene Glycol
PE	Polyethylene
Pen/Strep	Penicillin/Streptomycin
PGA	Poly(glycolic acid)
PHB	Poly(3-hydroxybutyrate)
PHBV	Poly(3-hydroxybutyrate-co-3-hydroxyvalerate)
PHEMA	Poly(2-hydroxyethyl methacrylate)
PK	Penetrating Keratoplasty
PLA	Poly(lactic acid)
PLGA	Poly(Lactic Acid-co-Glycolic Acid)
PLLA	Poly(L-Lactic Acid)
PMMA	Poly(methyl methacrylate)
S(%)	Swelling Ratio
SALK	Superficial Anterior Lamellar Keratoplasty
SDS-PAGE	Sodium Dodecyl Sulphate- Polyacrylamide Gel Electrophoresis
SEM	Scanning Electron Microscopy
TCPS	Tissue Culture Polystyrene
Tt	Transition Temperature
UTS	Ultimate Tensile Strength
UV	Ultra Violet
UXL	Uncrosslinked
v/v	volume/volume
WHO	World Health Organization
w/v	weight/volume
μm	micrometer

CHAPTER 1

INTRODUCTION

1.1 Cornea

The cornea is the most exterior, transparent surface of the eye which is roughly 500 µm thick in the center and the diameter is about 12 mm (Figure 1.1) (Z. Liu et al., 1999). There are two main functions of the cornea: (1) to protect the eye by serving as a barrier against external objects by virtue of its position. (2) To function as the principal optical element of the eye by refracting 70% of the light incoming into the eye (Buerman & Pedroza, 1996; Trinkaus-Randall, 2000; McLaughlin et al., 2009). Cornea is one of the avascular tissues in the body, a property essential for its transparency. Oxygen and glucose needed to maintain the normal metabolic functions of the cornea is supplied by diffusion from the tear film that forms on its external surface and the aqueous humor on the inside, respectively (Nishida, 2005).

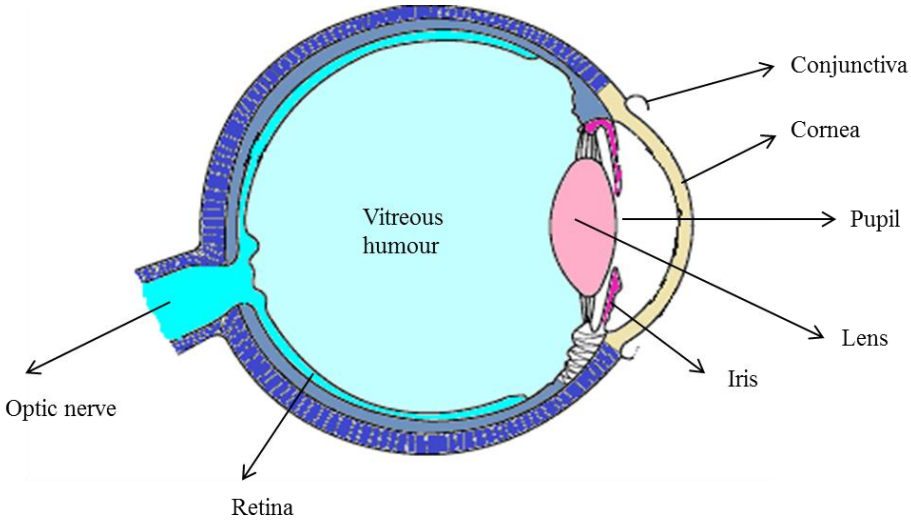

Figure 1.1: Scheme of the eye

1.1.1 Structure of the Cornea

Cornea has a layered structure composed of the Epithelium at the surface, Bowman's layer, Stroma, Descemet's membrane and Endothelium (Figure 1.2).

Corneal epithelium is 50-90 µm thick and forms the exterior layer of the cornea. Five-six layers of epithelial cells in the form of stratified, squamous and non-keratinized layers. Due to the strong junctions between the adjacent cells, the epithelium functions as a barrier against the microorganisms, and other

extraneous bodies. However, it is permeable to several molecules needed by the eye including CO_2, O_2, glucose, and sodium (Kaji, 2002).

Randomly arranged type I, III and IV collagen fibers and proteoglycans form the 12 µm Bowman's layer which is beneath the epithelium layer. Since the collagen fibers are formed by the secretion of

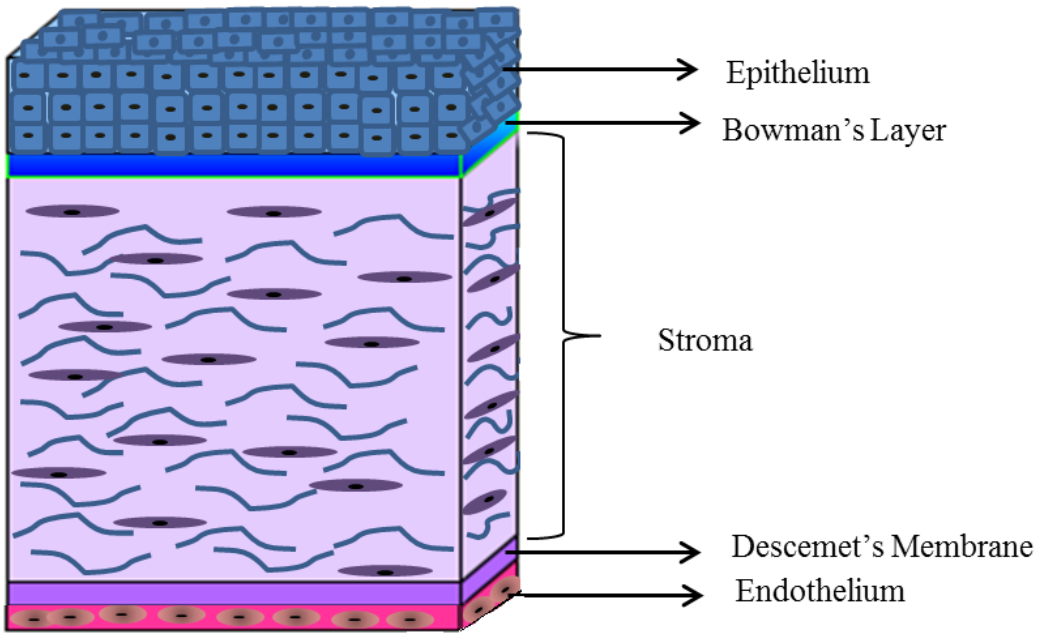

Figure 1.2: A schematic representation of the crosssection of the cornea

stromal keratocytes, it is considered as the anterior part of the stroma and its physiological function still remains unclear (Kaji, 2002; Nishida, 2005).

90% of the cornea is constituted by the stroma which is around 400 µm in thickness and it plays a major role in the protection, transmission and refraction by the cornea (Ruberti et al., 2007). Stroma is composed of mainly Type I collagen (70%) and glycosaminoglycans (GAGs), keratan sulfates (lumican, mimecan, and keratocan), and proteoglycans are the other extracellular matrix (ECM) components that make up the stroma (McLaughlin et al., 2009; Torbet et al., 2007). 3-10 % of the stroma (by volume) is composed of the stromal fibroblasts called keratocytes (Torbet et al., 2007).

Beneath the stroma, there is a 12 µm thick basement membrane named Descemet's membrane. Laminin and Type IV collagen are the main proteins of this layer (Kaji, 2002; Asbell & Brocks, 2011).

Endothelium is the innermost layer of the cornea and it is composed from 400,000 hexagonal cells. This layer is important for the maintenance of transparency of the cornea and the hydration of the stroma. Corneal hydration is controlled via a fluid pump mechanism driven by Na^+, K^+ ATPase in the endothelium (Ruberti et al., 2007; McLaughlin et al., 2009)

1.1.1.1 Cells of the Cornea

Cornea is composed of three different cell types, namely epithelial cells, keratocytes and endothelial cells.

The epithelium consists of a multilayered (five to seven layers) stratified squamous epithelium which has a continual turn over capability (every five to seven days) due to stem cells located at the corneal limbus. The limbus is situated in a transitional zone between the cornea and the conjunctiva. The stem

cells at the limbus are vital for the repair and regeneration of the corneal epithelium. There are three layers that form corneal epithelium; basal cell layer (next to the basement membrane), wing cell layers, and superficial cell layers. Among these layers, only the cells at the basal layer undergo mitosis. The cells derived from basal cells differentiate into wing and superficial cells. Superficial cell layer provides a protective barrier for the cornea (Suzuki et al., 2003; Vacanti & Vacanti, 2007).

Stromal keratocytes are mesenchyme-derived cells distributed throughout the collagen-proteoglycan matrix (3-10%, v/v) of the stroma. They play a major role in the maintenance of transparency of the cornea both by expression of crystalline proteins and also by preserving the organization of the stroma by producing proteoglycans continuously (Ruberti et al., 2007). Any cell loss or phenotype change in the stroma leads to a dramatic decrease in corneal transparency (Jester et al., 1999). Upon injury, the cells are stimulated either to go through apoptosis or to change phenotype to the repair phenotypes. In the case of apoptosis (observed when the epithelium layer is scraped away) the keratocytes beneath the epithelium undergo cell death and they are replaced with a new keratocyte population after a short time by mitosis of the neighboring cells. This response is thought to protect the cornea from further inflammation and loss of clarity (West-Mays & Dwivedi, 2006). In pathological corneas, during wound-healing process, keratocytes change their normal quiescent phenotypes into fibroblast and myofibroblasts and this change is characterized by reduced transparency due to a fibrotic extracellular matrix accumulation which is different from normal glycosaminoglycans of the stroma. Normal quiescent keratocytes express protein and mRNA for keratocan, aldehyde dehydrogenase class 3 and secrete keratan sulfate. On the other hand, repair transition is characterized by a high level of α-smooth muscle actin expression and the fibroblasts in the region start to repair the injury site by the secretion of biglycan, fibronectin, and collagen Type I and Type III (Funderburgh et al., 2003). Finally, this fibroblastic conversion is associated with the loss of transparency due to a decrease in expression of crystallins such as transketolase (TKT) (Jester et al., 1999; Muthusubramaniam et al., 2012). Following tissue repair, fibroblasts gradually gain keratocyte phenotype by becoming quiescent and transparent (Fini, 1999).

Corneal endothelium is composed of monolayer squamous endothelial monolayer that constitutes a barrier between the anterior chamber and the stroma. The main function of this layer is to maintain transparency by keeping cornea hydrated. It prevents corneal stroma from swelling by eliminating the excess fluid with the activity of Na^+/K^+ pumps and Mg^+ ionic pumps. Endothelium layer also provides nutrient to the avascular cornea by permitting the nutrients to go through. Thus, the barrier and pump functions of the endothelium are essential for the maintenance of the transparency, dehydrated state and the thickness of the cornea (Joyce, 2003; Bourne & McLaren, 2004; Teichmann et al., 2013).

1.1.1.2 Structure and Components of Stroma

The stroma is approximately 400 μm in thickness, containing 200-400 lamellae with 31 nm of uniform diameter and regular spacing to each other (Meek & Leonard, 1993). The lamellae forming the corneal stroma are parallel to the corneal surface and at right angles to adjacent lamellae forming a plywood-like structure (Figure 1.3 A, B). This organization of the fibrils is essential for both the biomechanical and the optical properties of the cornea (Meek, 2009). Mechanical properties are very important for the maintenance of normal functions of the cornea. The cornea must not be ruptured with traumatic impacts and withstand the tensile stress imposed by the intraocular pressure (IOP). This load bearing property is a result of the complex organization of the stromal tissue (Figure 1.3 B, C) (Ethier et al., 2004; Ruberti & Zieske, 2008). Corneal transparency is achieved mainly by the chemistry and the organization of the extracellular matrix (ECM) and by the stromal cells, keratocytes. Collagen Type I and Type V fibrils are the major constituents of the stroma and transparency is attributed to uniform fibril diameter, direction, and packing (Maurice, 1957; Meek & Fullwood, 2001). Proteoglycans are the second major group of molecules forming the stroma. Decorin contains chondroitin and dermatan sulfate and lumican, mimecan and keratocan contain keratan sulfate. Experiments with knock-out mice showed that keratocan deficient mice displayed cloudy corneas when mature. Cloudy corneas were also developed in the lumican deficient ones due to abnormal fibril diameter. This implies that lumican is an important GAG for the stromal collagen organization and together with other proteoglycans they are important for the clarity of the stroma and the cornea (Chakravarti et al., 2000; Meek & Boote, 2004).

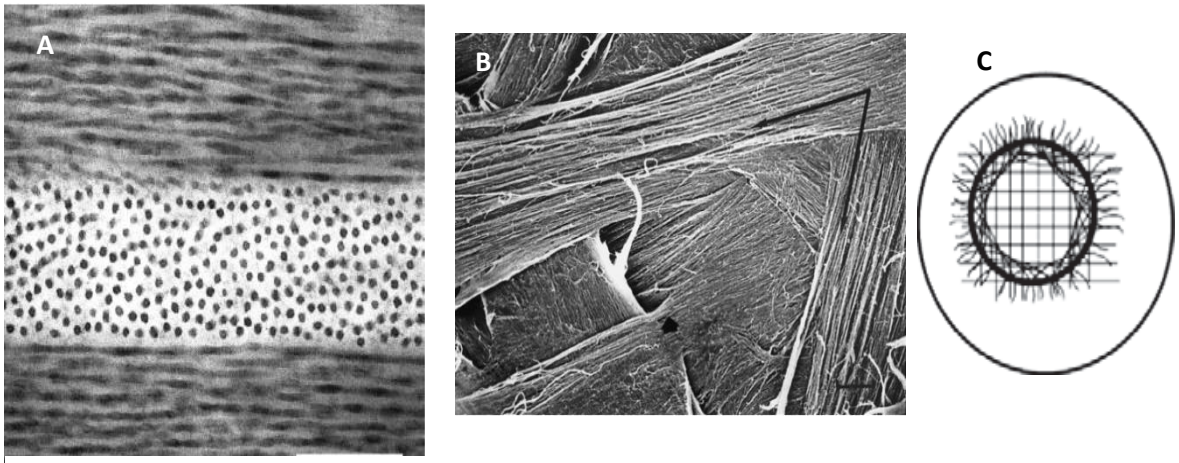

Figure 1.3: Structure of Stroma. A) Transmission electron micrograph shows the organization of the collagen fibrils in the crosssection of the stroma. In the top and bottom lamellae the fibrils are running from side to side whereas in the middle lamellae running toward the reader at right angles to the adjacent lamellae. The uniform diameter and regular spacing is seen in the middle lamellae (Adapted from Fullwood, 2004). B) Scanning electron micrograph shows the perpendicular arrangement of the collagen fibrils of the neighboring lamellae (Adapted from Meek & Fullwood, 2001). C) Possible fibril orientation model based on X-Ray synchrotron data (Adapted from Meek & Boote, 2004).

1.1.2 Corneal Diseases

Corneal diseases and wounds are the second major cause of blindness after cataract and are estimated to affect 27.9 million people worldwide of which 4.9 million with bilateral corneal blindness (Oliva et al., 2012). The major causes of corneal blindness are trachoma, ocular trauma and corneal ulcerations and childhood blindness.

Trachoma is a chronic and the most common infectious disease worldwide and it is estimated by World Health Organization (WHO) that 12 million people will develop trachoma related blindness by 2020. Thus, trachoma is placed in the intervention priority list of WHO. Trachoma is a result of repeated reinfection by an intracellular bacterium *Chlamydia trachomatis* and leads blindness 10- 40 years after infection (Dean et al., 2008). Chronic inflammation because of repeated infections results in the scarring of conjunctiva, in-turning of eyelashes (trichiasis) resulting from upper lid shortening and abrading of the cornea. Finally scarring, corneal opacity, and blindness are seen if the disease progresses and the cornea is not treated. Trachoma is found among poor populations and spread from eye to eye by close contact. WHO aims to prevent trachoma related blindness with the SAFE strategy; Surgery for trichiasis, Antibiotic treatment, Facial cleanliness, Environmental changes and improvements (Oliva et al., 2012).

Trauma is a major problem worldwide which causes unilateral visual impairment and corneal blindness due to severe eye injuries. There are 1.6 million blind people because of injuries and additional 19 million people suffer unilateral blindness or low vision and 2.3 million people are with bilateral low vision. Accidents are the most common causes of ocular traumas which are followed by sports activities, burns, traffic accidents, foreign bodies, and firearm accidents (Strahlman et al., 1990; Negrel & Thylefors, 1998).

Ulceration of cornea is another major sight-threatening problem. In this case, the epithelium is damaged and in severe cases stroma inflammation is seen. Loss of stromal tissue due to inflammation results in stromal lysis (Coster, 2002b). Ulceration can be a result of either external influences like physical trauma, heat or infection, exposure to chemicals or intrinsic influences like dystrophies and stem cell deficiency. The cornea can be destroyed in 24 h if the infected ulcer is not treated (Coster, 2002a).

The reasons of the childhood blindness vary between regions and by socioeconomic positions in that society. While high income countries are facing retinopathy due to prematurity, optic nerve hypoplasia, and cortical visual impairment, the causes in the low income countries are generally corneal scarring from measles, vitamin A deficiency, use of traditional eye remedies, and infectious keratitis and ophthalmia neonatorum (Isenberg et al., 2009). In general, the causes of childhood blindness can be classified as: genetic and chromosomal abnormalities, intra-uterine period problems like infections and toxins, causes that emerged at the time of birth or in the post-natal period like cerebral hypoxia, retinopathy, and ophthalmia neonatorum, and factors which are influential in the childhood such as vitamin A deficiency and trauma (Foster & Gilbert, 1992). In addition to these causes, herpes simplex virus (HSV) infections, keratoconjunctivitis and chemical keratitis are other potential sources of risk for childhood blindness (Whitcher et al., 2001).

1.1.2.1 Approaches for the Treatment of Corneal Damages

Cornea transplantation, penetrating keratoplasty (PK) is the most widely used treatment worldwide for permanently opacified, scarred or severely deformed corneas that clear vision cannot be achieved by spectacles or contact lenses. PK refers to full-thickness corneal replacement and among other organ transplantations it has the highest success rate (90%). However the success rate decreases dramatically in complex cases if the cornea develops edema or glaucoma, or if the cornea is highly vascularized and scarred. Cases with severe chemical burns, trachoma, dry eye syndrome, Stevens-Johnson syndrome, and vascularized corneas due to injury are also in the low success risk group for transplantation (Chirila et al., 1998).

In less complex cases where only some parts of the cornea are affected like in various corneal dystrophies, and keratoconus, lamellar keratoplasty (LK) is used instead of PK. In the case of Anterior lamellar keratoplasty (ALK), stroma, endothelium and Descemet's membrane are left intact while the diseased epithelium layer is removed. Superficial anterior lamellar keratoplasty (SALK) is used if the 30-40 % of the cornea is damaged and the diseased tissue is replaced with the same amount of healthy donor tissue. On the other hand, deep anterior lamellar keratoplasty (DALK) includes removal of diseased stroma and Descemet's membrane while leaving endothelium layer intact (Al-Kharashi et al., 2009). Anterior lamellar keratoplasty surgeries are more advantageous than PK surgeries where sutures are removed earlier and also the visual recovery occurs faster than normal PK procedures (Arenas et al., 2012).

Although success rate is very high in corneal transplantation when compared to other solid organs, and graft rejection is prevented extensively by topical steroids and immune-suppressive drugs, graft failure is still a serious problem (Panda et al., 2007). Shortage of donor tissue is major problem in corneal transplantation which leaves millions of patients untreated. The available corneal tissues decrease in number with the corneal surgeries like in situ keratomileusis (LASIK), infectious diseases like HIV and hepatitis, and with increasing age (Chirila, 2001; Muraine et al., 2002).

Keratoprostheses are the artificial corneas that are the only other choice for patients with several corneal graft rejection histories. Standard PK procedure is used to replace the damaged tissue with this artificial cornea to repair the function of the cornea. The first attempts to make an artificial cornea were made in the 19th century by De Quengsy with the first glass implantation to the rabbits (Chirila et al., 1998). However, unsuccessful results with glass samples due to high risk of removal of the material from the cornea lead to the use of synthetic polymers. Poly(methyl methacrylate) (PMMA) was the first polymer that was used as a keratoprosthetic material, and this attempt was followed by the use of other synthetic polymers. With the concept of "core-and-skirt" model where the porous skirt surrounds the central core material of the prostheses, it was aimed to obtain a good integration of the material with the host tissue. Today, most of the keratoprostheses designs are based on this model where the elastic, porous skirt allows ingrowth of the fibroblasts for anchorage of the cornea (Chirila et al., 1998; Griffith et al., 2009; Myung et al., 2008). However, due to problems like calcification, infection, and retinal detachment, keratoprostheses are used as an alternative to transplantation when the grafts fail repetitively (Griffith et al., 2011). Osteo-odonto keratoprosthesis (OOKP), Boston KPro, and AlphaCorKPro are three most commonly used types of keratoprostheses.

Osteo-odonto keratoprostheses (OOKP) was developed by Strampelli in 1963 where the mucous membrane covers the PMMA cylinder (Figure 1.4). Although OOKP ensures a good control over the immunological complications the surgical procedure is very complex and time consuming. Extrusion, glaucoma, retinal detachment and retroprosthetic membrane formation are the major problems associated with OOKP (C. Liu et al., 2005; Viitala et al., 2009).

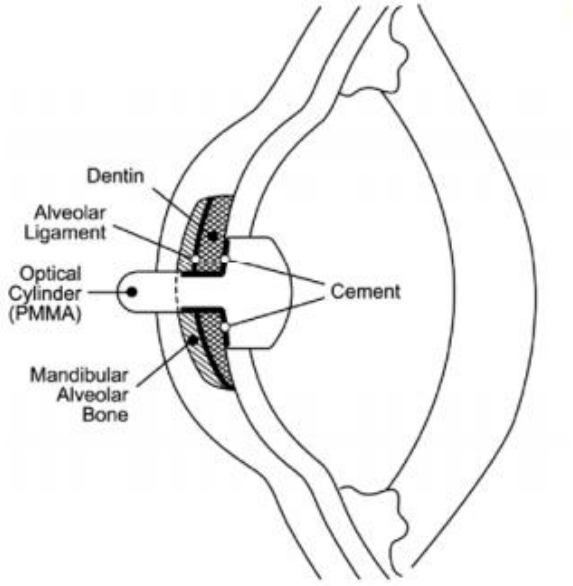

Figure 1.4: Scheme of the OOKP (Adapted from Laattala et al., 2011).

The Boston KPro uses a collar-button design where PMMA is used to form the front plate for carrying optical stem and back plate with holes to allow hydration and nourishment of the cornea. Titanium ring is used to lock the device to the donor corneal graft and then the device is sutured to the host (Robert & Harissi-Dagher, 2011). Although antibiotics like Vancomycin are extensively reduced the severe complications such as necrosis and endophthalmitis, glaucoma still remains a problem for Boston KPro patients (Güell et al., 2011).

The AlphaCorKPro, also known as Chirila keratoprosthesis, is made from crosslinked poly(2-hydroxyethyl methacrylate) (PHEMA) gel forming the central optic and the sponge skirt. With this design it was aimed to lower the mechanical stress, prevent leakage, and downgrowth of epithelium which are common problems with other designs. However, fibrous closure, white intraoptic deposits, and low sight due to complications are the reported problems associated with AlphaCor device (Gomaa et al., 2010; Hicks et al., 2006).

1.2 Tissue Engineering

The field of tissue engineering was originated from the biomaterials sciences in the last few decades and aims to replace, restore or improve the function of the tissues in the case of diseases or injuries by using cells, extracellular matrix components or biomaterials (Langer & Vacanti, 1993). Tissue engineering involves obtaining cells from the host's tissues and proliferating them on appropriate 3 dimensional tissue substitutes or scaffolds, which mimic the natural structure, composition and function of the tissue. The scaffolds play a significant role in supporting cell attachment, proliferation, and extracellular matrix (ECM) production by providing a framework. An ideal scaffold should mimic the natural human tissue by its micro and macrostructure (C. Liu et al., 2007). The scaffold should degrade in time

while the newly formed tissue takes its place. In the future, by tissue engineering it is aimed to reduce and eventually eliminate the need for organ transplants and problems associated with transplantation like limited number of donated organs and risk of disease transmission (L. G. Griffith & Naughton, 2002)

1.2.1 Corneal Tissue Engineering

1.2.1.1 Cells and Sources Used in Corneal Tissue Engineering

The cells used in corneal tissue engineering are specific to the targeted layer. Cells are obtained in two different ways: direct isolation from the tissue of the host (patient or the animal) or using stem cells that have the ability to differentiate into the desired cell type (Vacanti & Vacanti, 2007).

The epithelium cells used in tissue engineering purposes can be the cells at the basal layer or stem cells at the limbus and can be isolated by enzymatic digestion. The cells at the central cornea have proliferation capability only for two or three passages. On the other hand, the stem cells at the limbus have a higher proliferation potential (seven passages) and they grow much better in the culture compared to the central cornea cells (Germain et al., 2000). Stem cells isolated from other tissues like oral mucosal cells and bone marrow stem cells can also be used as an alternative to limbus stem cells (Chen et al., 2009; Jiang et al., 2010).

Keratocytes can be isolated from the corneal stroma after removing the epithelial layer and digesting the sample with dispase. Another option for isolation of the stromal cells is the obtaining them from keratocyte contaminant epithelium cell culture by changing the medium into a keratocyte culture medium. After several subculturing, the epithelial cells are lost due to inappropriate medium for them to proliferate (Germain et al., 2000).

The isolation of endothelial cells was a challenge earlier due to strong adherence of the cells to the Descemet's membrane and the common trypsin treatment damages cells that leads to degradation of the cells because of longer incubation times. Instead of usual trypsin treatment, collagenase type IV treatment works well and high numbers of free endothelial cells can be obtained. Another problem with the isolation of endothelial cells is the contamination of the culture with stromal cells which is solved by using a selective medium appropriate for endothelial cells that contains D-valine instead of L-valine (Engelmann et al., 1988; Engelmann et al., 2004).

Cornea seems to be an attractive tissue for tissue engineering to due to its simple, avascular and multilaminar structure. However, those three different cell types mentioned above need to be successfully cultured if a functional corneal equivalent is desired to be constructed (Ruberti et al., 2007). Although there are several studies attempted to construct tissue engineered cornea with three layers (McLaughlin et al., 2010; Vrana et al., 2008b), most of the studies focused on reconstructing one (Torbet et al., 2007; Wang et al., 2009) or two layers of the cornea (Zorlutuna et al., 2006; Builles et al., 2010).

1.2.1.2 Scaffolds Used in Corneal Tissue Engineering

1.2.1.2.1 Natural Origin Materials

Natural origin materials are widely employed in tissue engineering applications due to their various characteristics like biocompatibility, biodegradability, gelation ability, and water binding capacity. Additionally, they can be modified or conjugated with other molecules via chemical or enzymatic reactions. Natural polymers are hydrolyzed or degraded by the enzymes and metabolized by the biological systems (Sawhney & Drumheller, 1998). They also possess some disadvantages; induction of immune responses, variability with the source, batch-to-batch variability and limited sources. With the new processes and techniques of purification and production, these materials are being developed into better materials for tissue engineering (Correlo et al., 2011). Among the extremely broad range of polymers, three major classes of them are more widely used in tissue engineering than others; polyhydroxyalka-

noates, polysaccharidic polymers and protein-origin polymers. These polymers are obtained from plant, animal or algae sources and also microorganisms are employed to produce them via fermentation or enzymatic reactions (Hasırcı et al., 2001).

Polyhydroxyalkanoates are degradable and biocompatible and form a large family of polymers and the main molecules used in tissue engineering are mainly 3-hydroxybtyric acid (PHB) and copolymers of PHB with hydroxyalkanoates like 3-hydroxyvaleric acid (PHBV) (Hasırcı et al., 2001). They are promising polymers for biomedical field because of their mechanical strengths, biodegradability, and capability of fiber formation. For example, micropatterned films from PHBV have been used in the engineering of tissues like cornea (Zorlutuna et al., 2006; Zorlutuna et al., 2007), cartilage (Köse et al., 2005), bone (Köse et al., 2003; Kenar et al., 2006), cardiac (Kenar et al., 2011), and nerve (Yucel et al., 2010).

Polysaccharides are also used in cornea tissue engineering applications due to their biocompatibility, low cost in production, and non-toxicity. They can be obtained from a variety of sources such as microorganisms, animals and plants. Their chemical and physical properties vary according to their molecular weight and composition (Nair & Laurencin, 2007). Chondroitin sulfate is one of the polysaccharides used in the construction of foams together with collagen in cornea engineering and the scaffold was successfully populated with three cell types of the cornea (Vrana et al., 2008b). Rafat et al. (2008) used a chitosan-collagen blend in the construction of scaffolds for corneal epithelium. Their results showed that these scaffolds are biocompatible, elastic, optically clear and mechanically strong. Hyaluronic acid is another polysaccharide used in cornea reconstructs. Films consisting of collagen-gelatin-hyaluronic acid have been used and were shown to have appropriate hydrophilicity, mechanical strength and optical clarity. Additionally, corneal epithelial cells populated the scaffolds well which shows the suitability of this scaffold (Y. Liu et al., 2013).

Proteins are the major component of the extracellular matrices and they contribute to tissue regeneration, wound healing, and regulation pathways. Proteins are used for constructing sutures, scaffolds, and drug delivery systems. They degrade by hydrolysis via the enzymes of the host organism (Nair & Laurencin, 2007). Proteins produced by recombinant DNA technology avoid batch to batch variations risk of naturally occurring proteins by making the production of proteins with defined properties possible (Girotti et al., 2004). Collagen is thought to be an ideal scaffold material for corneal tissue engineering since it is the major component of the stroma. It has been shown that micropatterned, crosslinked collagen films helped alignment of human corneal keratocytes and improved the mechanical strength and the transparency of the scaffold (Vrana et al., 2008a; Vrana et al., 2007b). In another study, crosslinked collagen foams were shown to be populated well with the stromal cells (Vrana et al., 2007a). Silk fibroin is another protein used extensively in cornea engineering. RGD-functionalized silk protein constructs have been shown to replicate the normal lamellar structure of the corneal stroma and remain transparent. The scaffolds supported cell attachment, proliferation and alignment (Gil et al., 2010). Since collagen and elastin like recombinamers are used in the present study, they will be explained in more detail in the following section.

1.2.1.2.1.1 Collagen

Collagen is the major constituent of the mammalian tissues like cornea, skin, bone, cartilage and blood vessels. It has an important role in the attachment, regulation of proliferation, differentiation, anchorage, and survival of the cells (Wess, 2005). Three polypeptide chains constitute the motif of triple helix of the collagen with the repeating amino acid sequences Gly-X-Y. This repeating structure provides coiling to a left handed motif to each procollagen, and assembly into a right handed helix of the three chains to form triple-helix. After the secretion, the globular ends of the procollagen chains are cleaved leaving the collagen. Individual collagen molecules align parallel to each other to form fibril structure with a 64 nm gap (Cawston, 1998). The center of the triple helix is settled by Gly residues and the surface of the helix is situated by X and a Y residue where X is usually proline and Y is hydroxyproline. Hydroxyproline is an important amino acid for the stabilization of the triple helix.

There are more than twenty-seven genetically different types of collagen identified (Bou-Gharios & de Crombrugghe, 2008). However, type I collagen is the most abundant one and in the cornea it is the most studied protein for tissue engineering applications due to its abundance and unique chemical, physical and biological properties (Pachence et al., 2007). The collagen Type I fibrils are aligned parallel to each other in some tissues like tendons, or they form a random complex network in tissues like skin. The gaps between the neighboring chains seem to be filled by hydroxyapatite in the case of bone (Rossert & de Crombrugghe, 2002).

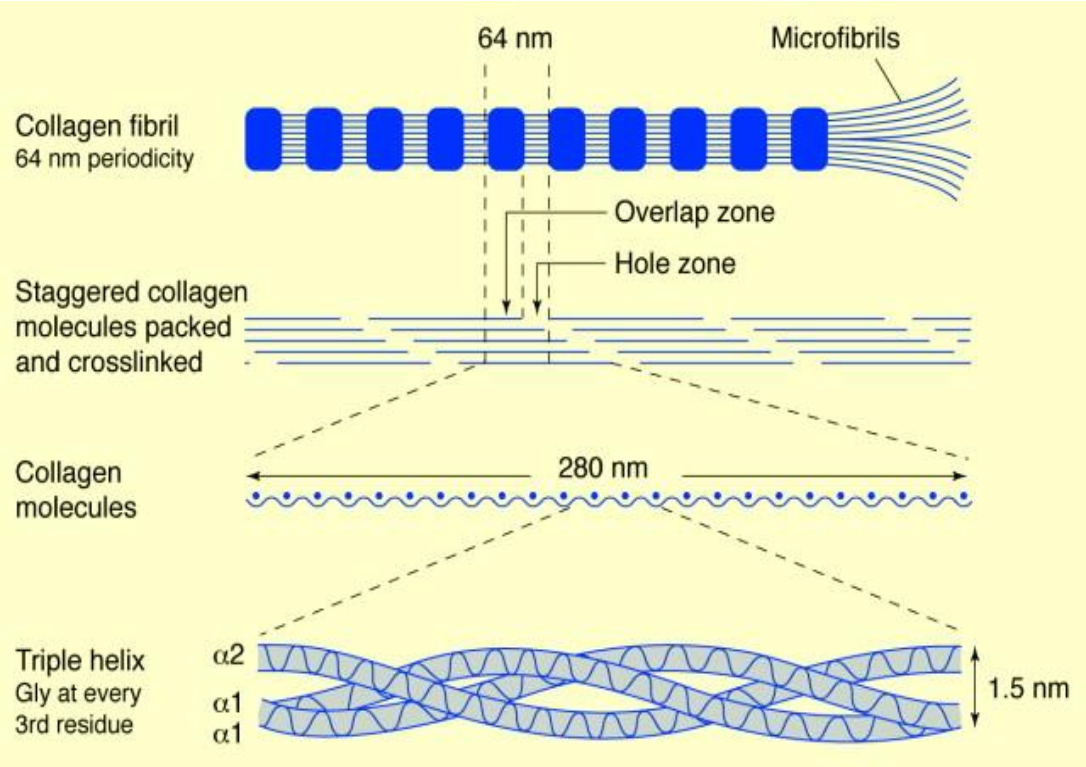

Figure 1.5: Schematic diagram of collagen structure and assembly (Adapted from Cawston et al., 1998)

Collagen can be isolated from the skin, bone and tendon of the animals (Senaratne et al., 2006; Rajan et al., 2007). Collagen is used in construction of scaffolds for a variety of tissues like bone (Ber et al., 2005; Murphy et al., 2010; Su et al., 2012; Amruthwar & Janorkar, 2012), vascular (Berglund et al., 2003; Boccafoschi et al., 2005; Zorlutuna et al., 2009; Pang et al., 2010), skin (Hafemann et al., 1999; Ma et al., 2003; Y. Liu et al., 2012), and cornea (Rafat et al., 2008; E. Vrana et al., 2008b; Merrett et al., 2009; Builles et al., 2010). Moreover, in the delivery of drugs and other active molecules collagen is used as a carrier (Vasantha et al., 1988; Olsen et al., 2003; Ruszczak & Friess, 2003; Kojima et al., 2012).

1.2.1.2.1.2 Elastin like Recombinamers

Elastin like polymers (ELPs) are artificial protein-based polymers which are very attractive in the field of biomaterials due to their unique compositions and high biocompatibility, and non-immunogenicity. ELPs consists of a pentapeptide repeats, valine-proline-glycine-X-glycine (VPGXG), where X stands for any amino acid except proline. Since ELPs are composed of amino acids, their metabolized products are amino acids and are not toxic for the system (Nair & Laurencin, 2007). Today,

with the combination of fermentation biology, molecular biology and genetic engineering techniques, it is possible to produce protein based polymers as recombinant proteins with the use of genetically modified organisms (bacteria). Research on recombinant polymers has shown that these proteins can be controlled to yield production of very precisely tailored biomaterials. Thus, ELPs (also known as Elastin like recombinamers, ELRs) possess an invaluable advantage because of the physical and chemical properties being well defined and controlled by the recombinant DNA technology used (Rodríguez-Cabello et al., 2009). ELRs are further developed into more sophisticated biomaterials by including short active peptides on the surface of the polymer. The first ELRs produced in this manner are RGD (R: L-Arginine, G: Glycine, and D: L-Aspartic Acid) that is shown to enhance cell binding, proliferation and spreading and REDV (R:L-Arginine, E: L-Glutamic acid, D: L-Aspartic acid, and V: L-Valine) known to stimulate endothelial cell adhesion and proliferation (Nair & Laurencin, 2007; Pachence et al., 2007; Rodríguez-Cabello et al., 2009).

All of the functional ELRs also exhibit Inverse Temperature Transition (ITT), which can be counted as one of their most interesting features. Below their transition temperature (Tt), these polymers expound but above this temp, the chains of the polymer get into more ordered confirmation which results in polymer to shrink (Ribeiro et al., 2009). Incorporation of proper guest residues at the fourth position of the molecule can lead to ELRs responding to other environmental stimuli like light, pH, and ionic strength (Nair & Laurencin, 2007).

ELRs have been shown to be very promising biomaterials in a wide variety of applications such as drug delivery (Bidwell III et al., 2007), coatings (Ozturk et al., 2009), and engineering of tissues engineering like bone (Amruthwar & Janorkar, 2012) cartilage (Betre et al., 2002), ocular (Martínez-Osorio et al., 2009), oral mucosa (Kinikoglu et al., 2011b), and liver (Janorkar et al., 2008).

The laminin YIGSR used in the present study (Y: L-Tyrosine, I: L-Isoleucine, G: Glycine, S: L-Serine, and R: L-arginine) is an adhesive peptide and interacts with 67 kDa laminin binding protein (LBP) (Figure 1.6). This protein has been shown to enhance binding, proliferation and spreading of several cell types like endothelial cells, smooth muscle cells, epithelial cells, and fibroblasts (Fittkau et al., 2005).

$\{[(VPGIG)_2\text{-}(VPGKG)_2\text{-}(VPGIG)_2]_2\text{-}(VPGIG)\text{----}DPGYIGSR\text{----}(VPGIG)_2\text{-}[(VPGIG)_2\text{-}(VPGKG)_2\text{-}(VPGIG)_2]_2\}_8$

Figure 1.6: Monomer composition of the elastin-like recombinamer (ELR), YIGSR.

1.2.1.2.2 Synthetic Origin Materials

Biodegradable synthetic polymers are attractive alternatives for the natural origin biopolymers due to their following advantages: 1) Most biodegradable synthetic polymers are biocompatible and when compared with some of the natural origin ones, they do not initiate any immunological responses; 2) Their mechanical properties and degradation rates can be altered without changing the bulk features of the polymer by changing the process conditions and components; 3) They can be processed to take on various forms and properties that to enhance the tissue ingrowth (Gunatillake & Adhikari, 2003; Tian et al., 2012).

Polyesters are the most commonly used synthetic polymers because of their biodegradability and biocompatibility. They undergo degradation by hydrolysis of the ester linkage and the degradation products are excreted from the body by metabolic pathways. Poly(glycolic acid) (PGA), poly(L-lactic

acid) (PLLA), and poly(lactide-co-glycolic acid) (PLGA) and are the most widely used polyesters in the field of tissue engineering including cornea tissue engineering (Gunatillake & Adhikari, 2003; Pachence et al., 2007). Zorlutuna et al. (2007) used the blend of PLGA and PHBV in the production micropatterned 2D scaffolds for epithelial and fibroblastic cells. Their study showed that the blend of these two polymers can be successfully used in the corneal tissue engineering applications. In another study, Hu et al. (2005) used PGA scaffolds to study the change in transparency over time. They observed that the stromal equivalent became nearly transparent in 8 weeks.

1.3 Approach of This Study

1.3.1 Contact Guidance

The cells and the tissue growth are extensively influenced by the surface properties of the substrate like topography that is formed by the cells and the extracellular matrix (ECM) proteins. This effect, contact guidance, significantly influences the wound healing process and tissue growth (Zhang et al., 2005). It has been shown that, a wide range of materials used to create topography affect the cell behavior. These include metals like gold, titanium, inorganic compounds like silica and lithium niobate, and polymers like nylon, cellulose acetate, fibrin, and collagen. The topographies that the cells interact can be channels, spikes, tunnels and dots, fibers, cylinders, and meshes. While the cells react with the surface topography, their orientation and organization changes, extension is enhanced, movements are modified and polarized, adhesion strength changes and activation of the signaling pathways is seen. Studies have shown that most types of cells including chondrocytes, fibroblasts, epithelial cells, osteocytes, and smooth muscle cells react with the surface (Curtis & Wilkinson, 1997).

In this study, in order to alter the behavior of the cells (alignment, ECM secretion, adhesion, etc.) micropatterning was used. It can be achieved via a variety of methods. Photolithography, the one used in this study, is one of the micropatterning techniques (Figure 1.7). In this technique UV light is used to transfer a desired pattern through a quartz (glass) photomask onto a photoresist (light-sensitive) on the surface. After removal of the reacted (or unreacted) resist, the substrate is washed and then the exposed

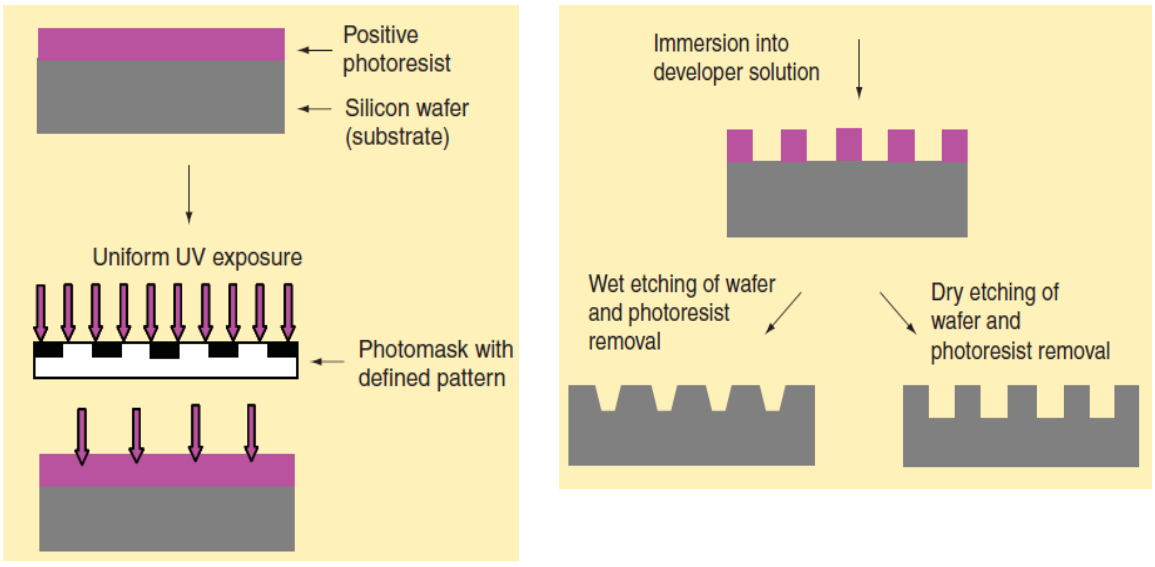

Figure 1.7: Schematic representation of photolithography (Adapted from Hasirci & Kenar, 2006).

parts are etched. Thus, the material under the photoresist receives the patterns after further chemical treatments (Falconnet et al., 2006; Subramani, 2010). If the final treatment is done by wet chemical etching by using hydrofluoric acid, walls with slopes occur like the one used in this present study or vertical walls are formed if the surface is etched by the reactive ions created by an electric field (Figure 1.7) (Hasirci & Kenar, 2006). The film to seed the cells on is obtained by using the etched substrate as a template. The pattern on the film is then used to guide the cells for a successful tissue engineering construct.

1.4 Novelty of This Study

Corneal stroma is composed of 200-400 lamellae parallel to corneal surface and at right angles to the adjacent lamellae like plywood (Meek & Leonard, 1993). This alignment and orientation of the stroma is vital for the maintenance of mechanical and optical properties of the cornea (Meek, 2009). In the present study, the natural structure of the stroma was mimicked by using micropatterned collagen-based films that helped alignment of the cells. These films were used in the construction of 3D, multilayered scaffolds by stacking the micropatterned films perpendicular to adjacent films. Collagen has an important role in cell attachment, proliferation and survival of the cells (Maurice, 1957; Wess, 2005). Elastin Like Recombinamers (ELR) are artificial protein based polymers produced by recombinant DNA technology. Recently, they find increasing use in the field of tissue engineering due to their biocompatibility (Nair & Laurencin, 2007). Studies conducted using ELRs with YIGSR sequences showed that this sequence increased the cell binding, migration and proliferation of wide range of cells including endothelial cells, epithelial cells, fibroblasts and smooth muscle cells (Fittkau et al., 2005). In this study these ELRs were used for the first time with stromal keratocytes to improve cell adhesion and proliferation. Collagen and ELR were used together in the construction of scaffolds which were stabilized with dehydrothermal crosslinking and their in vitro performance was tested by using human corneal keratocytes.

CHAPTER 2

MATERIALS AND METHODS

2.1 Materials

Bovine serum albumin (BSA), sodium cacodylate trihydrate, glutaraldehyde (25%), 4',6- diamine-2-phenylindole dihydrochloride (DAPI), FITC-conjugated phalloidin, amphotericin B, Collagenase type II from *Clostridium Histolyticum*, paraformaldehyde, monoclonal mouse anti-human collagen type I antibody, and Coomassie brilliant blue were purchased from Sigma-Aldrich (USA). New born calf serum, Dulbecco's Modified Eagle Medium/ Ham's Nutrient Mixture F12 (DMEM:F12, 1:1) with and without Phenol red, Trypsin-EDTA (0.25%), Penicillin/Streptomycin, and SnakeSkin dialysis tubing were obtained from HyClone, Thermo Scientific (USA). Ethanol, sodium dihydrogen phosphate dihydrate, disodium hydrogen phosphate heptahydrate, acetic acid (HAc), sodium chloride, Anti-keratan sulfate antibody, clone EFG-11 and goat anti-mouse IgG (H+L), Alexa Fluor® 488 conjugate were purchased from Merck (Germany). Human basic fibroblast growth factor (hFGF basic/ FGF2) with carrier was purchased from Cell Signaling Technology, Inc. (USA). Spectra ™ Multicolor broad range protein ladder was obtained from Fermentas, Thermo Scientific (USA). Dimethyl sulfoxide (DMSO) and Triton X-100 were bought from AppliChem (USA). Alamar Blue was purchased from Invitrogen Inc (USA). Nucle-oCasette was obtained from ChemoMetec (Denmark). Dithiothreitol (DTT) was bought from Bio-Rad Laboratories (USA). Poly(dimethylsiloxane) (PDMS) precursor and curing agent (Sylgard 184) were purchased from Dow Corning, USA.

Male Sprague-Dawley rat tails for isolation of collagen type I were kindly provided by Tayfun İde (DVM), GATA Animal Experiments Laboratory (Turkey).

2.2 Methods

2.2.1 Collagen Type I Isolation

Collagen type I was isolated from male Spraque-Dawley rat tails as described previously (Kinikoglu et al., 20011a). Briefly, the skins of tails were cut along their length, tendons were removed, and dissolved in cold acetic acid (0.5 M) for 2-3 days at 4 ^{o}C. The suspension was filtered through glass wool and dialyzed in a dialysis tubing (CO 10000) against phosphate buffer (5 L, 12.5 mM NaH_2PO_4, 11.5 mM Na_2HPO_4, pH 7.2) at 4 ^{o}C for 1 week by changing buffer daily. The resulting white solid precipitate of collagen was centrifuged at 1600 g for 10 min (Sigma 3K30, Germany) and the pellet was dissolved overnight at +4 ^{o}C in 0.15 M acetic acid, NaCl (25 g) was added, incubated overnight at 4 ^{o}C and centri-fuged. The pellet was dissolved in 0.15 M acetic acid and dialyzed for 1 week against phosphate buffer (pH 7.2) at 4 ^{o}C. The collagen pellets obtained following centrifugation were sterilized by storing in 70% ethanol for 2 days. After centrifugation the pellet was frozen at -80 ^{o}C (Sanyo MDF-U53865, Japan) and lyophilized (Labconco Freezone 6, USA) for 12 h. Yellowish collagen powder was stored at 4 ^{o}C.

2.2.1.1 Collagen Characterization

Purity of Collagen was determined by sodium dodecyl sulphate-polyacrylamide gel electrophoresis (SDS-PAGE). 20 µL, 0.2% collagen solution (w/v, in 0.15 M acetic acid) was denatured at 95 ^{o}C for 3 min in mercaptoethanol, and loaded in SDS-PAGE gels (separating gel- 10% acrylamide/bisacrylamide, and stacking gel- 4.2% acrylamide/bisacrylamide). Samples were run at 30 mA for 2.5 h and stained with 0.2% (w/v) Coomassie Brilliant Blue by incubation overnight and visualized after destaining with Water:Methanol:Acetic acid = 4:5:1

2.2.2 Elastin-like Recombinamer Isolation

The elastin-like recombinamer (ELR) was produced, purified and characterized at the University of Valladolid (Spain). Briefly BLR (DE3) strain of recombinant *Escherichia coli* (*E.coli*) that contains the gene which expression results in the production of the polymer named as YIGSR ([(VPGIG)2-VPGKG-VPGIG)2 DPGYIGSR-(VPGIG)2-VPGKG-VPGIG)2]8). *E.coli* was induced to express genes in a 2 L terrific broth medium (TB) containing 0.1 mg/mL Amphiciline and 0.8 % glycerol at 37 ^{o}C, 250 rpm. Next day the fermentation was stopped after obtaining an optical density difference over 4 at 600 nm. After several washes, the culture was lysed by disruption and the debris was removed by centrifugation at 12,000 rpm, 4 ^{o}C, for 30 min and incubated at 40 ^{o}C. Following centrifugation at 40 ^{o}C, the pellet was resuspended and cold and warm centrifugations were repeated 2 times more. The protein was frozen at -24 ^{o}C and lyophilized.

2.2.2.1 ELR Characterization

2.2.2.1.1 SDS PAGE

SDS-PAGE was performed to assess the purity of the YIGSR produced. 6 µL of YIGSR solution (1 mg/mL in Milli Q) in mercaptoethanol was loaded in a polyacrylamide gel (separating gel- 12% acrylamide/bisacrylamide, and stacking gel- 4% acrylamide/bisacrylamide). The presence and purity of the polymer was detected by the intense band around 90 kDa.

2.2.2.1.2 MALDI-TOF

Matrix-Assisted Laser Desorption/ Ionization Time-of-Flight (MALDI-TOF) mass spectroscopy was also used to determine the purity and molecular weight of the YIGSR containing ELR. Voyager STR (Applied Biosystems) was used in linear mode and with an external calibration using bovine serum albumin (BSA).

2.2.3 Preparation of Template to Create Ridge-Valley Patterned Films

The silicon template used in the preparation of ridge-valley patterned films was kindly provided by Prof. Dr. Atilla Aydınlı (Bilkent University, Physics department, Ankara). The silicon template was produced by photolithography and chemical etching (Figure 2.1) and PDMS templates were prepared using this silicon master. Briefly the PDMS prepolymer-catalyst mixture was poured onto the silicon wafers and cured at 70 ^{o}C for 3 h. Resulting PDMS template was peeled off from the silicon wafer mechanically. Final templates had the inverse dimensions of the silicon template.

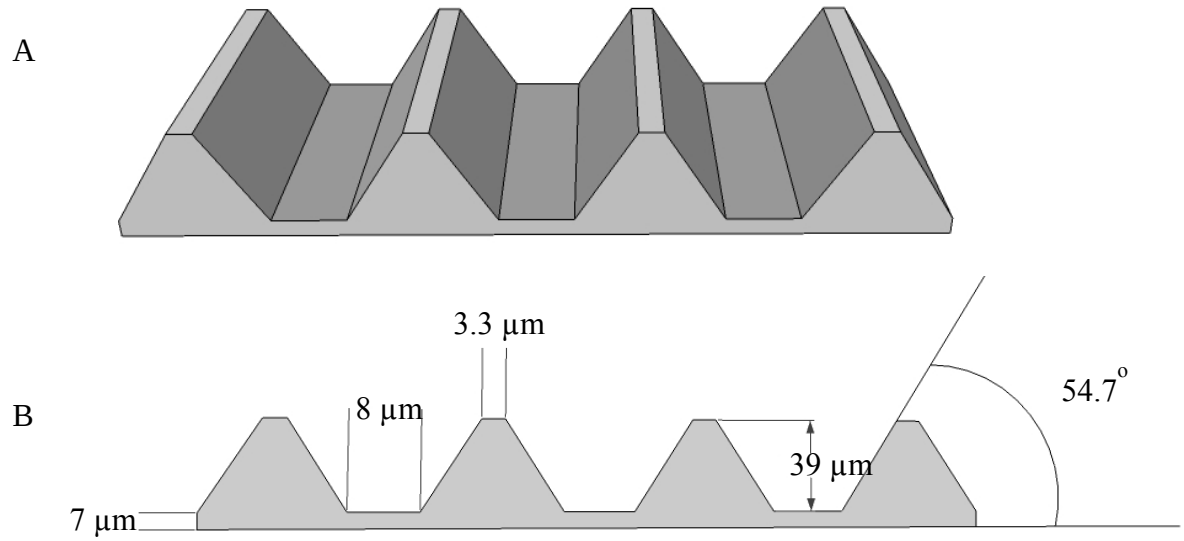

Figure 2.1: Template for patterned films. A) Schematic representation of the surface of the template, B) dimensions of the template.

2.2.4 Scaffold Preparation

2.2.4.1 Micropatterned Collagen Film

Solvent casting method was used to prepare the micropatterned collagen films to seed the cells on. Collagen solution (15 mg/mL in 0.5 M acetic acid) was prepared at 29 ^{o}C with continuous stirring until complete dissolution. 1 mL was poured onto the patterned PDMS templates and allowed to dry in air for 2 days. The dry films were removed from the template with a forceps and stored at 4 ^{o}C until use.

2.2.4.2 Unpatterned Collagen Film

Unpatterned (Smooth) Teflon sheets (2 cm x 2 cm) were used as the template to prepare unpatterned collagen films which were processed as described above.

2.2.4.3 Micropatterned Collagen:ELR Film

ELR was prepared in PBS (15 mg/mL, pH 7.4) and 1 volume of this solution was mixed with 5 volume of collagen solution (15 mg/mL in 0.5 M acetic acid) and 1 mL of this solution was poured onto the patterned PDMS templates. Air-dried films were removed and stored at 4 ^{o}C.

2.2.4.4 Multilayer Scaffold Preparation

4 layers of collagen or collagen-ELR films were prepared as follows; a film was taken and 10 µL droplets of collagen solution were placed at the 4 corners. Then the next film was put perpendicular to the first film and again 4 droplets (10 µL) were put on the corners. Similarly, two more films were placed on top each being orthogonal to the film above and below (Figure 2. 2)

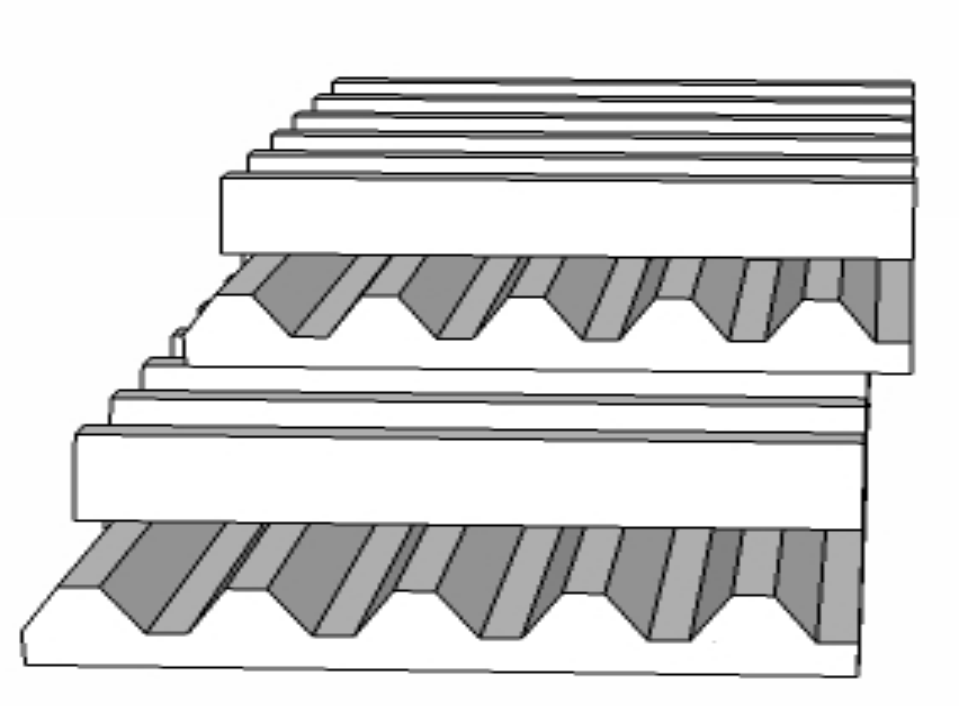

Figure 2. 2: Organization of the single layer films in the multilayer construct.

2.2.4.5 Crosslinking of the Films

Single or multilayered films were crosslinked physically by dehydrothermal treatment (DHT). The films were incubated under vacuum at 105 ^{o}C 24 h, 140 ^{o}C 24 h, or 150 ^{o}C 24 h under vacuum (vacuum oven Model 281A, Cole-Parmer, USA).

2.2.5 Characterization of the Scaffolds

2.2.5.1 Measurements of Film Thickness

Thickness of the films was measured by a micrometer (Erste Qualitat, Germany) to a sensitivity of 0.1 μm and an average of 3 measurements from each of 6 samples was made.

2.2.5.2 In situ Degradation Test

To study the degradation profile, films were incubated in 10mM PBS pH 7.4 at 37 ^{o}C with continuous shaking and the films were examined at 1, 2, 3 and 4 weeks. After removal from PBS, the films were rinsed with distilled water 3 times, lyophilized and the extent of weight loss determined gravimetrically.

2.2.5.3 Enzymatic Degradation with Collagenase

The stability of the films against enzymatic degredation was determined using Collagenase Type II as described previously (Vrana et al., 2007b). Briefly pre-weighed films were incubated in Collagenase

Type II solution (0.1 mg/ mL in PBS pH 7.4) for 2 h, rinsed with distilled water for 3 times, lyophilized, and weighed.

2.2.5.4 Determination of Water Contact Angle

The contact angle of the films with water was determined using a commercial contact angle goniometer KSV Cam 200 (KSV Instruments Ltd., Finland). Distilled water (5 µL) was placed at 5 different locations on the films and cross-sectional image of the water droplet- on the surface was obtained by the digital camera system of the goniometer. Contact angles were calculated by processing these images with the software of the system.

2.2.5.5 Swelling Test

Patterned collagen and collagen:ELR films were tested for water retention. The dry weights of four samples from each film were determined and these films were incubated in PBS (10 mM, pH 7.4) for 2, 4, 6, and 24 h. At each time point the samples were taken and after removing the excess water with a tissue paper the wet weight was determined. Water Content was calculated according to the following equation:

$$WC\ (\%) = \frac{W_w - W_d}{W_w} \text{ x}100 \quad (1)$$

where
WC (%): Water Content (%, w/w)
W_d: Dry weight of the samples (mg)
W_w: Wet weight of the samples (mg)

2.2.5.6 Stereomicroscopy

The films were examined under a stereomicroscope (Nikon, SMZ1500, USA).

2.2.5.7 SEM

The films (1 cm^2) were placed on carbon tapes on SEM stubs and coated with Au-Pd under vacuum and observed under a scanning electron microscope (JEOL, JSM- 6400, USA) equipped with NORAN System 6 X-Ray Microanalysis System and with SEM (QUANTA, 400F Field Emission SEM, USA and SEC, Mini-SEM, South Korea) at 5-20 kV.

2.2.6 In vitro Studies

2.2.6.1 Human Keratocyte Cell Culture

Human Keratocytes from Passage 5 to 13 were used. Cells were stored frozen in their medium and 15% DMSO, at -196 ^oC. Following thawing, cells were incubated in a CO_2 incubator (Sanyo MCO-17 AIC, Sanyo Electric Co. Ltd., Japan) at 37 ^oC and 5% CO_2. The medium contained Dulbecco's Modified Eagle Medium/Ham's Nutrient Mixture F12 (DMEM/F12; 1:1), New born calf serum (10%), amphotericin B (1 µg/mL), penicillin (100 UI/mL), and streptomycin (100 µg/mL). Cells were cultured in tissue culture polystyrene (TCPS) flask in a CO_2 incubator at 37 ^oC, and 5% CO_2. Growth medium was changed every two days.

2.2.6.2 Sterilization of the Scaffolds

Scaffolds crosslinked at 150 ^{o}C for 24 h were already sterile due to high temperature. Additional sterilization was done by exposing both sides of the films to UV in a laminar flow hood for 15 min at room temperature.

2.2.6.3 Cell Seeding onto the Scaffolds

Scaffolds were incubated in a sterile PBS pH 7.4 for 24 h to swell and then allowed to air-dry for 2-3 h to allow cell penetration. Cells were detached from the surface of TCPS flask by Trypsin-EDTA (1:1 0.25% EDTA: PBS pH 7.4) at 37 ^{o}C for 5 min, and the effect of trypsin was blocked with addition of keratocyte growth medium and centrifuged at 3000 g for 5 min. After suspending the cells in the medium cell number was determined via Nucleocounter (ChemoMetec, Denmark). Cells were seeded onto the films at a density of $1x10^4$ cells/cm^2. For multilayer scaffolds $1x10^4$ cells/cm^2 were seeded onto top and on each of the other layers using an insulin syringe. The cell seeded scaffolds were incubated in a CO_2 incubator at 37 ^{o}C for 2 h to allow the cells attach to the scaffolds. Finally, 2 mL of keratocyte growth medium was put into each well which was changed every two days.

2.2.6.4 Alamar Blue Cell Viability Assay

Proliferation of the cells on the scaffolds was determined by Alamar Blue assay. Scaffolds were washed twice with DMEM HAM's F12 1:1 colorless and incubated in 10% Alamar Blue solution in DMEM HAM's F12 1:1 growth medium supplemented by amphotericin B (1µg/mL), penicillin (100 UI/mL), and streptomycin (100 µg/mL) for 1h at 37 ^{o}C and 5% CO_2. After incubation the reduced solution (200 µL) was transferred into 96-well plates, the scaffolds were washed twice with colorless medium, keratocyte growth medium was added and then incubated. Intensity of the reduced dyes was determined at 570 and 595 nm by using an Elisa plate reader (Molecular Devices, USA). The absorbances were converted to percent reduction values and then to cell numbers using a calibration curve.

Percent reduction was calculated according to the following equation:

$$\text{Reduction (\%)} = \frac{((\varepsilon_{ox})_{\lambda_2} \text{ x } A_{\lambda_1}) - ((\varepsilon_{ox})_{\lambda 1} \text{ x } A_{\lambda 2})}{((\varepsilon_{red})_{\lambda 1} \text{ x } A'_{\lambda 2}) - ((\varepsilon_{red})_{\lambda 2} \text{ x } A'_{\lambda 1})} \text{ x100} \qquad (2)$$

where,

λ_1= 570 nm $\quad$ λ_2 = 595 nm
$(\varepsilon_{ox})\lambda_2$ = 117.216 $\quad$ $(\varepsilon_{red})\lambda_1$ = 155.677
$(\varepsilon_{ox})\lambda_1$ = 80.586 $\quad$ $(\varepsilon_{red})\lambda_2$ = 14.652

$A_{\lambda 1}$= Absorbance of test well,
$A_{\lambda 2}$= Absorbance of test well,
$A'_{\lambda 1}$= Absorbance of negative control well (blank)
$A'_{\lambda 2}$= Absorbance of negative control well.

2.2.6.5 Microscopical Studies

2.2.6.5.1 Fluorescence Microscopy

2.2.6.5.1.1 DAPI-Phalloidin Staining

Single layer films were stained as they are while multilayer films were separated into single layer films and then stained. Briefly, growth medium of the cells was discarded, fixed directly with 4% (w/v) paraformaldehyde at room temperature for 30 min and cell membrane was permeabilized with Triton X-100 (1% v/v in PBS pH 7.4) at room temperature for 5 min. After washing, samples were incubated in BSA (1% w/v in PBS) at 37 ^{o}C for 30 min. FITC-labeled Phalloidin, (1:200 w/v, prepared in 0.1% BSA, w/v in PBS), was added directly on the samples and they were stored at 37 ^{o}C for 1 h. After washing three times with 0.1% BSA, the samples were incubated with DAPI (1:3000 w/v, in 0.1% BSA) for 5 min at 37 ^{o}C. Samples were washed with PBS three times and stored in PBS solution until examination using a Zeiss Axio Imager M2 (Germany) fluorescent microscope.

2.2.6.5.2 SEM

Scaffolds were fixed with 2.5% v/v glutaraldehyde in cacodylate buffer pH 7.4 for 2 h at room temperature. After washing several times with cacodylate buffer and distilled water, samples were lyophilized and examined with SEM as described before.

Samples used for fluorescent microscopy analysis were washed with distilled water and observed with SEM after lyophilization.

2.2.6.5.3 Confocal Laser Scanning Microscopy

2.2.6.5.3.1 Immunostaining

2.2.6.5.3.1.1 Collagen Type I Staining

Extracellular matrix (ECM) secretion of keratocytes was examined by indirect immunostaining of collagen type I. Films were fixed in 2.5% formaldehyde for 15 min. After washing with PBS, cell membranes were permeabilized by incubation in with 1% Triton X-100 for 5 min. After washing, samples were incubated in 1% BSA w/v solution in PBS for 1 h at 37 ^{o}C. Anti-human collagen type I antibody produced in mouse (1:200 dilution) in 0.1% w/v BSA in PBS was added onto the samples which were incubated for 1 h at 37 ^{o}C. Samples were washed several times with 0.1% BSA and incubated with AlexaFluor 488 conjugate anti-mouse antibody produced in goat (1:100 dilution) in 0.1% BSA for another 1 h at 37 ^{o}C. After washing with PBS, samples were stored in PBS at 4 ^{o}C. Samples were examined by confocal laser scanning microscope (Zeiss LSM 9100, Germany) between 500-550 nm with 488 nm Argon laser for collagen deposition and between 555-650 nm with 532 nm Argon laser for autofluorescence.

2.2.6.5.3.1.2 Keratan Sulfate Staining

Keratocyte specific proteoglycan keratan sulfate was determined by indirect keratan sulfate staining. Films were fixed in 2.5% formaldehyde for 15 min and then with 1% Triton X-100 for 5 min. Samples were washed with PBS several times and incubated with 1% w/v BSA in PBS for 1 h at 37 ^{o}C. After washing, anti-human keratan sulfate antibody produced in mouse (1:100 dilution) in 0.1% w/v in PBS was added on the samples and incubated for 1 h at 37 ^{o}C. Samples were washed and incubated with AlexaFluor 488 labeled anti-mouse antibody produced in goat (1:100 dilution) in 0.1% BSA (w/v in PBS) at 37 ^{o}C for 1 h. After washing with PBS samples were stored in PBS at 4 ^{o}C and observed with a Zeiss

LSM 9100 (Germany) confocal laser scanning microscope between 500-550 nm with 488 nm Argon laser for keratan sulfate deposition and between 555-650 nm with 532 nm Argon laser for autofluorescence.

2.2.6.6 Transparency of the Films

In order to determine the light transmittance of the films they were scanned in the range 250 nm-700 nm by using Shimadzu 2100-S UV-Vis Spectrophotometer (Japan). Films were attached on the wall of the quartz cuvette and their transparency was measured on days 0, 1, 20, and 30.

2.2.6.7 Mechanical Tests

Patterned collagen and collagen:ELR films were tested with an Instron 3366 tensile tester (Instron Corp., USA) at 0.2 mm/min strain rate until failure. At least six specimens were used for each time point (days 1 and 30). The dimensions for the test samples were 2 cm x 2 cm x 45 μm and the tests were done by Prof. Ahmed El-Sheikh (University of Liverpool, UK) with his specially designed test rig.

2.2.7 Statistical Analysis

Statistical analysis was carried out by using the Student's t-test; p values smaller or equal to 0.05 were considered statistically significant.

CHAPTER 3

RESULTS AND DISCUSSION

3.1 Collagen Type I Isolation and Purification

Collagen Type I was isolated from tails of Sprague-Dawley as previously described in Section 2.2.1. SDS-PAGE analysis was performed (Section 2.2.1.1) in order to demonstrate the purity of the isolated collagen Type I. Middle lane shows the protein ladder with bands 260 kDa, 140 kDa, 100 kDa, and 70 kDa from top to bottom. First and the third lanes show the isolated and commercial collagen, respectively. Collagen type I has doublets at molecular weights of 115 and 130 kDa, and at 215 and 235 kDa (data sheet obtained from Sigma-Aldrich Co.). Isolated collagen had the same band pattern with commercial collagen type I (Figure 3.1) and absence of other bands indicates the purity of the collagen isolated from rat tail.

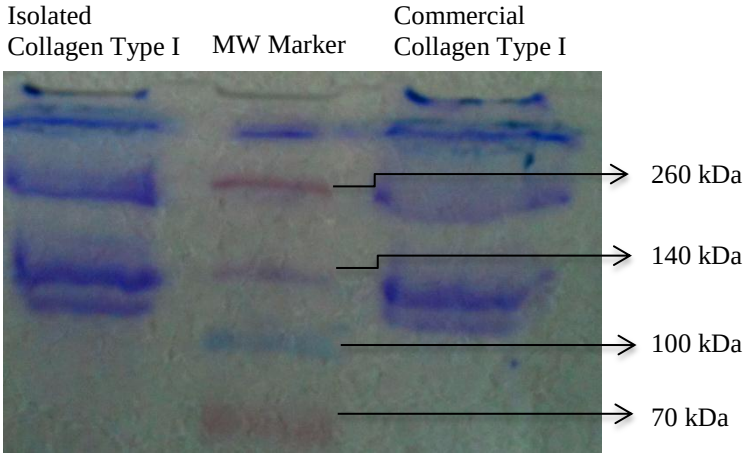

Figure 3.1: SDS-PAGE of collagen isolated from rat tail tendons.

3.2 Elastin like Recombinamers Isolation and Purification

ELRs are isolated and purified from the bacterial lysate by using their temperature responsive behavior where below their transition temperature (Tt) they are soluble in water and above this temperature they remain as precipitate. MALDI-TOF and SDS PAGE tests show the purity and the correctness of the molecular weight of the ELRs, YIGSR (Figure 3.2). The theoretical mass of the polymer is 89366 Da and both of the results demonstrate that the isolated polymer was pure and molecular weight matched the expected data well. A peak at 89455 Da of the MALDI-TOF spectrum gives the mass of the polymer that is quite close to the theoretical value and peak at 44707 is due to doubly charged species. An intense band around 89 kDa and absence of any other bands at the SDS-PAGE proves the purity of the isolated polymer.

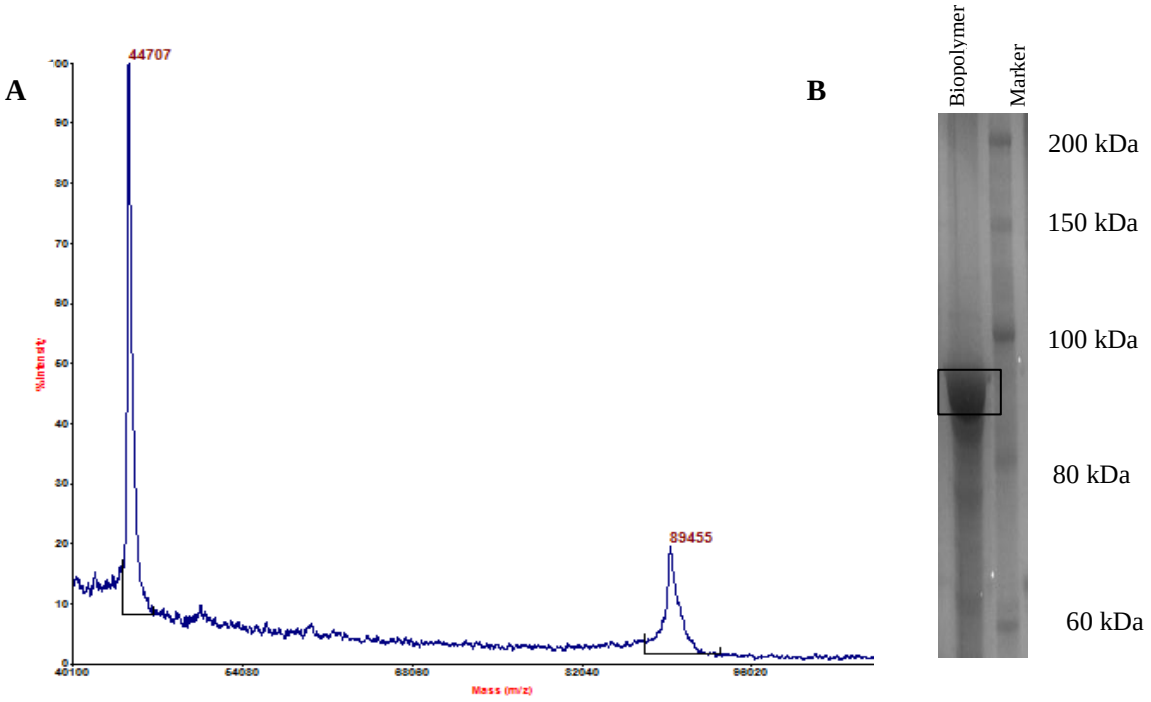

Figure 3.2: MALDI-TOF and SDS gel electrophoresis of the ELR with the bioactive sequence of YIGSR. Theoretical molecular weight is 89.366 kDa. A) MALDI-TOF analysis of the polymer, and B) the gel electrophoresis.

3.3 Scaffold Characterization

3.3.1 Characterization of the Collagen Films

Before studying in vitro performance of the scaffolds, the physical properties of them was studied which affect behavior of the cells. Thus, film thickness, properties of the patterns, optimization of the crosslinking temperature, transparency at different temperatures, contact angles, and degree of swelling of the scaffolds were determined.

The thickness of the collagen films was measured with a micrometer as 45.5 ± 2.0 μm. Surface of the films was characterized by scanning electron microscopy (SEM) and SEM micrographs of the uncrosslinked and crosslinked films showed that pattern fidelity is quite high and the patterns were not disturbed with the crosslinking (Figure 3.3).

Collagen Type I isolated from rat tail is highly soluble in water. Thus, crosslinking of the scaffolds should be done in order to stabilize the collagen films and to decrease pattern deterioration in culture conditions. The crosslinking method greatly influences the final characteristics of the scaffolds such as strength, biocompatibility, and antigenicity. Collagen can be crosslinked chemically or physically.

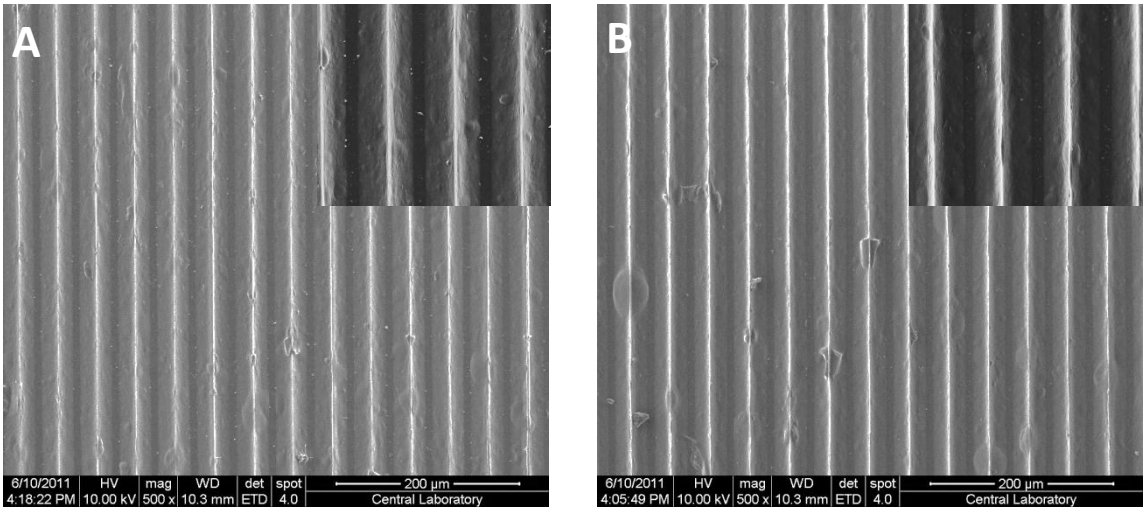

Figure 3.3: SEM micrographs of patterned collagen films. A) Uncrosslinked, B) Crosslinked at 150 ^{o}C 24 h. Magnifications (x500), insets (x2000).

Although chemical crosslinkers like glutaraldehyde and formaldehyde provide high mechanical strength, their poor biocompatibility, risk of cytotoxicity, and problem of calcification cause great concern. On the other hand, physical crosslinking methods like dehydrothermal (DHT) do not have these disadvantages and provides a highly biocompatible surface with moderate mechanical strength. However, one disadvantage with DHT treatment is the long crosslinking hours at very high temperatures which are reported to cause partial degradation of the collagen (Weadock et al., 1995). In this study, DHT treatment was used in order to crosslink the films and different temperatures were tested to find the optimal crosslinking temperature (which does not deteriorate the pattern of the films during tissue culturing). Degradation profiles in collagenase Type II and in PBS, transparency, and water contact angles after different DHT treatments were studied.

3.3.1.1 Enzymatic Degradation Profile of Films

Collagen fibrils of cornea are highly ordered and densely packed when compared to any other tissue of the body. Cornea should be transparent to perform its function and this ordered structure and avascularity of the cornea leads to its transparency. Corneal stromal keratocytes have an important role in the collagen metabolism, both in the synthesis and the degradation of the collagen fibrils. The matrix degrading enzymes and matrix metalloproteinases are produced by corneal keratocytes (Hao et al., 1999). Thus, in order to preserve transparency and other vital functions of the cornea, the organization of the scaffold should not be disrupted by the enzymes until the cells secrete their own ECM and compensates for the degraded collagen. In this study, in order to test the stability of the films against proteolytic enzymes, films were incubated with collagenase type II (Figure 3.4) Uncrosslinked films (UXL) and films crosslinked at 105 ^{o}C for 24 h (DHT105) degraded totally after 2 h incubation with the collagenase, but films crosslinked at 140 ^{o}C (DHT140) and 150 ^{o}C (DHT150) for 24 h resisted to degradation to some extent. When compared with DHT140 films (28% remained), the DHT150 films were very stable (88% remained). As a control, PBS (pH 7.4) was used as the degradation medium and the films retained their forms in PBS during 2 h incubation except UXL films where only a very small portion (21%) of the films was remained (Figure 3.4). Thus, experiments in the degradation medium showed that in situ degradation of the films at this 2 h interval was negligible.

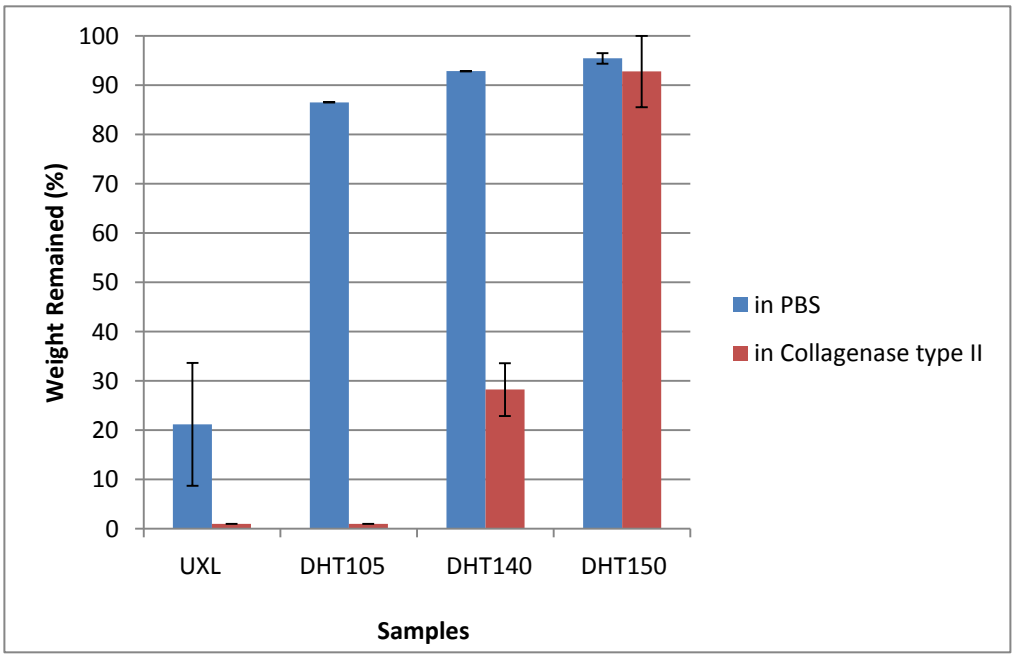

Figure 3.4: Degradation profile of the crosslinked patterned collagen films in PBS, pH 7.4 and in collagenase type II solution (0.1 mg/mL in PBS pH 7.4) at 37 ^{o}C, after 2 h.

The effect of the proteolytic enzymes on the patterns was also studied with scanning electron microscopy (SEM) (Figure 3.5). UXL and DHT105 films were totally degraded. The patterns of the DHT140 films were highly deteriorated and the collagen fragments were seen all over the surface (Figure 3.5 A). On the other hand, the patterns on the DHT150 films were conserved and no collagen fragments were observed. Although the pattern features were not as sharp as the untreated ones (Figure 3.3), the main form and the dimensions of the patterns were not affected after such a vigorous hydrolytic treatment (Figure 3.5 B).

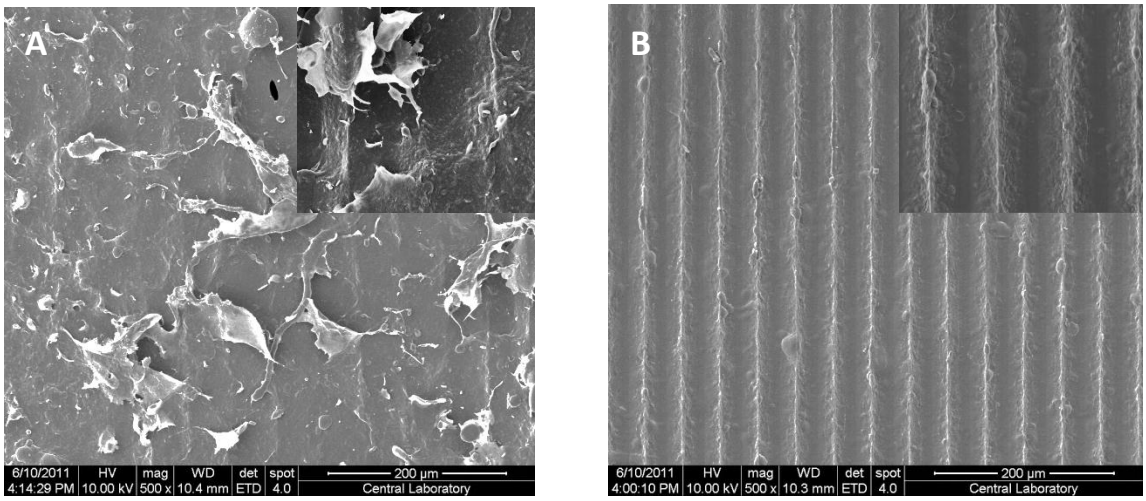

Figure 3.5: SEM micrographs of the films after 2h treatment with collagenase. A) DHT140 film, and B) DHT150 film. Inset magnifications are x2000.

The surface of the films was also studied after incubation in a milder environment, PBS pH 7.4 for 2 h (Figure 3.6). Although UXL film did not degrade totally in PBS after 2 h, there were missing the patterns and fragments (Figure 3.6 A). The patterns of the DHT105 films were also deteriorated in PBS, however, they still retained their pattern form and dimensions (Figure 3.6 B). DHT140 and DHT150 films were not affected by PBS (Figure 3.6 C, D).

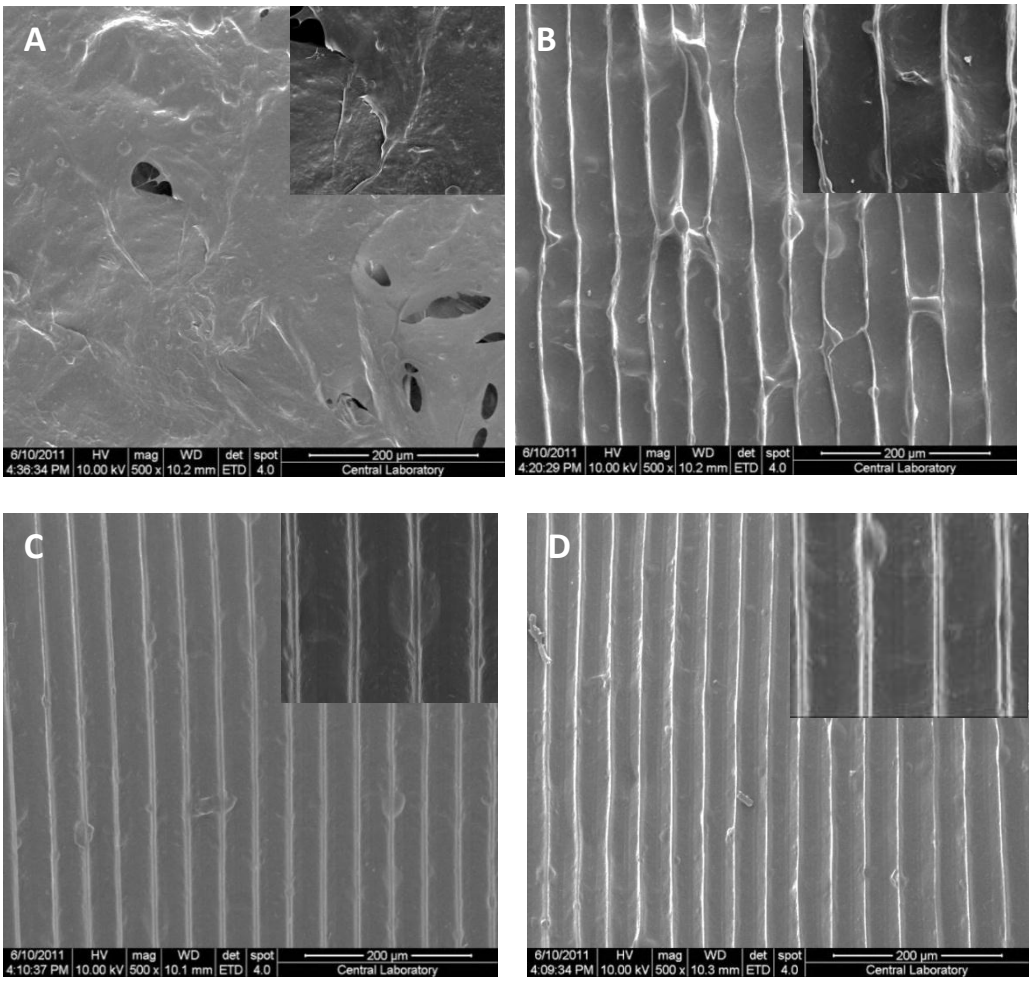

Figure 3.6: SEM micrographs of patterned films after 2h incubation in PBS (pH 7.4). A) UXL Film, B) DHT105 film, C) DHT140 film, and D) DHT150 film. Magnifications (x500), insets (x2000).

3.3.1.2 In situ Degradation Test

The degradation profile of the scaffolds in culture conditions and in the integration with the host tissue is an important property since the rate of the degradation affects the performance of the scaffold that it should carry out until it is fully compensated by the ECM products. If degradation occurs too fast, the structural support may not be provided due to insufficient number of cells and protein matrix ingrowth from the neighboring healthy tissue. On the other hand, if the degradation proceeds too slowly, the scaffold can be recognized as a foreign material and inflammation is started which results in scaffold rejection (Williams et al., 1999). In order to mimic the culture conditions, crosslinked and uncrosslinked films were incubated in PBS (pH 7.4, 37 ^{o}C) for 4 weeks (Figure 3.7). While UXL films degraded completely in one week, crosslinked ones resisted degradation for much longer. Among the crosslinked films, DHT150 was the most stable in the weight of which there was a small decrease. In the first week it lost 15% of its weight and at the end of fourth week the loss was 18%. DHT140 was also stable but not as much as DHT150; it lost 28% of its weight in the first week and this loss was 38% at the end of 4th week. DHT105 was the least stable among the crosslinked films where after 4 weeks only 15% of the film was remained.

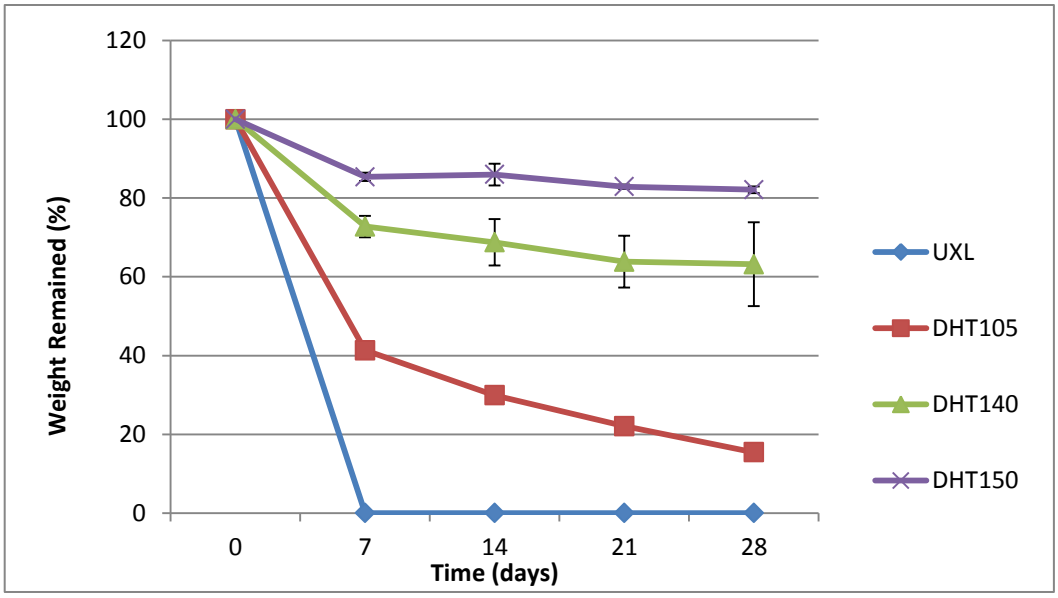

Figure 3.7: In situ degradation profile of the crosslinked and uncrosslinked films incubated for 4 weeks in PBS (pH 7.4, 37 ^{o}C).

3.3.1.3 Transparency Measurements

Cornea is avascular and it is transparent which are among its most important properties. Cornea transmits more than 90% of the light in the visible spectrum (Jester, 2008) and therefore any corneal equivalent should be transparent enough to be used in place of the natural cornea. In order to study transparency, the light transmittance of the films was measured in the range 250-700 nm and all the films showed light transmittance in between 77-85% (Figure 3.8). In the visible range, UXL films had the highest light transmittance (85%) and significantly different from others ($p \leq 0.05$). The DHT105 and DHT140 films showed about 80% of transmittance, while DHT150 films showed the lowest transmittance which was still around 77%. Although the difference in light transmittance of DHT105 and DHT140 was not significant, this small decrease could be explained with an increase in crosslinking which decreased the hydration of the films. Additionally, with increasing temperature a slight yellowish color (probably a result of oxidation) was observed in the films which also be explained with incubation at high temperatures and this also may be another reason for the decrease in transmittance.

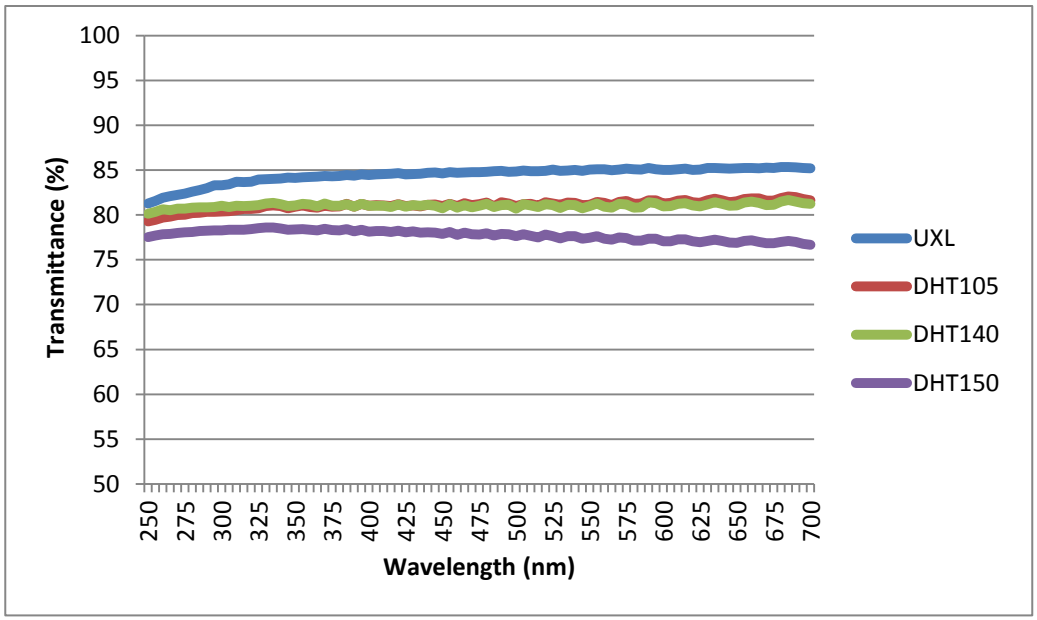

Figure 3.8: Transparency of the patterned films in the UV-Vis range.

3.3.1.4 Contact Angle

The determination of contact angles is essential to estimate the hydrophilicity of a sample which is needed to understand the behavior of the material in the biological environment and thus its biocompatibility. According to one classification materials that have a contact angle above 80^{o} hydrophobic, those with contact angles in the range 48-62^{o} are moderately wettable, and those with a contact angle less than 35^{o} are wettable or hydrophilic (Menzies & Jones, 2010). Highly hydrophobic or highly hydrophilic surfaces were shown to be unsuitable for protein adhesion. Experiments conducted with human fibroblasts showed that while the surfaces with moderately wettable properties supported cell growth, and proliferation of the cells was linear, on the highly hydrophobic or hydrophilic surfaces the cell number decreased by time. This probably is because for cell attachment and proliferation, protein adherence on the surface plays an important role and this in turn is affected significantly by the wettability of the surface (Faucheux et al., 2004).

Water contact angle measurements of the various samples are shown in Table 3.1. The results show that all films were highly hydrophobic (Figure 3.9) and the contact angles of the patterned films were not significantly different from each other (in the range of 113-120 degrees) ($p \leq 0.05$). However, contact angles do not reveal all the aspects of the wetting of these samples. Although the initial contact angles were as high as tabulated, the films started to absorb the droplets and a linear decrease in the contact angle by time was observed. The contact angles measured during 5 minutes (by 1 minute intervals) and they were decreased dramatically and significantly after 5 min (Table 3.1). One reason for this initial high contact angle may be the placement of the drops on the patterns (Figure 3.10). In order to test this hypothesis, contact angles of the UXL and DHT150 unpatterned films were measured. It is clearly seen that in the absence of patterns hydrophobicity decreased and this difference between the initial contact angles of the patterned and unpatterned samples were significant ($p \leq 0.05$). This observation was supported by the literature where nano and micro patterned surfaces are employed to obtain super-hydrophobic surfaces ((Feng et al., 2002)).

Table 3.1: Contact angle measurements of collagen films at different temperatures

Sample	Contact angle (deg)	Contact angle (deg) after 5 min.
UXL Patterned	114.82 ± 7.99	102.34 ± 9.28
UXL Unpatterned	98.09 ± 0.84	88.33 ± 4.92
DHT105	113.52 ± 2.74	103.02 ± 7.44
DHT140	119.16 ± 4.09	106.33 ± 6.72
DHT150	117.13 ± 1.19	106.80 ± 4.53
DHT150 Unpatterned	95.61 ± 2.48	82.57 ± 1.22

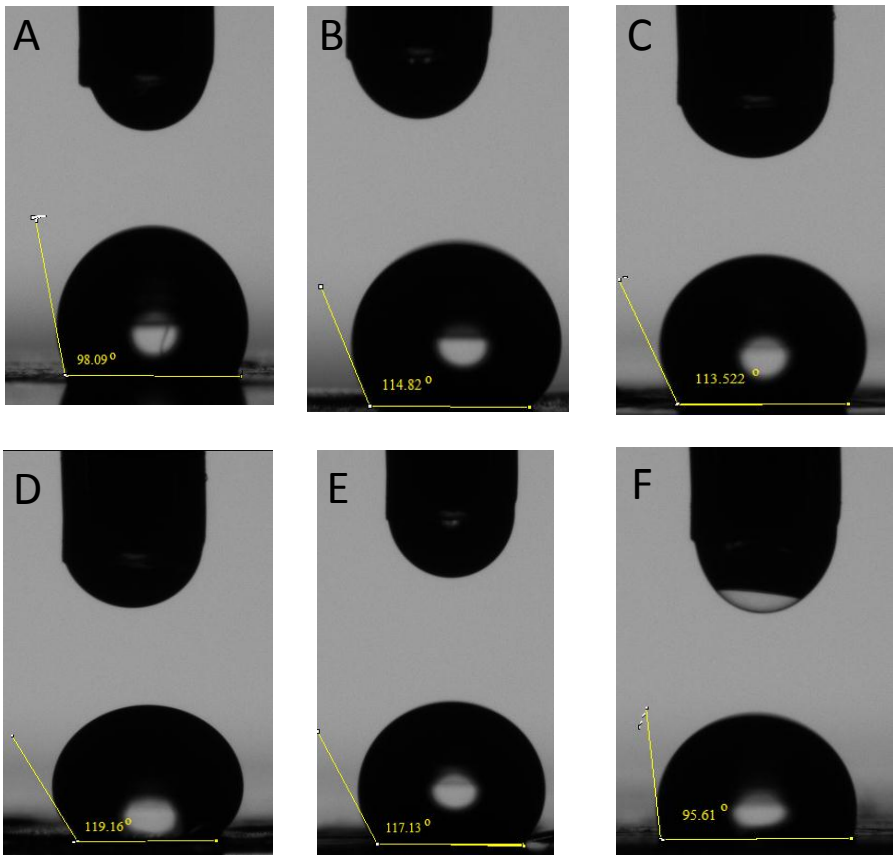

Figure 3.9: Water contact angles of collagen films. A) UXL unpatterned, B) UXL patterned, C) DHT105, D) DHT140, E) DHT150, and F) DHT150 unpatterned.

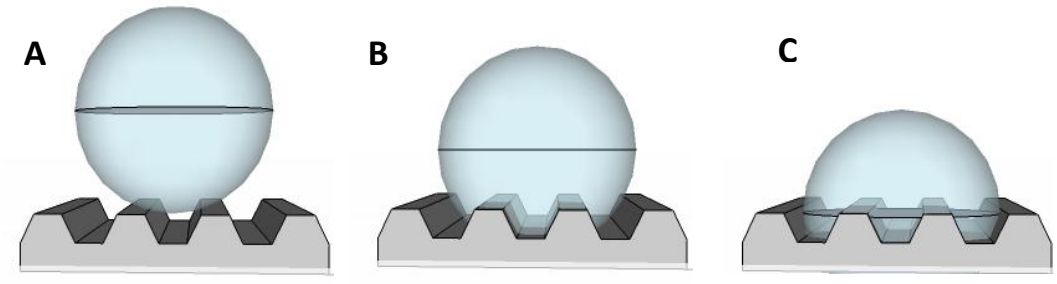

Figure 3.10: Scheme of the water droplet on the patterned surface. A) Immediate, B) after 5 min, and C) after total filling of the patterns.

Ber et al. (2005) used the same method to study the wettability of the surfaces of unpatterned collagen films. Their study showed that the contact angle of the DHT films was 74.53 ± 0.70 where for UXL films it was 72.08 ± 0.57. Their result is highly different from the result presented in this study and the reason may be the concentration of the collagen where they used 1 % collagen and it was 1.5 % in this study. In another study Taraballi et al. (2012) prepared 1% collagen films from collagen type I isolated from equine tendon and found the contact angle of the UXL films as 110^{o}. These results show that, water contact angle is affected by the surface topography, material source, and concentration of the samples used.

In this study degradation in enzyme solution and DHT treatments have shown that DHT150 films maintain their surface features and integrity and therefore the best. In the rest of the study 150 ^{o}C and 24 h DHT treatment was used as the crosslinking conditions.

3.3.2 Characterization of Collagen:ELR Films

Dry film thickness was measured as 60.0 ± 1.9 μm for Collagen:ELR (Col:ELR) films and this did not change after crosslinking. The thickness of these films was expected to be the similar to that of the collagen films (45.5 ±2.0 μm) because the same volume and concentration was used but they were significantly different ($p \leq 0.05$). It is most probably because the ELR chains are mixed with the collagen molecules preventing their packing, because the ELRs are shorter and more hydrophilic. Surface characterization with SEM showed that the fidelity of the patterns was not disturbed in the presence of ELRs (Figure 3.11).

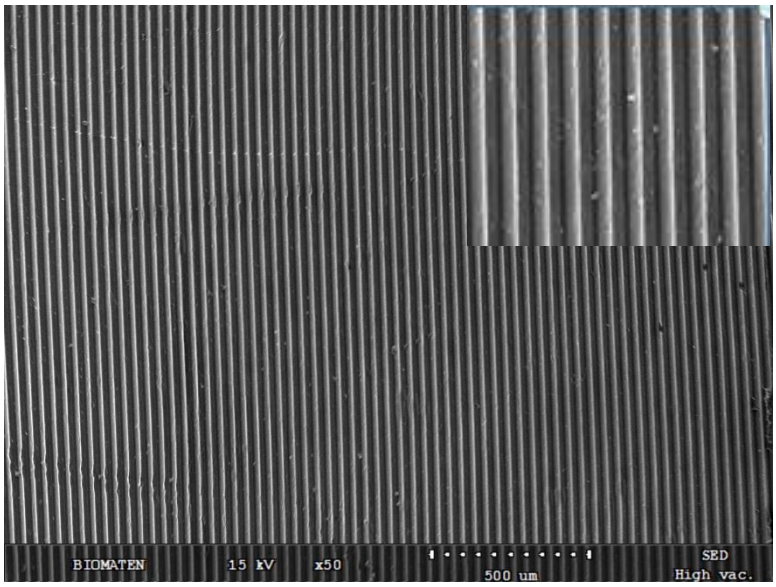

Figure 3.11: SEM micrograph of uncrosslinked Col:ELR films. Magnifications (x50), insets (x150).

3.3.2.1 Collagenase Stability of the Col:ELR films

Enzymatic degradation of Col:ELR films was studied (Figure 3.12). According to the results, 85.48% of the weight remained after 2 h where it was quite similar for collagen films (88.12%) and the difference was not significant ($p \leq 0.05$) which shows that the presence of ELR in the structure did not affect susceptibility to enzymatic attack. UXL Col and Col:ELR films, on the other hand, were degraded totally after 2h enzyme treatment.

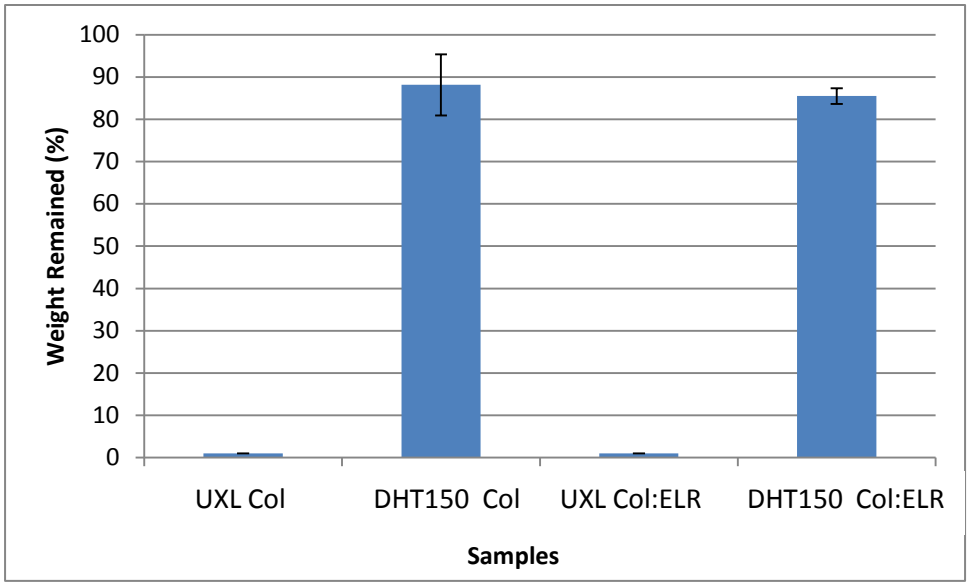

Figure 3.12: Degradation profile of patterned Col and Col:ELR films in collagenase type II solution (0.1 mg/mL in PBS, pH 7.4) at 37 ^{o}C, after 2 h.

3.3.2.2 In situ Degradation Test

The stability of the Col:ELR films in the culturing conditions was tested by incubation of the films in PBS (37 ^{o}C , pH 7.4) for 4 weeks. The results for crosslinked samples presented in Figure 3.13 show first a distinct decrease of about 20% which was followed by a steady decrease for 3 weeks. On the whole 82% of the DHT150 Col films remained after 4 weeks while 67% of DHT150 Col:ELR films remained. Although the DHT150 Col:ELR films seems to have a higher degradation rate than DHT150 Col films, the remaining weight (%) after 4 weeks was still higher than other DHT films (Section 3.3.1.2). The reason why the DHT150 Col:ELR films had higher degradation rate may be the less effective crosslinking of Col:ELR films because ELR was homogenously mixed with the collagen molecules and the interaction between the collagen molecules was disturbed which must have prevented further crosslinking. Also the shorter ELR chains may have gradually dissolved in water leaving behind only collagen. Meanwhile, the UXL forms of both films degraded totally in the first week.

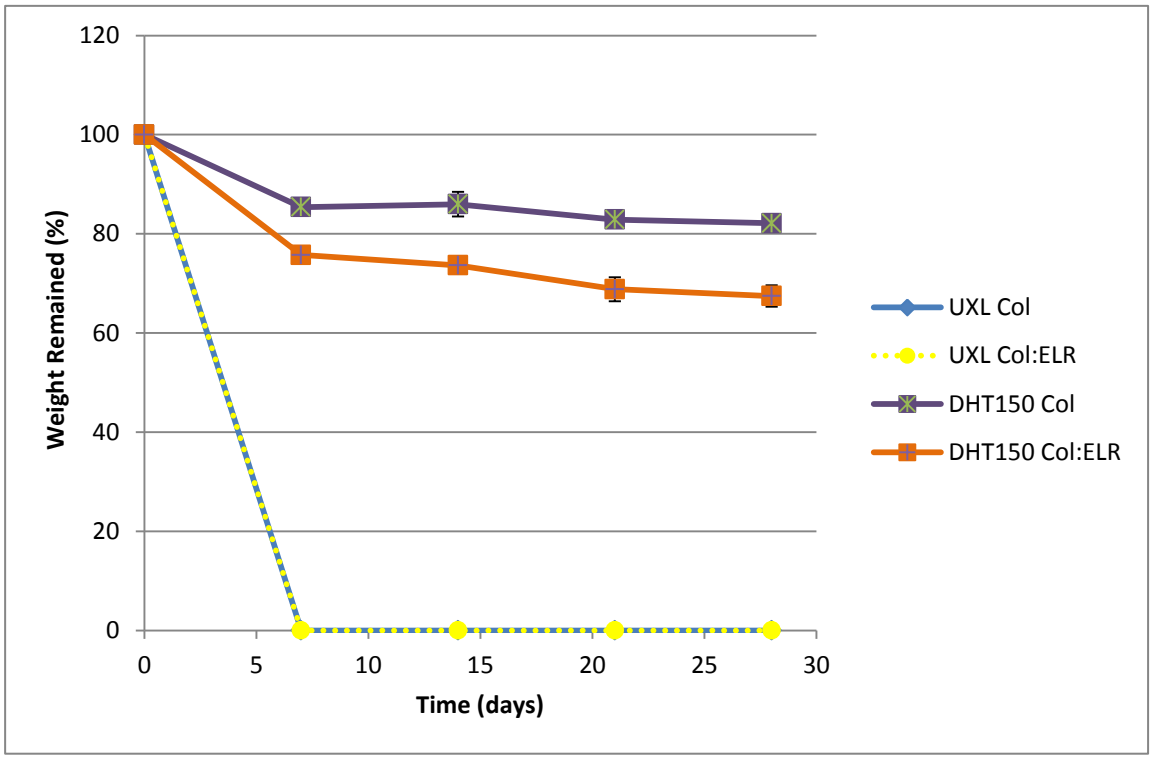

Figure 3.13: In situ degradation profile of the patterned films incubated for 4 weeks in PBS (pH 7.4, 37 ^{o}C).

3.3.2.3 Transparency Measurements

The light transmittance of the Col:ELR films was measured in the UV-Vis range 250 nm- 700 nm and the spectrum is presented along with those of UXL Col and DHT150 Col films (Figure 3.14**)**. The results show that incorporation of ELR into the structure increased the light transmittance in comparison to Col film. Light transmittance at 700 nm for DHT150 Col:ELR films has 83 % while it was 77 % for DHT150 Col films and 85 % for UXL Col films. When compared to other DHT films (Section 3.3.1.3), ELR enhanced the transmission of light especially in the visible range.

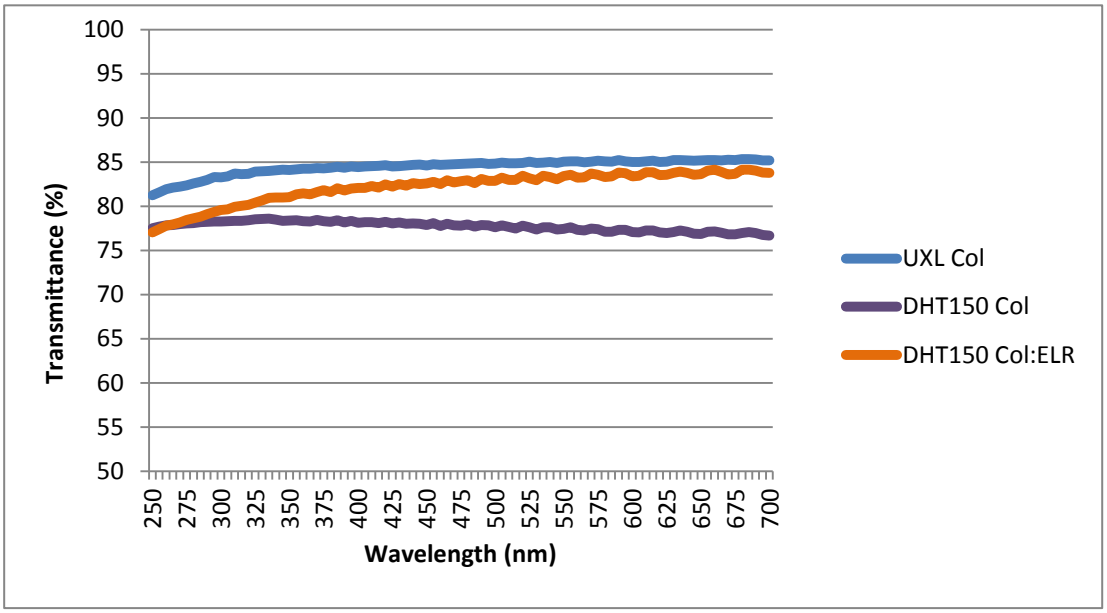

Figure 3.14: Transparency of the patterned Col and Col:ELR films in the UV-Vis range

In order to have a visual proof of the transparency of the films, stereomicrographs of the films in hydrated state were taken (Figure 3.15). As can be seen in the micrographs, DHT150 Col:ELR films are more transparent than others because the letters appear sharper.

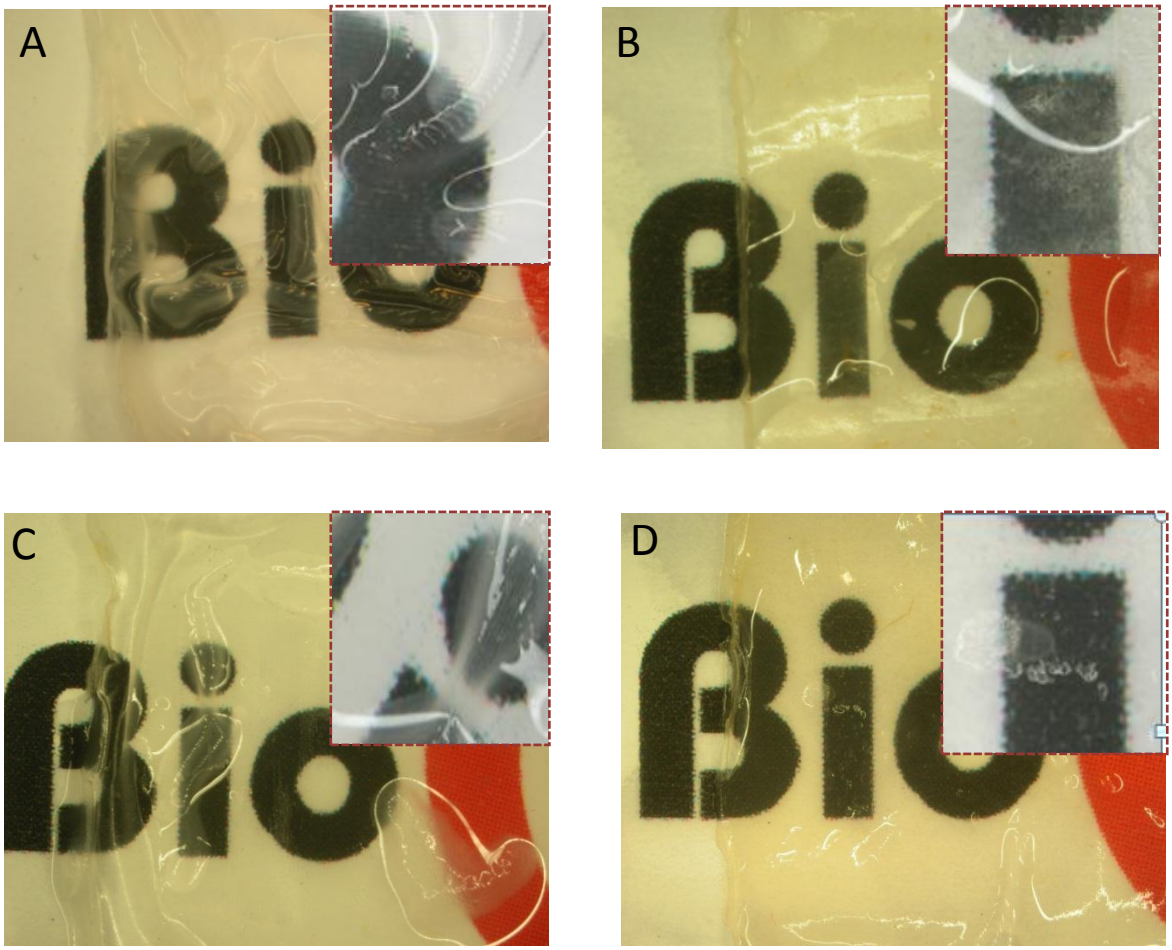

Figure 3.15: Transparency of the single layer films is shown by stereomicrographs. A) UXL Col, B) DHT150 Col, C) UXL Col:ELR, D) DHT150 Col:ELR. Magnifications (x3), insets (x8).

3.3.2.4 Contact Angle

Water contact angle measurements of Col:ELR films are presented in Table 3.2 and Figure 3.16 together with the results of UXL Col and DHT150 Col films for comparison. Incorporation of ELR into the film structure appears to have no significant effect on the hydrophilicity of the surface in comparison to other collagen samples ($p<0.05$). The contact angles of the surfaces were decreased significantly after 5 min of initial measurement (Table 3.2) which yielded a more hydrophilic surface as was reported in Section 3.3.1.4.

Table 3.2: Contact angle measurements of patterned Col:ELR films at different temperatures

Sample	Contact angle (deg)	Contact angle (deg) after 5 min.
UXL Col	114.82 ± 7.99	102.34 ± 9.28
DHT150 Col	117.13 ± 1.19	106.80 ± 4.53
UXL Col:ELR	117.34 ± 0.92	101.31 ± 7.91
DHT150 Col:ELR	117.26 ± 4.45	106.46 ± 4.95

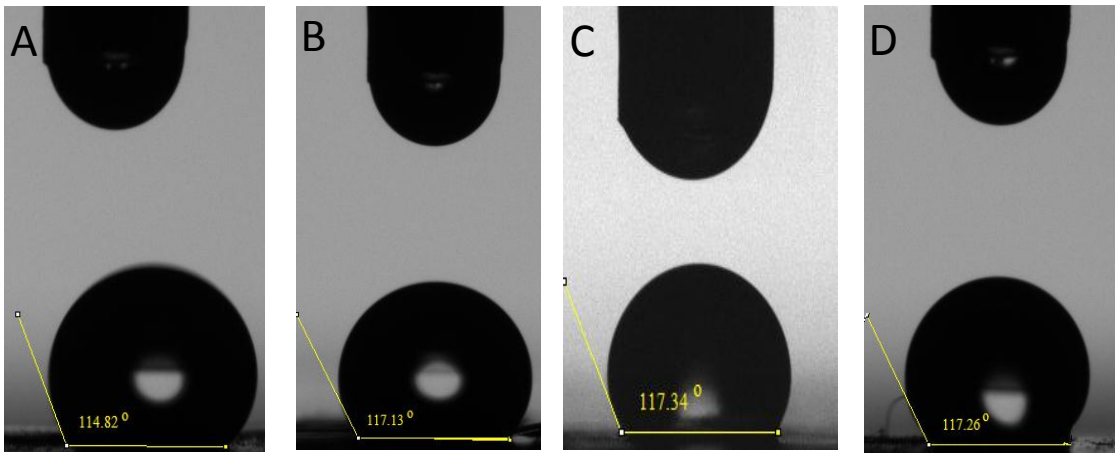

Figure 3.16: Water contact angles. A) UXL Col, B) DHT150 Col, C) UXL Col:ELR, and D) DHT150 Col:ELR.

3.3.2.5 Swelling Test

Degree of equilibrium swelling and the time taken for this are important parameters for the corneal scaffolds. The weights of the DHT150 Col and DHT150 Col:ELR films increased rapidly in the first 2 h of incubation and they reached equilibrium after 4 h and further incubation until 24 h did not lead to a measurable change in the weights of the films. Table 3.3 shows the water contents (%) and the thicknesses of the films after 4 h incubation.

Table 3.3 Water Content, WC (%), and the thickness of the DHT150 films after 4 h incubation.

Sample	WC (%)	Thickness (μm)
DHT150 Col	64.59 ± 0.86	73 ± 6
DHT150 Col:ELR	65.73 ± 2.99	70 ± 3
Native Cornea	78.0 ± 3.0	500

The table show that there is no significant difference in the degrees of swelling of the DHT150 Col and DHT150 Col:ELR films. The water content (%) of the samples was comparable with the native human cornea (78.0 ± 3.0%) (Y. Liu et al., 2013). Thicknesses of the films were not significantly different from each other at the end of the test. Thus, the presence of ELR in the film did not affect the swelling ratio or thickness of the films even though a somewhat higher swelling was expected with the ELR carrying film.

3.3.3 Characterization of Multilayer Scaffolds

Stroma of the natural cornea has lamellae which are parallel to the surface of the cornea and at right angles to adjacent lamellae like in plywood (Section 1.1.1.2). This and the resultant alignment of the cells are very important for the mechanical and optical properties of the cornea (Meek, 2009). Thus, in order to mimic the natural structure of the corneal stroma, multilayer 3D scaffolds were constructed by stacking four single layers of UXL Col or Col:ELR films (Figure 3.17). In order to stabilize the films in this form collagen solution was placed at the four corners of the first film and the second film was placed on top with its patterns orthogonal to those of the first film. Two more films were placed on top of each other in a similar fashion.
Natural corneal stroma is around 400 μm thick while the multilayer structure constructed in this study was about 200 μm in dry state and about 300 μm in wet state. Only four layers were used for ease of construction and in vitro studies.

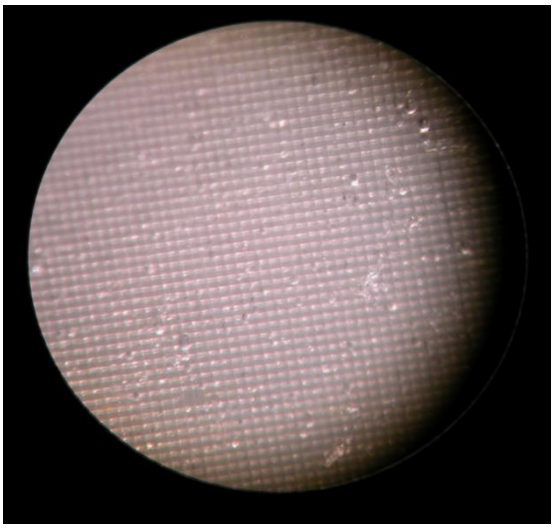

Figure 3.17: Stereomicrograph of multilayer scaffold with 4 layers of UXL Col film. Magnification: x45.

Transparency of the stacked scaffold was assessed by stereomicroscopy and when compared with the single layers films it was observed that the transparency was better in the single films. Yellowish color was seen in crosslinked samples which decrease transparency in comparison to uncrosslinked scaffolds (Figure 3.18). DHT150 Col:ELR films yielded better transparency then DHT150 Col films because the letters were sharper.

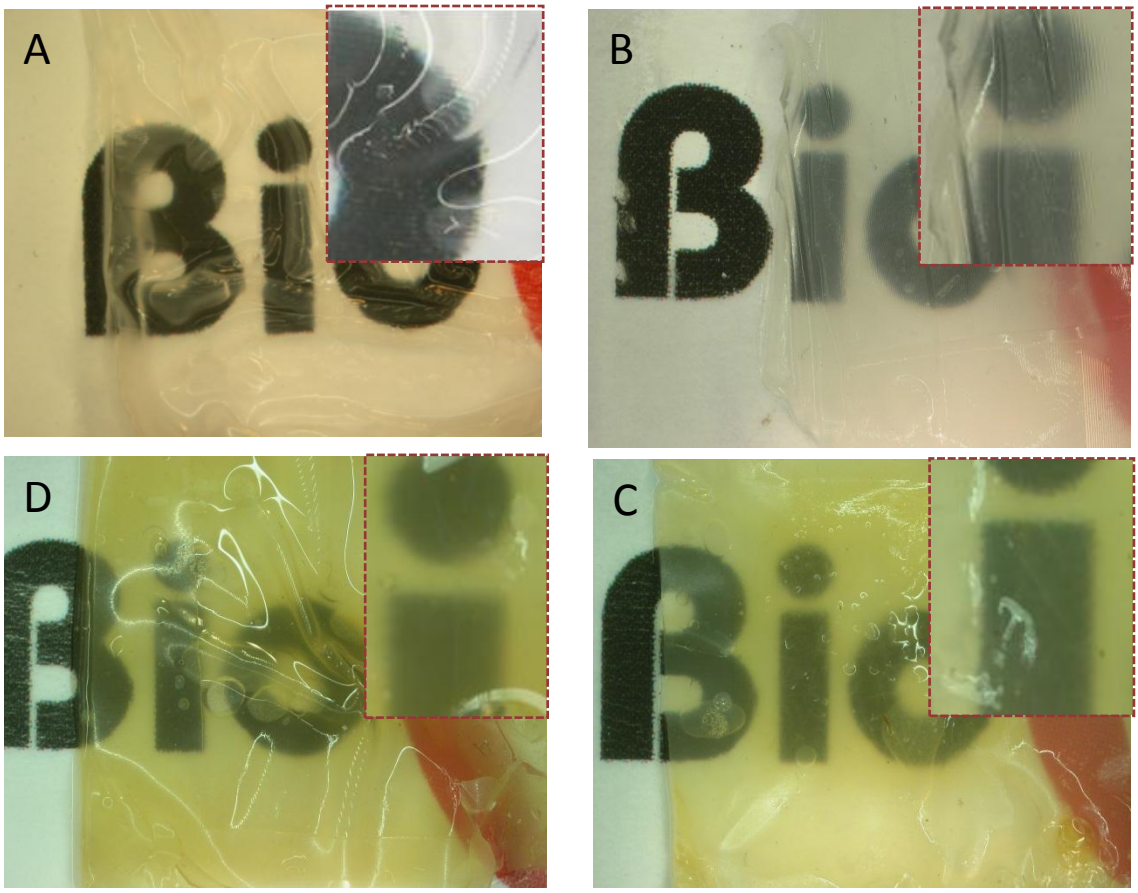

Figure 3.18: Stereomicrographs of the films for transparency. A) Single layer UXL Col film, B) multilayer UXL Col scaffold, C) multilayer DHT150 Col scaffold, and D) Multilayer Col:ELR scaffold. Magnifications (x3), insets (x8)

3.4 In vitro studies

3.4.1 Single Layer Films

3.4.1.1 Cell Proliferation

Cell proliferation was determined by using the Alamar Blue assay. The number of cells on both the films was practically same for the duration of the test (3 weeks) (Figure 3.19). None of the films appeared to be superior to the other neither in cell adhesion nor in proliferation. The main observation was that the cell growth curve was triphasic: an initial linear increase in the first week, a very slow increase in the second week and then a very rapid cell proliferation in the third week. This higher proliferation in the 3rd week can be because of the ECM secretion of the cells which creates more area for the cells to proliferate on; an indication of this was observed by the fluorescence microscope. Gil et al. (2010) used RGD- functionalized, patterned silk films which were seeded with human corneal keratocytes. The cell number showed a linear increase in the 14 day period. In another study, Lawrence et al. (2009) reported a similar result for a 6 day culture for human keratocytes seeded on silk films. However, both studies lack the 3rd week data where in this study a sharp increase was observed between Days 14 and 21.

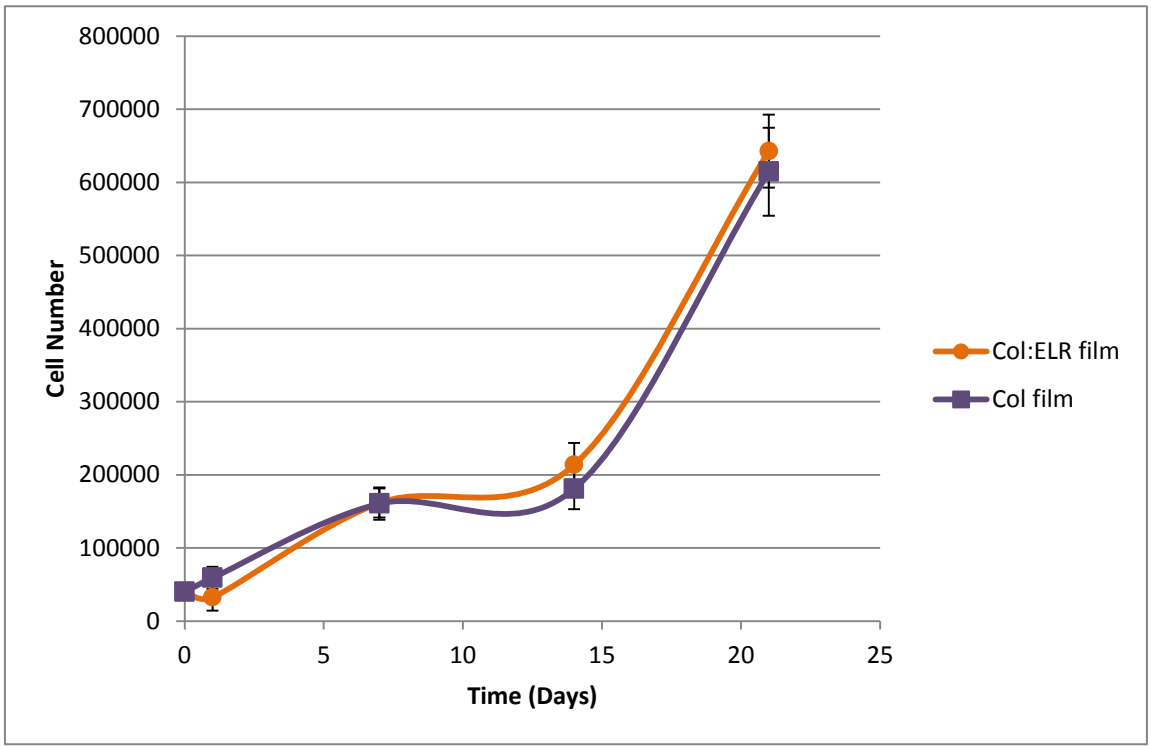

Figure 3.19: Proliferation of keratocytes on Col and Col:ELR films in 3 weeks. (Initial cell seeding density per sample: $4x10^4$)

3.4.1.2 Microscopy Studies

3.4.1.2.1 Fluorescence Microscopy

3.4.1.2.1.1 DAPI Staining

Human keratocytes seeded on the patterned collagen films were stained with DAPI and observed under fluorescence microscopy. DAPI is a blue stain that shows the nuclei of the cells and is useful to study indications of alignment and state of health (proper adhesion, apoptosis etc.). Figure 3.20 shows the SEM micrograph of the patterned films and it is presented just to show that on these films there are unpatterned regions between the patterned fields. Figure 3.21 shows the keratocytes on patterned Col films, Figure 3.22 on unpatterned Col films, and Figure 3.23 on patterned Col:ELR films. Keratocytes on the patterned films responded to the patterns of the films and aligned along the direction of the grooves on Day 1. The alignment was maintained in the 7^{th} and 21^{st} days of incubations. This can be seen that the nuclei are lined up in one direction and also they are slightly more elliptical than usual. The aspect ratios of the nuclei of the cells on patterned films were significantly higher at each time point than the nuclei of the cells on unpatterned films (Table 3.4) ($p \leq 0.05$). The ratios show that the nuclei of the cells on the unpatterned surfaces also became elliptical significantly in 3 weeks in comparison to Day 1 data ($p \leq 0.05$). However, their elliptic shape was individual rather than in unition with other cells. In the second and following weeks cells on patterned films at various depths were detected. This could be due to the ECM secretion by the cells which filled the grooves and allowed the multilayers to form. Keratocytes on unpatterned Col films proliferated well and no special alignment was observed during the three weeks of incubation (similar with those cells in the tissue culture flask) (Figure 3.22). This unaligned appearance was seen in the smooth regions between the patterned fields of the patterned films, too (Figure 3.20).

Table 3.4: Aspect ratio of the nuclei of the cells on unpatterned and patterned Col films.

Time (Days)	Unpatterned Film	Patterned Film
1	1.31 ± 0.18	1.66 ± 0.28
7	1.64 ± 0.21	2.41 ± 4.23
21	2.17 ± 4.31	3.01 ± 0.6

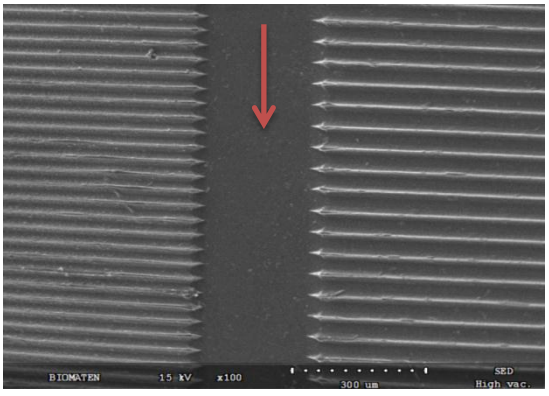

Figure 3.20: SEM micrograph of patterned collagen film. Arrow shows the unpatterned region. Magnification (x100).

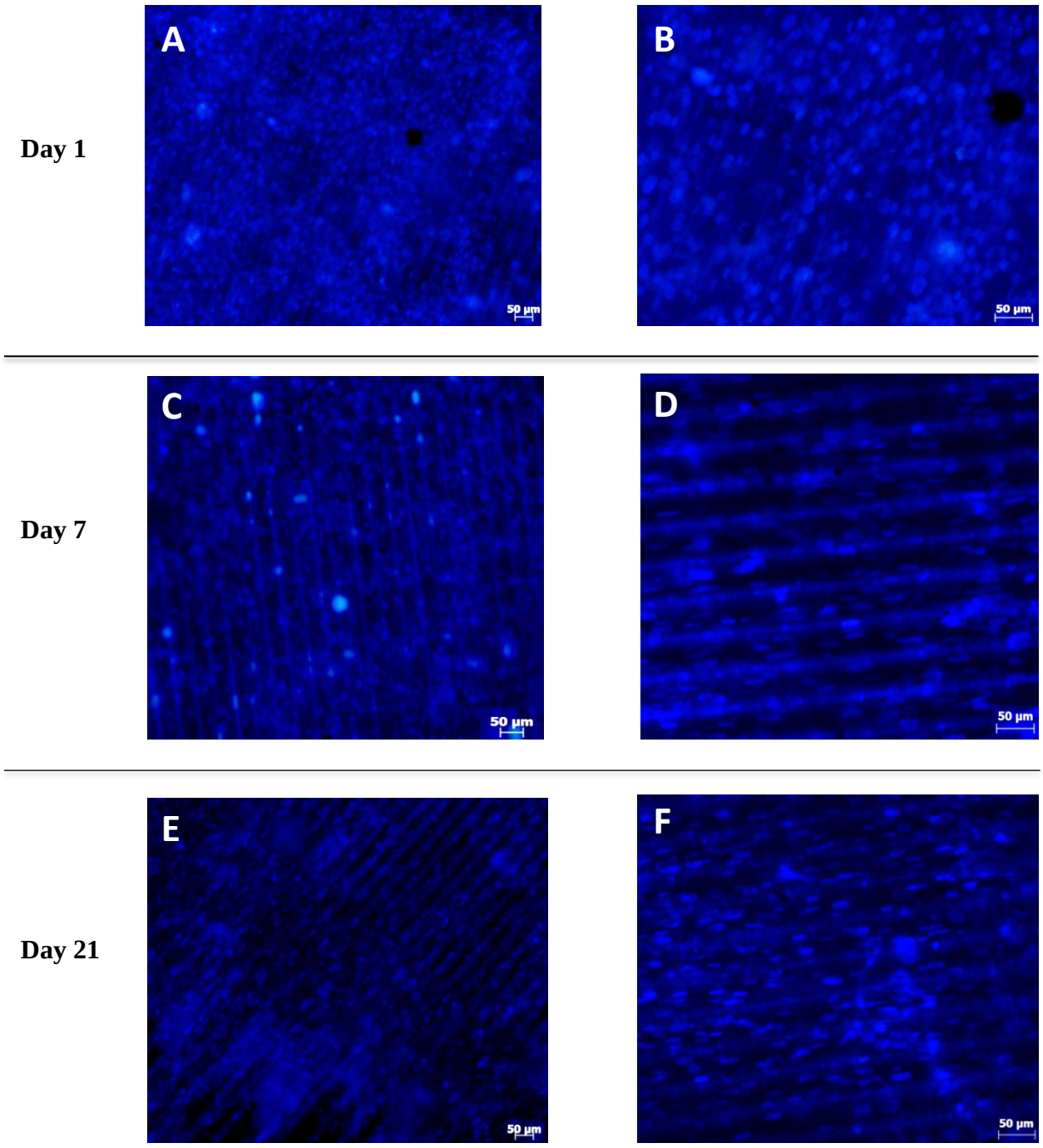

Figure 3.21: Fluorescence micrographs of DAPI stained human keratocytes on patterned Col films. Time of incubation (days): A, B) 1, C, D) 7, and E, F) 21. Scale bars: 50 µm.

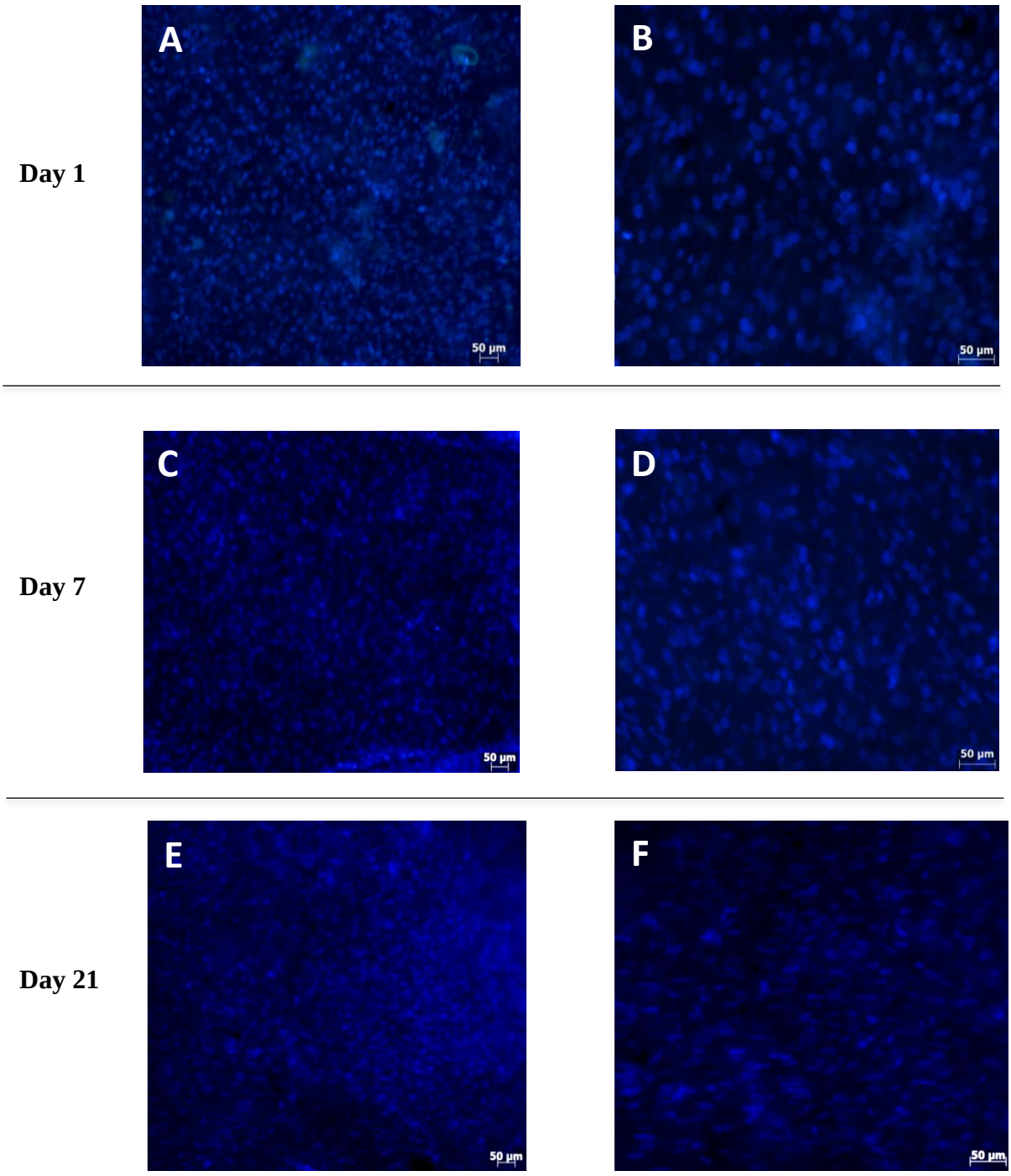

Figure 3.22: Fluorescence micrographs of DAPI stained human keratocytes on unpatterned Col films. Time of incubation (days): A, B) 1, C, D) 7, and E, F) 21. Scale bars: 50 µm.

Keratocytes on patterned Col:ELR films behaved similarly to those on patterned Col films. They were also aligned along the grooves of the films (Figure 3.23) and formed multilayers after.

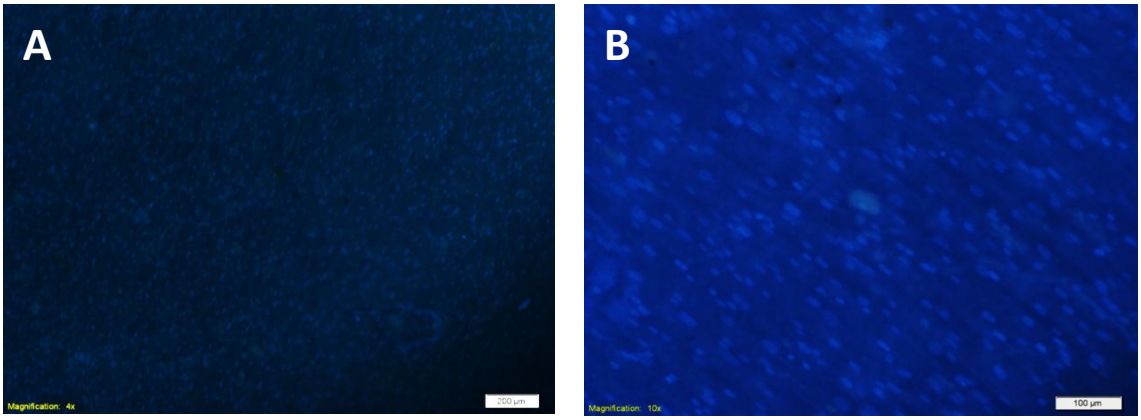

Figure 3.23: Fluorescence micrographs of DAPI stained human keratocytes on patterned Col:ELR films on Day 14. Scale bars: A) 200 µm, B) 100 µm.

3.4.1.2.1.2 Phalloidin Staining

FITC-labeled phalloidin stains the actin fibers of cells and in this study they were used to stain the human corneal keratocytes. It was observed that while the cytoskeleton of the keratocytes on unpatterned Col films randomly distributed, the cells on the patterned films aligned along the grooves (Figure 3.24). Since cytoskeleton of a cell is more flexible then the nucleus, covers a much large portion of the cell and consists of fibers that can be stained. Phalloidin staining was a more effective indication of cell alignment.

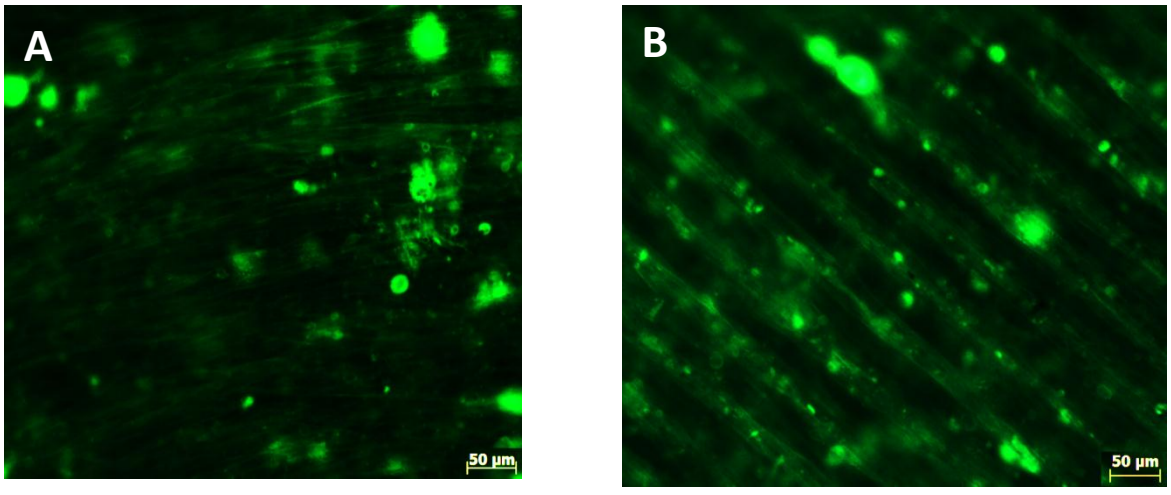

Figure 3.24: Fluorescence micrographs of human corneal keratocytes on collagen films stained with phalloidin-FITC after 14 days of incubation. A) Unpatterned Col film, B) patterned Col film. Scale bars: 50 µm.

Cells on unpatterned films also showed regions of but these regions were not continuous and constituted patches on the surface aligned in different directions (Figure 3.25 A). This was very similar to the behavior of the cells on the tissue culture flasks (Figure 3.25 D) (Guo et al., 2007). Interestingly, after reaching confluency, the second layer of cells grew almost perpendicular to the first layer of the cells. This was not observed in the patterned collagen films where the multilayer of cells continued to grow along the patterns (within the grooves) (Figure 3.24 B). This aligned behavior of the cells on the patterned films allows one to control the orientation of the cells on the multilayer constructs.

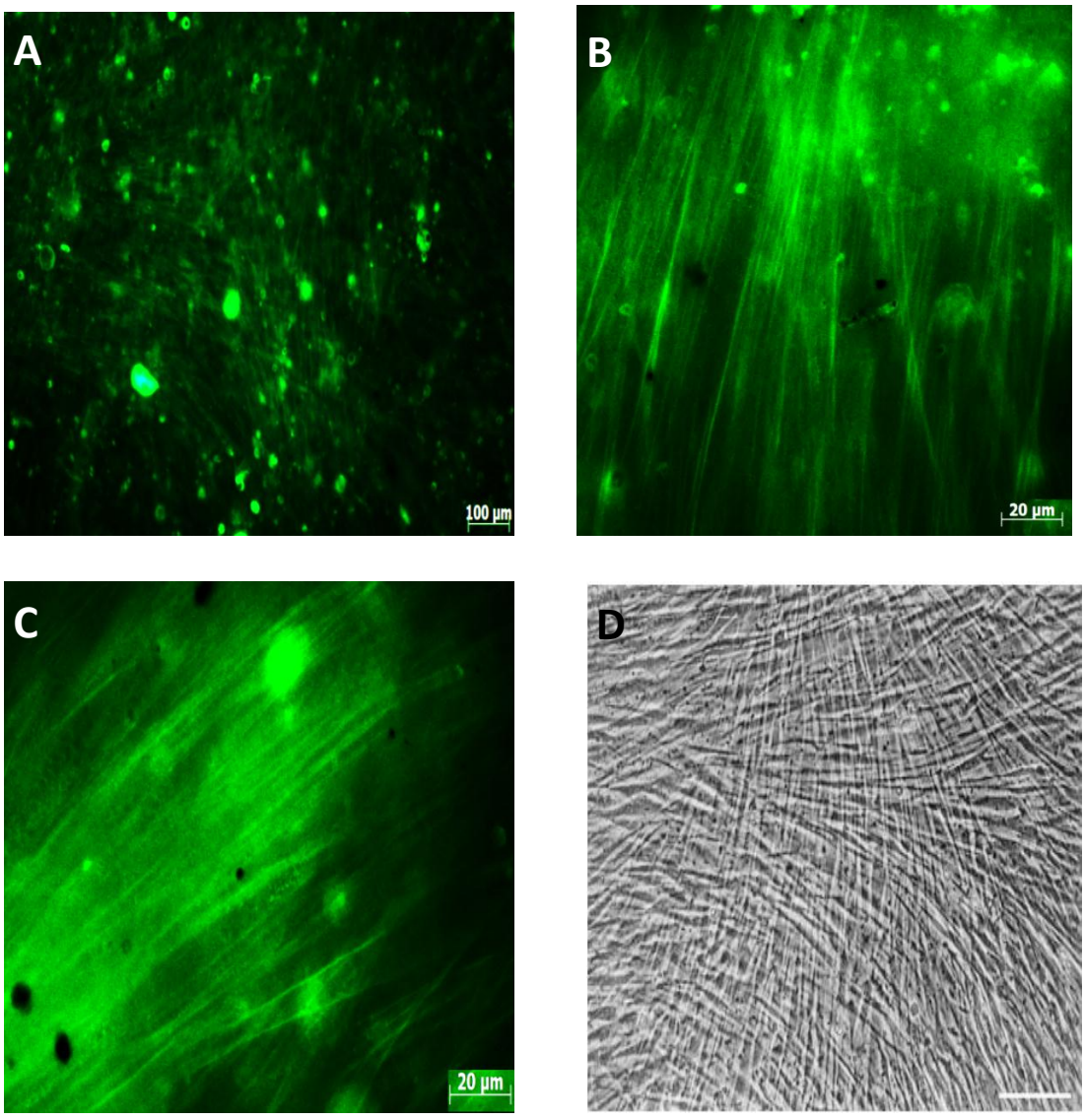

Figure 3.25: Behavior of human corneal keratocytes. A-C) Fluorescence micrograph of human corneal keratocytes on unpatterned Col films stained with phalloidin-FITC on day 14. Scale bar is: A) 100 µm, B, C) 20 µm. D) Phase contrast image of human corneal keratocytes on transwell membrane after 1 week. Scale bar: 20 µm (Adapted from Guo et al., 2007).

Keratocytes seeded on the patterned Col:ELR films exhibited the same behavior with the cells seeded on the patterned collagen films (Figure 3.26). Thus, the presence of ELR in the composition of the film did not affect the behavior and morphology of the cells on the patterned films.

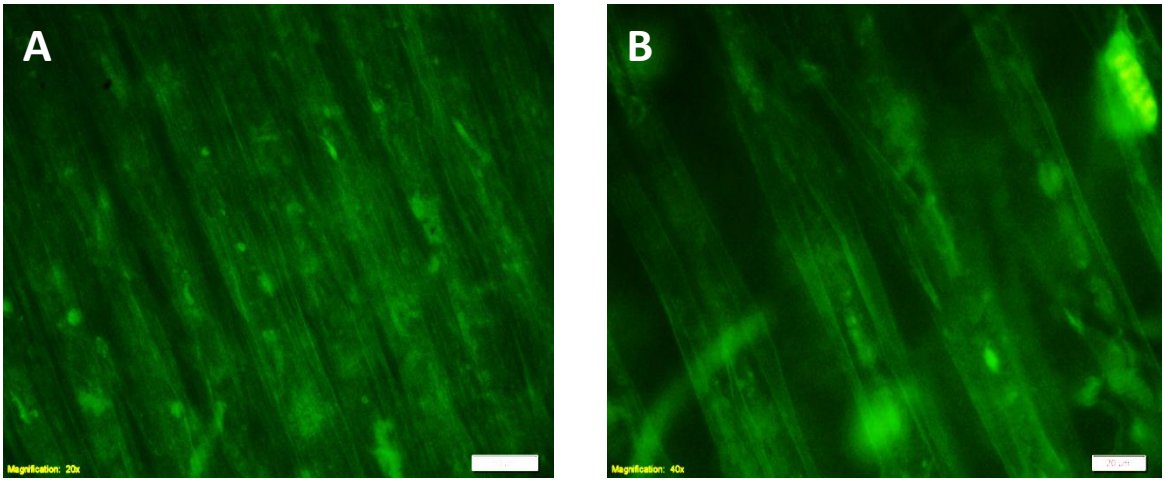

Figure 3.26: Fluorescence micrograph of human corneal keratocytes on Col:ELR films stained with phalloidin FITC after 14 days of incubation. Scale bars are: A) 50 μm, B) 20 μm.

3.4.1.2.2 SEM

Keratocytes seeded on the patterned Col films were studied with SEM which showed the orientation of the cells clearly. Cells on Day 1 attached to the surface of the unpatterned films and they were away from each other and no alignment was observed (Figure 3.27 A, B). After 7 days they populated the films and made contacts with each other (Figure 3.27 C, D) and spread on the film like they did on TCPS (Section 3.4.1.2.1.2). The keratocytes seeded on the patterned Col films, however, were aligned just after 1 day of incubation (Figure 3.28 A, B). On Day 7 the cells on the unpatterned films had not reached confluency but multilayer patches with their own orientations could be detected (arrow in Figure 3.27 C).

The arrow on Figure 3.28 A shows the unpatterned border region between the patterned fields on the Col films and it is seen that in these regions the cells were randomly distributed. This shows that for the preservation of alignment pattern continuity was very important and cells could not maintain their orientation across a relatively short unpatterned gap. Micrographs shows that the cells proliferated well and the ECM secretions filled the grooves in most of the parts and the alignment was not lost after 7 days of incubation (Figure 3.28 C, D). The advantage of using patterned substrate is that even if the cells are not confluent the independent patches they are all aligned along the grooves thus, when they eventually cover the whole surface they would all be aligned.

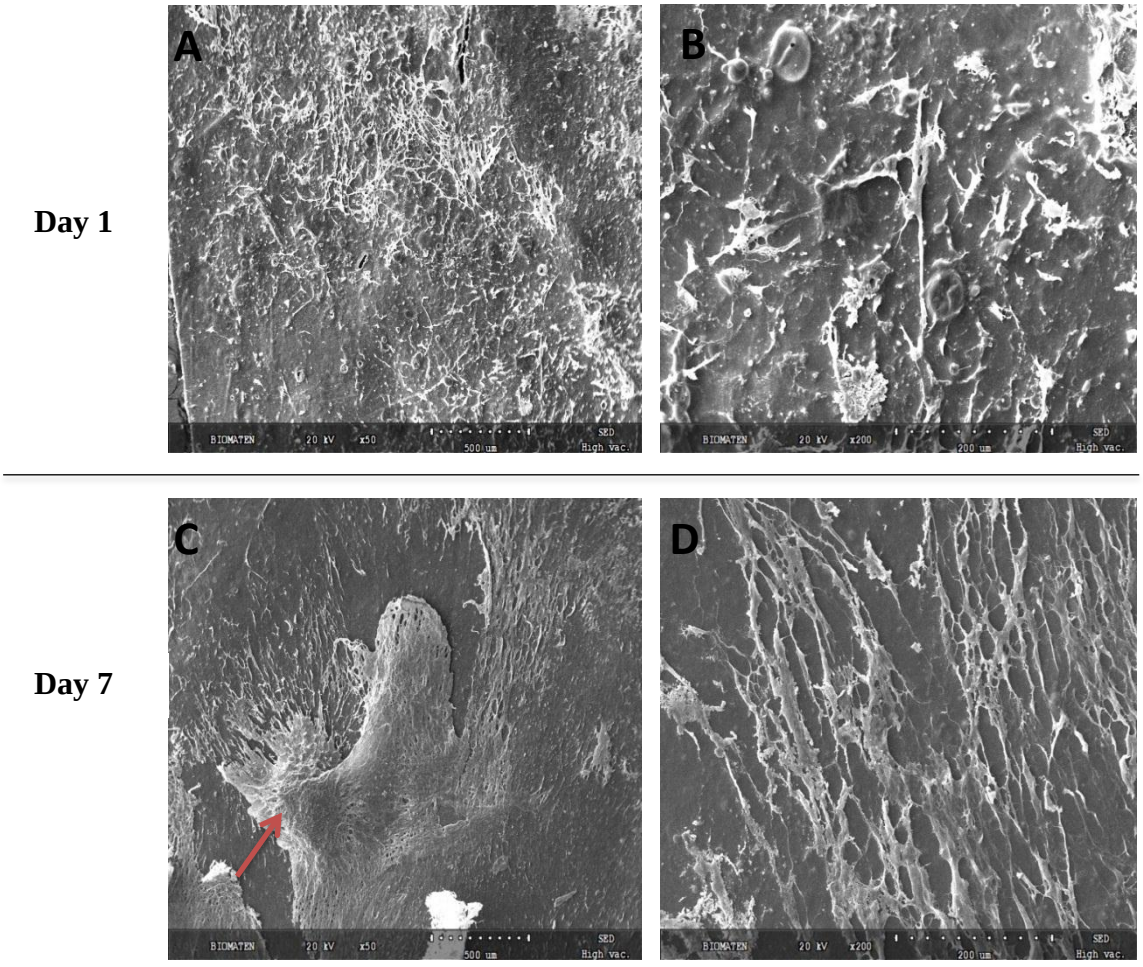

Figure 3.27: SEM micrographs of human corneal keratocytes on unpatterned Col films. Time of incubation (days): A, B) 1, and C, D) 7. Magnifications A, C) x50, and B, D) x200.

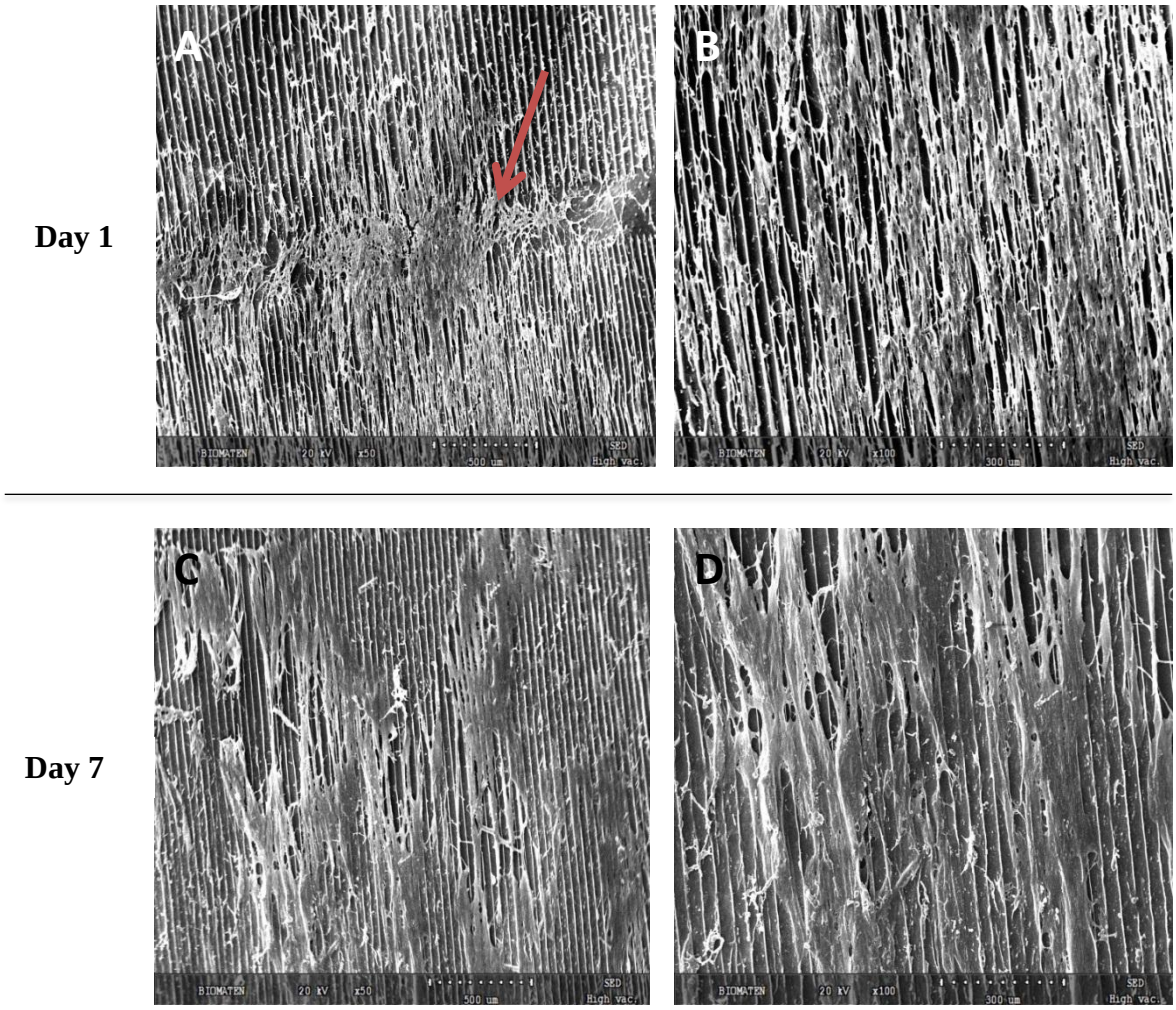

Figure 3.28: SEM micrographs of human corneal keratocytes on patterned Col films. Time of incubation (days): A, B) 1, and C, D) 7. Magnifications: A, C) x50, and B, D) x100.

3.4.1.3 Transparency Measurements

Transparency is very important for the artificial cornea constructs to fulfill function properly. Transparency of the natural cornea is provided by ECM and keratocytes. ECM contributes to the transparency with its proteoglycans and the organization of the collagen fibrils and keratocytes keep the cornea transparent by the continuous synthesis of proteoglycans and crystalline proteins (Maurice, 1957; Ruberti et al., 2007). Thus, the transparency of the any cornea equivalent should be improved by the corneal keratocytes over time by proteoglycan and crystalline protein synthesis to match that of the native cornea. Patterned Col and Col:ELR films were tested in vitro over one month for their transparency.

In the first day, the wet Col films had 80 % transmittance in the visible range (700 nm), and the Col:ELR films had 85 % (Figure 3.29 A). In three weeks transparency of Col films increased to 87% and to 92 % after 30 days. Transparency of the Col:ELR films was higher than that of the Col films at each time point; 91% on the third week and 93% on 30^{th} day (Figure 3.29 B, C). Both these values are comparable with that of the native cornea where the transmittance is 98 % at 700 nm (Meek et al., 2003; Shah et al., 2008). Thus, incorporation of ELR into the structure slightly enhanced the transparency of the collagen constructs. The transparency for both types, however, was increased by almost 5% over a 30 day period. The increase in the transparency of both films was due to an increase in the organization of the films and the alignment of the cells over the grooves. The crosslinking method, DHT, probably also contributed to the transparency of the films since studies conducted with other crosslinking agents like glutaraldehyde, 1-ethyl-3-(3-dimethylaminopropyl) carbodiimide hydrochloride (EDC), and cyanamide resulted in opaque films with much higher swelling degrees than with DHT crosslinking (Crabb & Hubel, 2008). Degradation of the films during this period may also contribute to the increase in transparency, however, the in situ degradation was not so high over the 1 month test period and besides the ECM secretion and the proliferation of the cells on the films probably compensated this loss. For comparison transmittance (%) at 700 nm of 0 (unseeded), 1, 20, and 30 days for both films were given in Figure 3.30 in order to view the improvement over time better.

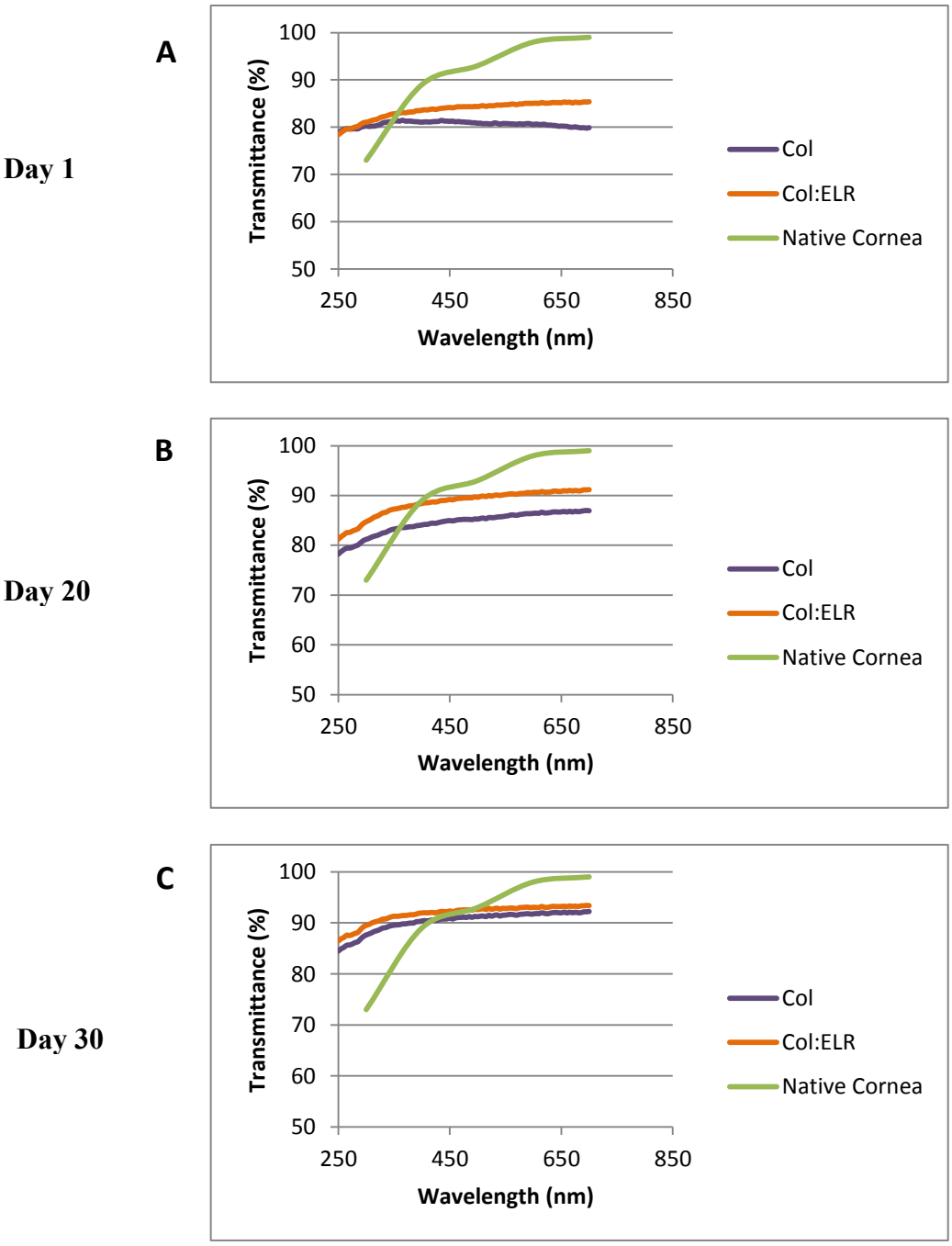

Figure 3.29: Transparency of the Col and Col:ELR films. Days A) 1, B) 20, and C) 30. Transparency of the films was compared with transparency of native cornea (Meek et al., 2003).

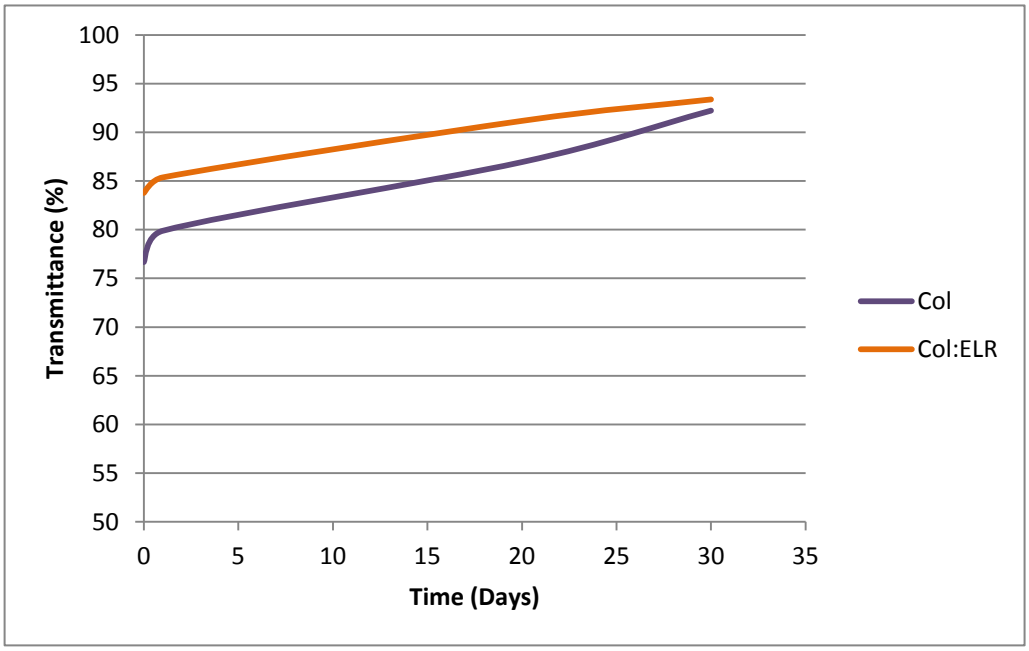

Figure 3.30: Improvement of transparency over 30 days at 700 nm. A) Col films, and B) Col:ELR films.

3.4.1.4 Mechanical Tests

Mechanical properties of the scaffold are also very important in tissue engineering because the cells sense and respond the mechanical features of the surfaces they attach to. The mechanical properties of the surface influence the orientation, proliferation, and differentiation of the cells (Last et al., 2009). Collagen is responsible for the mechanical properties of the soft tissues in the body including cornea where the organization of the collagen fibrils also plays an important role. The regular alignment of the collagen fibrils in the cornea is very important for the optical and biomechanical features of the cornea as mentioned earlier (Section 1.1.1.2). Cornea is subjected to shear forces created by the eyelids and tear films. Any artificial cornea construct should be strong enough for handling during implantation and to be able to withstand the external forces afterwards.

In order to study the mechanical features of the films Col and Col:ELR samples were tested over a 30 day period. To have an idea about the initial properties the unseeded Col and Col:ELR films were maintained in the culture medium for 1 day and then tensile tested. Figure 3.31 shows the typical stress strain curve obtained by using the unseeded Col films after 1 day incubation. It is observed that there is a long period as if the film components are orienting after which it starts straining. The film does not show any significant plastic deformation. Mechanical strength of the seeded and unseeded films was measured after 30 days of incubation (Table 3.5). Results presented in the table show that the ultimate tensile strength (UTS) of the unseeded and seeded Col:ELR films was higher than the Col films in all test categories. UTS of both films decreased significantly after 30 days of incubation whether they were seeded or not ($p \leq 0.05$). This was interesting since a preservation of the strength or even an increase was expected. The unseeded films incubated for 30 days had higher UTS than their seeded counterparts. The difference in UTS of the seeded and unseeded samples after 30 days incubation was not statistically significant for Col:ELR films but it was significant for Col films ($p \leq 0.05$). Young's modulus (E) calculations gave the similar results with the UTS (Figure 3.32). Unseeded films on Day 1 had higher E values than their 30 day incubated seeded and unseeded counterparts. Col films had slightly higher E values at all time points but the difference was not significant ($p \leq 0.05$). Vrana et al. (2007b) conducted a similar study and observed that the mechanical strength of the patterned collagen films increased in 14 days in the presence of human

corneal keratocytes while the strength of their unseeded equivalents were decreased and the main difference between that and the present study was the different crosslinking methods used. They used chemical crosslinking where it provides higher mechanical strength in comparison to physical methods. Zorlutuna et al. (2007) obtained similar results with polyester based films. On the other hand Crabb & Hubel (2008) reported very similar results to those of the present study. They did not observe any increase in UTS or a significant difference between the seeded and unseeded samples in 4 weeks. Thus, the contribution of the cells and the ECM secreted by these cells to the mechanical strength of the films was negligible when compared with the initial properties of the films. In the present study, the cells on the samples were fixed with 4 % paraformaldehyde before measuring the mechanical properties and may be as a result of this, any small difference in the strength of the films was masked.

Table 3.5: Ultimate tensile strength of the Col and Col:ELR films

Samples	Ultimate Tensile Strength (UTS) (MPa)
Col Day 1 unseeded	0.995 ± 0.400
Col Day 30 unseeded	0.164 ± 0.028
Col Day 30 seeded with keratocytes	0.069 ± 0.049
Col:ELR Day 1 unseeded	1.294 ± 0.803
Col:ELR Day 30 unseeded	0.331 ± 0.197
Col:ELR Day 30 seeded with keratocytes	0.267 ± 0.197

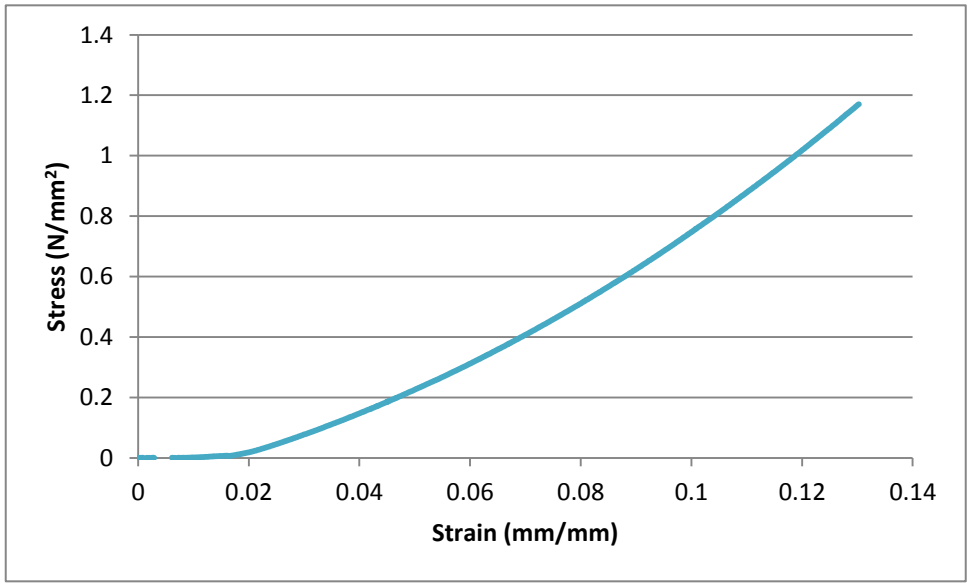

Figure 3.31: A representative stress-strain curve of unseeded Col film after 1 day in the incubation medium. The rest of these curves are presented in Appendix B.

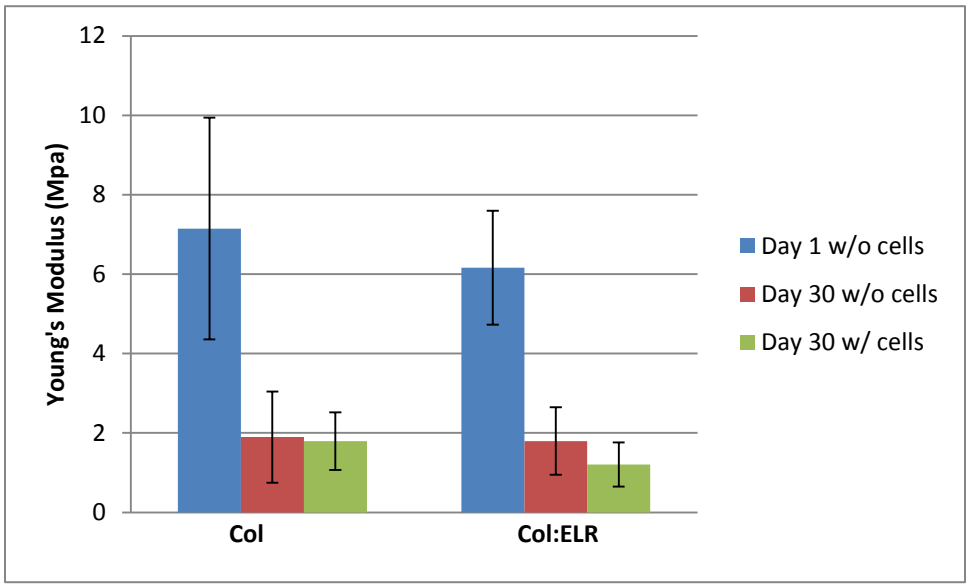

Figure 3.32: Young's modulus of the Col and Col:ELR films

3.4.2 Multilayer Scaffolds

3.4.2.1 Cell Proliferation

Cell proliferation on multilayer scaffolds was determined by Alamar Blue assay (Figure 3.33). Initial number of cells was $4x10^4$. On the first day, the cell numbers on the two scaffolds (Col and Col:ELR) were not significantly different from each other ($p \leq 0.05$) and they were lower than the seeded amount. The number of cells increased significantly in the following 3 weeks. Results show that the cells proliferated better on the Col films than on the Col:ELR films at each time point. At the end of 21 days of incubation number of cells on the Col films were twice as high as the Col:ELR films.

On the multilayer scaffolds, the number of cells increased 7 fold in 3 weeks but 17 fold on single Col films. The decrease in rate in the multilayer structures was more dramatic for Col:ELR films: The increase in 21 days was 2.5 fold for the multilayer while it was 17 fold for the single layer Col:ELR films. Interestingly, however, the slow or no cell number increase in the second week observed with the single layer films was also observed with the multilayer films. Thus, the cellular behavior apparently has not changed when the number of layers is increased. The main reason for the lower rate of proliferation may be the poor oxygen and nutrient level between the layers of the scaffold leading to poor metabolic activity.

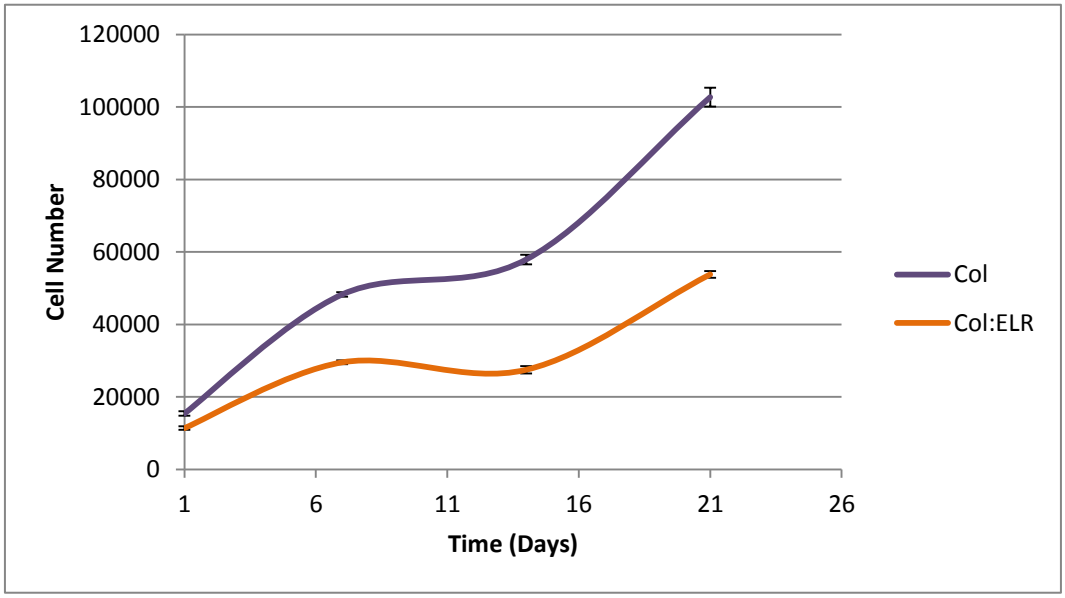

Figure 3.33: Cell proliferation on multilayer Col and Col:ELR scaffolds after 21 days of incubation.

3.4.2.2 Confocal Laser Scanning Microscopy (CLSM)

3.4.2.2.1 Immunostaining

3.4.2.2.1.1 Collagen Type I Staining

Structure of the cornea is predominantly composed of collagen type I and its turnover is done by the keratocytes. Thus, in order to study the effects of the patterns and multilayer construct on the collagen type I deposition, immunostaining was done against human collagen type I after 10 days in the culture medium (Figure 3.34). Since the collagen is autofluorescent at almost every wavelength studied, it was difficult to obtain a signal for collagen type I from multilayer construct using CLSM. Also, penetration of the dyes into the layers of the construct was not homogenous. For this reason, the layers were separated and then immunostaining was carried out. To stain the deposited collagen Alexafluor488 labeled anti-mouse Ig antibody was used and was represented in green in the figures. As a control for the autofluorescence the signals coming from green and red region were overlaid where the regions with total overlap were seen in yellow and collagen deposited regions in green. Results show that after 10 days of incubation no distinct green regions were observed as was the case with the unseeded control samples indicating that the cells did not synthesize collagen Type I during this time period. Vrana et al. (2007b) conducted a similar study by using collagen patterned films and they had observed collagen type I deposition after 7 days. In another study, Builles et al. (2007) developed a hemicornea (epithelized stroma) from Collagen-GAG-Chitosan substrates and showed that after 5 weeks of culture their construct had newly synthesized collagen type I. The main reason for the constructs used in this study not to secrete collagen type I could be due to the lack of oxygen between the layers of the construct which might have led to apoptosis of the cells. This also can explain the lower cell number observed with the multilayer constructs. Also, the relatively short incubation time may have prevented the collagen type I deposition. Cell seeding with higher density, culturing for longer periods and using bioreactors for proper oxygen transport can enhance collagen type I deposition and proliferation of the cells.

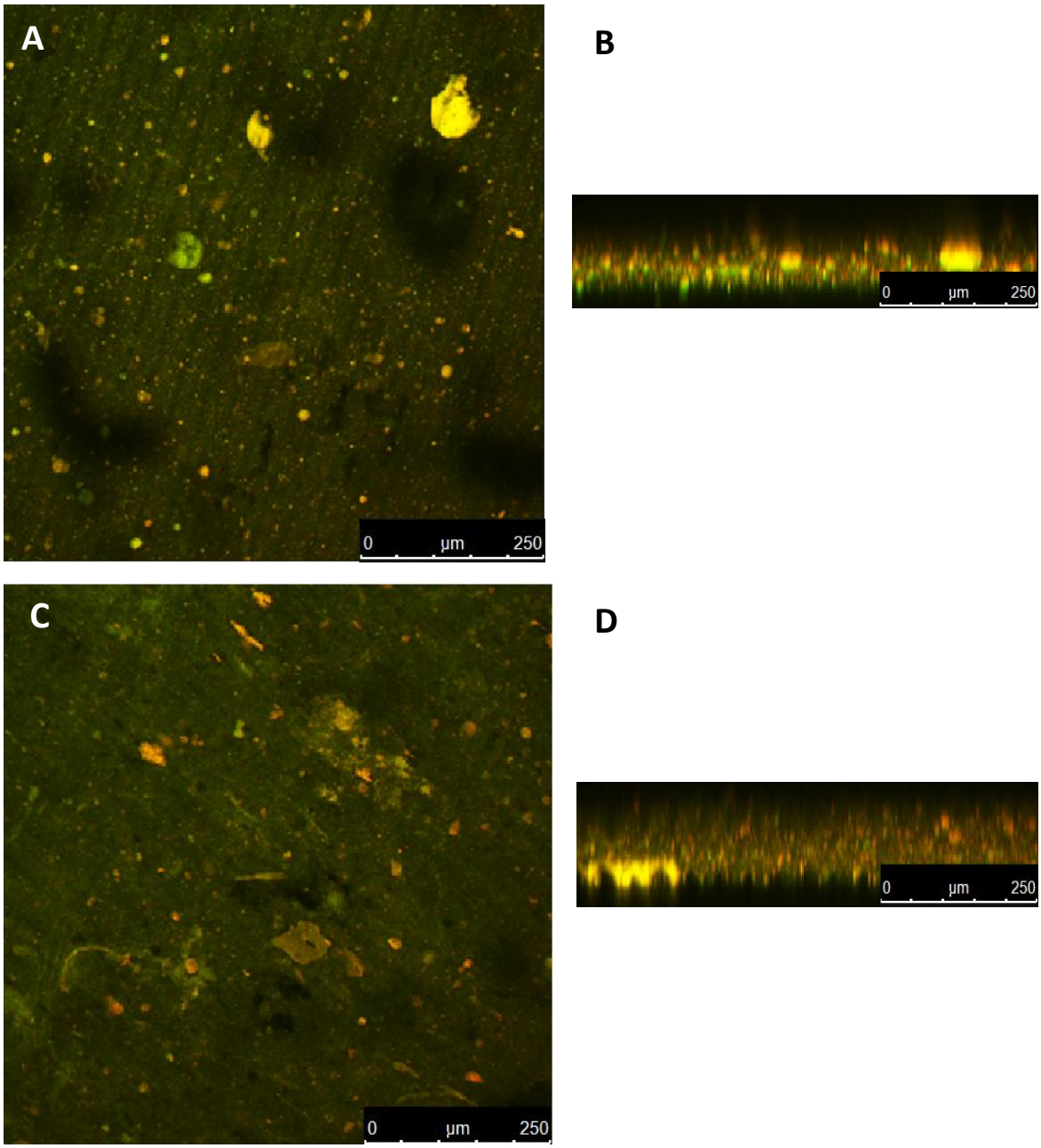

Figure 3.34: CSLM Images of Collagen Type I immunostaining after 10 days. A) Control, B) cross section of the control, C) top layer of the Col multilayer construct, and D) cross section of the top layer. Scale bars: 250 µm

3.4.2.2.1.2 Keratan Sulfate Staining

Keratocytes are characterized by their expression of various GAGs including keratan sulfate and it is a good indication for the preservation of keratocyte phenotype. Keratan sulfate deposition was examined by immunostaining of the layers of the multilayer constructs on Day 10 (Figure 3.35). If there is deposited keratan sulfate, it is presented in green color since Alexafluor488 labeled anti-mouse Ig antibody was used. Since collagen has autofluorescence at every wavelength of the range in question an overlay of the background and the dyes was done. Distinctive green color (which means no overlapped regions) indicated the presence of keratan sulfate deposition. The layers of the multilayer construct were stained separately like in Collagen type I staining. CSLM images showed no distinct green coloring in the cell seeded constructs like in the control samples. This indicates that either the cells did not secrete any keratan sulfate during the 10 days of culture or they lost their keratocyte phenotype. Normally keratocytes express GAG like keratan sulfate but when their phenotype is changed into repair type they start the repair process by secreting collagens, type I and type III, biglycan, and fibronectin (Funderburgh et al., 2003). However, in this study the immunostaining against human collagen type I also did show any secretion of collagen type I. Apperantly, the 10 days of culture and the number of cells seeded may not be enough for the secretion of keratan sulfate.

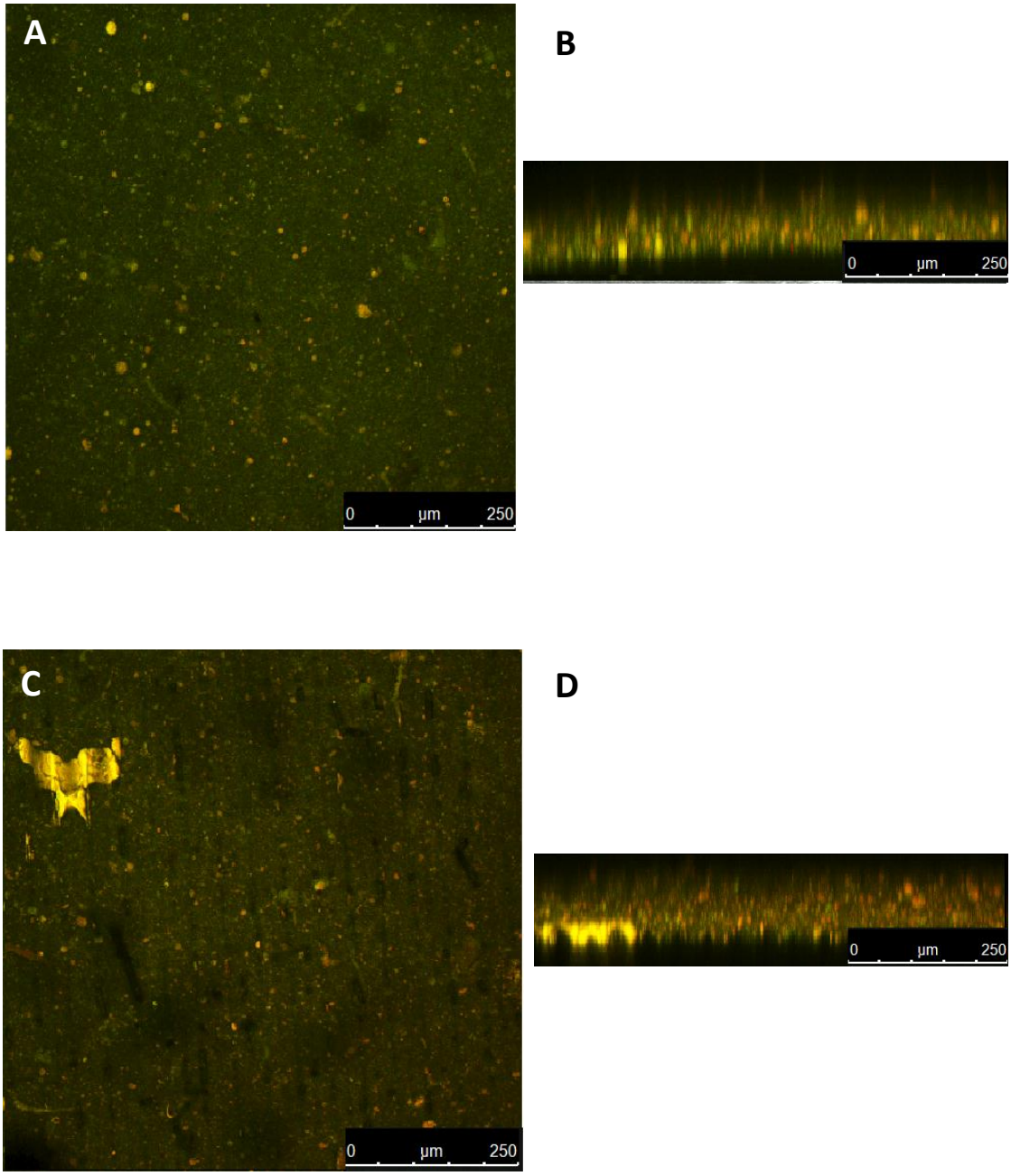

Figure 3.35: CSLM images of keratan sulfate staining on Day 10. A) Control, B) cross section of the control film, C) top layer of the Col multilayer construct, and D) cross section of the top layer.

CHAPTER 4

CONCLUSION AND FUTURE STUDIES

Corneal diseases and injuries are the second most common causes after cataract that leads to corneal blindness. Transplantation and keratoprostheses are the only options for the failed corneas but due to drawbacks of these treatments tissue engineering field has emerged in the last few decades with the aim to restore the function of the damaged tissues by using scaffold and the cells of the patient.

In this study a 3D scaffold was constructed from Col and Col:ELR patterned films that attempt to mimic the natural structure and organization of the corneal stroma.

The Col and Col:ELR films and constructs were shown to support cell attachment and proliferation. Alignment of the cells on the patterned films was achieved even after 1 day of incubation and their transparency was increased significantly over a 30 day period. The constructs appear to have the potential for use as a stroma equivalent and their performance should be enhanced before *in vivo* studies. ELR amount in the structure needs to be increased or optimized in order to show its effect more distinctly. The seeded cell number also needs to be increased to achieve better results. The ECM secretion has to be shown microscopically and quantified if possible. The layers can be stacked on top of each other by using bioadhesives. Bioreactors should be used to achieve better culture conditions for tissue formation and then the samples should be tested *in vivo* on rabbits by using rabbit corneal keratocytes before attempting clinical trials.

REFERENCES

Al-Kharashi, S. A., Al-Obailan, M. M., Almohaimeed, M., & Al-Torbak, A. A. (2009). Deep anterior lamellar keratoplasty. *Saudi Journal of Ophthalmology, 23*(3–4), 203-209. doi: 10.1016/j.sjopt.2009.10.004

Amruthwar, S. S., & Janorkar, A. V.In vitro evaluation of elastin-like polypeptide–collagen composite scaffold for bone tissue engineering. *Dental Materials*, (0) doi: 10.1016/j.dental.2012.10.003

Arenas, E., Esquenazi, S., Anwar, M., & Terry, M. (2012). Lamellar corneal transplantation. *Survey of Ophthalmology, 57*(6), 510-529. doi: 10.1016/j.survophthal.2012.01.009

Asbell, P., & Brocks, D. (2011). Cornea overview. In D. A. Dartt, P. Bex, P. D'Amore, R. Dana, L. K. Mcloon & J. Y. Niederkorn (Eds.), *Ocular periphery and disorders* (pp. 134). San Diego: Academic Press.

Ber, S., Torun Köse, G., & Hasırcı, V. (2005). Bone tissue engineering on patterned collagen films: An in vitro study. *Biomaterials, 26*(14), 1977-1986. doi: 10.1016/j.biomaterials.2004.07.007

Berglund, J. D., Mohseni, M. M., Nerem, R. M., & Sambanis, A. (2003). A biological hybrid model for collagen-based tissue engineered vascular constructs. *Biomaterials, 24*(7), 1241-1254. doi: 10.1016/S0142-9612(02)00506-9

Betre, H., Chilkoti, A., & Setton, L. A. (2002). A two-step chondrocyte recovery system based on thermally sensitive elastin-like polypeptide scaffolds for cartilage tissue engineering. *Engineering in Medicine and Biology, 2002. 24th Annual Conference and the Annual Fall Meeting of the Biomedical Engineering Society EMBS/BMES Conference, 2002. Proceedings of the Second Joint, , 1* 829-830 vol.1.

Bidwell III, G. L., Fokt, I., Priebe, W., & Raucher, D. (2007). Development of elastin-like polypeptide for thermally targeted delivery of doxorubicin. *Biochemical Pharmacology, 73*(5), 620-631. doi: 10.1016/j.bcp.2006.10.028

Boccafoschi, F., Habermehl, J., Vesentini, S., & Mantovani, D. (2005). Biological performances of collagen-based scaffolds for vascular tissue engineering. *Biomaterials, 26*(35), 7410-7417. doi: 10.1016/j.biomaterials.2005.05.052

Bou-Gharios, G., & de Crombrugghe, B. (2008). Chapter 15 - type I collagen structure, synthesis, and regulation. In John P. Bilezikian A2Lawrence G. Raisz and T. John MartinA2 John P. Bilezikian,Lawrence G.Raisz, & T. John Martin (Eds.), *Principles of bone biology (third edition)* (pp. 285-318). San Diego: Academic Press. doi: 10.1016/B978-0-12-373884-4.00034-3

Bourne, W. M., & McLaren, J. W. (2004). Clinical responses of the corneal endothelium. *Experimental Eye Research, 78*(3), 561-572. doi: 10.1016/j.exer.2003.08.002

Buerman, R. W., & Pedroza, L. (1996). Ultrastructure of the human cornea. *Microscopy Research and Technique, 33*(4), 320.

Builles, N., Janin-Manificat, H., Malbouyres, M., Justin, V., Rovère, M., Pellegrini, G., Ruggiero, F. (2010). Use of magnetically oriented orthogonal collagen scaffolds for hemi-corneal reconstruction and regeneration. *Biomaterials, 31*(32), 8313-8322. doi: 10.1016/j.biomaterials.2010.07.066

Cawston, T. (1998). Matrix metalloproteinases and TIMPs: Properties and implications for the rheumatic diseases. *Molecular Medicine Today, 4*(3), 130-137. doi: 10.1016/S1357-4310(97)01192-1

Chakravarti, S., Petroll, W. M., Hassell, J. R., Jester, J. V., Lass, J. H., Paul, J., & Birk, D. E. (2000). Corneal opacity in lumican-null mice: Defects in collagen fibril structure and packing in the posterior stroma. *Investigative Ophthalmology & Visual Science, 41*(11), 3365-3373.

Chen, H. J., Chen, H., Lai, J., Chen, C., Tsai, Y., Kuo, M., Ma, D. H. (2009). Persistence of transplanted oral mucosal epithelial cells in human cornea. *Investigative Ophthalmology & Visual Science, 50*(10), 4660-4668. doi: 10.1167/iovs.09-3377

Chirila, T. V., Hicks, C. R., Dalton, P. D., Vijayasekaran, S., Lou, X., Hong, Y., Constable, I. J. (1998). Artificial cornea. *Progress in Polymer Science, 23*(3), 447-473. doi: 10.1016/S0079-6700(97)00036-1

Chirila, T. V. (2001). An overview of the development of artificial corneas with porous skirts and the use of PHEMA for such an application. *Biomaterials, 22*(24), 3311-3317. doi: 10.1016/S0142-9612(01)00168-5

Correlo, V. M., Oliveira, J. M., Mano, J. F., Neves, N. M., & Reis, R. L. (2011). Chapter 32 - natural origin materials for bone tissue engineering – properties, processing, and performance. In Anthony Atala, Robert Lanza, James A. Thomson and Robert M. Nerem (Eds.), *Principles of regenerative medicine (second edition)* (pp. 557-586). San Diego: Academic Press. doi: 10.1016/B978-0-12-381422-7.10032-X

Coster, J. D. (2002a). Corneal ulceration. In S. Lightman (Ed.), *Fundamentals of clinical ophthalmology* (pp. 41-64). London: BMJ Publishing Group.

Coster, J. D. (2002b). Foundations of keratology. In S. Lightman (Ed.), *Fundamentals of clinical ophthalmology* (pp. 1-34). London: BMJ Publishing Group.

Crabb, R. A., & Hubel, A. (2008). Influence of matrix processing on the optical and biomechanical properties of a corneal stroma equivalent. *Tissue Engineering.Part A, 14*(1), 173-182. doi: 10.1089/ten.a.2007.0139; 10.1089/ten.a.2007.0139

Curtis, A., & Wilkinson, C. (1997). Topographical control of cells. *Biomaterials, 18*(24), 1573-1583. doi: 10.1016/S0142-9612(97)00144-0

Dean, D., Kandel, R. P., Adhikari, H. K., & Hessel, T. (2008). Multiple chlamydiaceae species in trachoma: Implications for disease pathogenesis and control. *PLoS Med, 5*(1), e14.

Engelmann, K., Böhnke, M., & Friedl, P. (1988). Isolation and long-term cultivation of human corneal endothelial cells. *Investigative Ophthalmology & Visual Science, 29*(11), 1656-1662.

Engelmann, K., Bednarz, J., & Valtink, M. (2004). Prospects for endothelial transplantation. *Experimental Eye Research, 78*(3), 573-578. doi: 10.1016/S0014-4835(03)00209-4

Ethier, C. R., Johnson, M., & Ruberti, J. (2004). Ocular biomechanics and biotransport. *Annual Review of Biomedical Engineering, 6*(1), 249-273. doi: 10.1146/annurev.bioeng.6.040803.140055

Falconnet, D., Csucs, G., Michelle Grandin, H., & Textor, M. (2006). Surface engineering approaches to micropattern surfaces for cell-based assays. *Biomaterials, 27*(16), 3044-3063. doi: 10.1016/j.biomaterials.2005.12.024

Faucheux, N., Schweiss, R., Lützow, K., Werner, C., & Groth, T. (2004). Self-assembled monolayers with different terminating groups as model substrates for cell adhesion studies. *Biomaterials, 25*(14), 2721-2730. doi: 10.1016/j.biomaterials.2003.09.069

Feng, L., Li, S., Li, Y., Li, H., Zhang, L., Zhai, J., Zhu, D. (2002). Super-hydrophobic surfaces: From natural to artificial. *Advanced Materials, 14*(24), 1857-1860. doi: 10.1002/adma.200290020

Fini, M. E. (1999). Keratocyte and fibroblast phenotypes in the repairing cornea. *Progress in Retinal and Eye Research, 18*(4), 529-551. doi: 10.1016/S1350-9462(98)00033-0

Fittkau, M. H., Zilla, P., Bezuidenhout, D., Lutolf, M. P., Human, P., Hubbell, J. A., & Davies, N. (2005). The selective modulation of endothelial cell mobility on RGD peptide containing surfaces by YIGSR peptides. *Biomaterials, 26*(2), 167-174. doi: 10.1016/j.biomaterials.2004.02.012

Foster, A., & Gilbert, C. (1992). Epidemiology of childhood blindness. *Eye (London, England), 6*(2), 173-176.

Fullwood, N. J. (2004). Collagen fibril orientation and corneal curvature. *Structure, 12*(2), 169-170. doi: 10.1016/j.str.2004.01.019

Funderburgh, J. L., Mann, M. M., & Funderburgh, M. L. (2003). Keratocyte phenotype mediates proteoglycan structure: A Role for Fibroblasts in Corneal Fibrosis. *Journal of Biological Chemistry, 278*(46), 45629-45637. doi: 10.1074/jbc.M303292200

Germain, L., Carrier, P., Auger, F. A., Salesse, C., & Guérin, S. L. (2000). Can we produce a human corneal equivalent by tissue engineering? *Progress in Retinal and Eye Research, 19*(5), 497-527. doi: 10.1016/S1350-9462(00)00005-7

Gil, E. S., Mandal, B. B., Park, S., Marchant, J. K., Omenetto, F. G., & Kaplan, D. L. (2010). Helicoidal multi-lamellar features of RGD-functionalized silk biomaterials for corneal tissue engineering. *Biomaterials, 31*(34), 8953-8963. doi: 10.1016/j.biomaterials.2010.08.017

Girotti, A., Reguera, J., RodrÃguez-Cabello, J., Arias, F., Alonso, M., & Testera, A. (2004). Design and bioproduction of a recombinant multi(bio)functional elastin-like protein polymer containing cell adhesion sequences for tissue engineering purposes. *Journal of Materials Science: Materials in Medicine, 15*(4), 479-484. doi: 10.1023/B:JMSM.0000021124.58688.7a

Gomaa, A., Comyn, O., & Liu, C. (2010). Keratoprostheses in clinical practice: A review. *Clinical & Experimental Ophthalmology, 38*(2), 211-224. doi: 10.1111/j.1442-9071.2010.02231.x

Griffith, L. G., & Naughton, G. (2002). Tissue engineering--current challenges and expanding opportunities. *Science, 295*(5557), 1009-1014. doi: 10.1126/science.1069210

Griffith, M., Jackson, W. B., Lagali, N., Merrett, K., Li, F., & Fagerholm, P. (2009). Artificial corneas: A regenerative medicine approach. *Eye (London, England), 23*(10), 1985-1989.

Griffith, M., Fagerholm, P., Lagali, N., Latorre, M. A., Hackett, J., & Sheardown, H. (2011). Chapter 49 - regenerative medicine in the cornea. In Anthony Atala, Robert Lanza, James A. Thomson and Robert M. Nerem (Eds.), *Principles of regenerative medicine (second edition)* (pp. 911-924). San Diego: Academic Press. doi: 10.1016/B978-0-12-381422-7.10049-5

Güell, J. L., Arcos, E., Gris, O., Aristizabal, D., Pacheco, M., Sanchez, C. L., & Manero, F. (2011). Outcomes with the boston type 1 keratoprosthesis at instituto de microcirugía ocular IMO. *Saudi Journal of Ophthalmology, 25*(3), 281-284. doi: 10.1016/j.sjopt.2011.04.010

Gunatillake, P. A., & Adhikari, R. (2003). Biodegradable synthetic polymers for tissue engineering. *European Cells & Materials, 5*, 1-16; discussion 16.

Guo, X., Hutcheon, A. E. K., Melotti, S. A., Zieske, J. D., Trinkaus-Randall, V., & Ruberti, J. W. (2007). Morphologic characterization of organized extracellular matrix deposition by ascorbic Acid–Stimulated human corneal fibroblasts. *Investigative Ophthalmology & Visual Science, 48*(9), 4050-4060. doi: 10.1167/iovs.06-1216

Hafemann, B., Ensslen, S., Erdmann, C., Niedballa, R., Zühlke, A., Ghofrani, K., & Kirkpatrick, C. J. (1999). Use of a collagen/elastin-membrane for the tissue engineering of dermis. *Burns, 25*(5), 373-384. doi: 10.1016/S0305-4179(98)00162-4

Hao, J., Nagano, T., Nakamura, M., Kumagai, N., Mishima, H., & Nishida, T. (1999). Galardin inhibits collagen degradation by rabbit keratocytes by inhibiting the activation of pro-matrix metalloproteinases. *Experimental Eye Research, 68*(5), 565-572. doi: 10.1006/exer.1998.0637

Hasırcı, V., Lewandrowski, K., Gresser, J. D., Wise, D. L., & Trantolo, D. J. (2001). Versatility of biodegradable biopolymers: Degradability and an in vivo application. *Journal of Biotechnology, 86*(2), 135-150. doi: 10.1016/S0168-1656(00)00409-0

Hasirci, V., & Kenar, H. (2006). Novel surface patterning approaches for tissue engineering and their effect on cell behavior. *Nanomedicine (London, England), 1*(1), 73-90.

Hicks, C. R., Crawford, G. J., Dart, J. K. G., Grabner, G., Holland, E. J., Stulting, R. D., Bulsara, M. (2006). AlphaCor: Clinical outcomes. *Cornea, 25*(9), 1034-1042 10.1097/01.ico.0000229982.23334.6b.

Hu, X., Lui, W., Cui, L., Wang, M., & Cao, Y. (2005). Tissue engineering of nearly transparent corneal stroma. *Tissue Engineering, 11*(11-12), 1710-1717. doi: 10.1089/ten.2005.11.1710

Isenberg, S., Rutar, T., Lietman, T., Nischal, K., Wilson, E., Murray, T., Traboulsi, E. (2009). 138: International childhood blindness. *Journal of American Association for Pediatric Ophthalmology and Strabismus, 13*(1), e34. doi: 10.1016/j.jaapos.2008.12.140

Janorkar, A. V., Rajagopalan, P., Yarmush, M. L., & Megeed, Z. (2008). The use of elastin-like polypeptide–polyelectrolyte complexes to control hepatocyte morphology and function in vitro. *Biomaterials, 29*(6), 625-632. doi: 10.1016/j.biomaterials.2007.10.022

Jester, J. V. (2008). Corneal crystallins and the development of cellular transparency. *Seminars in Cell & Developmental Biology, 19*(2), 82-93. doi: 10.1016/j.semcdb.2007.09.015

Jester, J. V., Moller-Pedersen, T., Huang, J., Sax, C. M., Kays, W. T., Cavangh, H. D., Piatigorsky, J. (1999). The cellular basis of corneal transparency: Evidence for 'corneal crystallins'. *Journal of Cell Science, 112 (Pt 5)*(Pt 5), 613-622.

Jiang, T. S., Cai, L., Ji, W. Y., Hui, Y. N., Wang, Y. S., Hu, D., & Zhu, J. (2010). Reconstruction of the corneal epithelium with induced marrow mesenchymal stem cells in rats. *Molecular Vision, 16*, 1304-1316.

Joyce, N. C. (2003). Proliferative capacity of the corneal endothelium. *Progress in Retinal and Eye Research, 22*(3), 359-389. doi: 10.1016/S1350-9462(02)00065-4

Kaji, Y. (2002). Anatomy of the cornea, limbus and sclera. In D. J. Apple, L. Buratto, J. L. Alio, S. K. Pandey & A. Agarwal (Eds.), *Textbook of ophthalmology*. New Delhi: Jaypee.

Kenar, H., Köse, G. T., & Hasirci, V. (2006). Tissue engineering of bone on micropatterned biodegradable polyester films. *Biomaterials, 27*(6), 885-895. doi: 10.1016/j.biomaterials.2005.07.001

Kenar, H., Kose, G. T., Toner, M., Kaplan, D. L., & Hasirci, V. (2011). A 3D aligned microfibrous myocardial tissue construct cultured under transient perfusion. *Biomaterials, 32*(23), 5320-5329. doi: 10.1016/j.biomaterials.2011.04.025

Kinikoglu, B., Rodriguez-Cabello, J. C., Damour, O., & Hasirci, V. (2011a). A smart bilayer scaffold of elastin-like recombinamer and collagen for soft tissue engineering. *Journal of Materials Science.Materials in Medicine, 22*(6), 1541-1554. doi: 10.1007/s10856-011-4315-6

Kinikoglu, B., Rodríguez-Cabello, J. C., Damour, O., & Hasirci, V. (2011b). The influence of elastin-like recombinant polymer on the self-renewing potential of a 3D tissue equivalent derived from human lamina propria fibroblasts and oral epithelial cells. *Biomaterials, 32*(25), 5756-5764. doi: 10.1016/j.biomaterials.2011.04.054

Kojima, C., Suehiro, T., Watanabe, K., Ogawa, M., Fukuhara, A., Nishisaka, E., Magata, Y. (2012). Doxorubicin-conjugated dendrimer/collagen hybrid gels for metastasis-associated drug delivery systems. *Acta Biomaterialia*, (0) doi: 10.1016/j.actbio.2012.11.013

Köse, G. T., Korkusuz, F., Korkusuz, P., Purali, N., Özkul, A., & Hasırcı, V. (2003). Bone generation on PHBV matrices: An in vitro study. *Biomaterials, 24*(27), 4999-5007. doi: 10.1016/S0142-9612(03)00417-4

Köse, G. T., Korkusuz, F., Özkul, A., Soysal, Y., Özdemir, T., Yildiz, C., & Hasirci, V. (2005). Tissue engineered cartilage on collagen and PHBV matrices. *Biomaterials, 26*(25), 5187-5197. doi: 10.1016/j.biomaterials.2005.01.037

Laattala, K., Huhtinen, R., Puska, M., Arstila, H., Hupa, L., Kellomäki, M., & Vallittu, P. K. (2011). Bioactive composite for keratoprosthesis skirt. *Journal of the Mechanical Behavior of Biomedical Materials, 4*(8), 1700-1708. doi: 10.1016/j.jmbbm.2011.05.025

Langer, R., & Vacanti, J. (1993). Tissue engineering. *Science, 260*(5110), 920-926. doi: 10.1126/science.8493529

Last, J. A., Liliensiek, S. J., Nealey, P. F., & Murphy, C. J. (2009). Determining the mechanical properties of human corneal basement membranes with atomic force microscopy. *Journal of Structural Biology, 167*(1), 19-24. doi: 10.1016/j.jsb.2009.03.012

Lawrence, B. D., Marchant, J. K., Pindrus, M. A., Omenetto, F. G., & Kaplan, D. L. (2009). Silk film biomaterials for cornea tissue engineering. *Biomaterials, 30*(7), 1299-1308. doi: 10.1016/j.biomaterials.2008.11.018

Liu, C., Paul, B., Tandon, R., Lee, E., Fong, K., Mavrikakis, I., Hamada, S. (2005). The osteo-odonto-keratoprosthesis (OOKP). *Semin Ophthalmol, 20*(2), 113-128. doi: 10.1080/08820530590931386

Liu, C., Xia, Z., & Czernuszka, J. T. (2007). Design and development of three-dimensional scaffolds for tissue engineering. *Chemical Engineering Research and Design, 85*(7), 1051-1064. doi: 10.1205/cherd06196

Liu, Y., Ma, L., & Gao, C. (2012). Facile fabrication of the glutaraldehyde cross-linked collagen/chitosan porous scaffold for skin tissue engineering. *Materials Science and Engineering: C, 32*(8), 2361-2366. doi: 10.1016/j.msec.2012.07.008

Liu, Y., Ren, L., & Wang, Y. (2013). Crosslinked collagen–gelatin–hyaluronic acid biomimetic film for cornea tissue engineering applications. *Materials Science and Engineering: C, 33*(1), 196-201. doi: 10.1016/j.msec.2012.08.030

Liu, Z., Huang, A. J., & Pflugfelder, S. C. (1999). Evaluation of corneal thickness and topography in normal eyes using the orbscan corneal topography system. *The British Journal of Ophthalmology, 83*(7), 774-778.

Ma, L., Gao, C., Mao, Z., Zhou, J., Shen, J., Hu, X., & Han, C. (2003). Collagen/chitosan porous scaffolds with improved biostability for skin tissue engineering. *Biomaterials, 24*(26), 4833-4841. doi: 10.1016/S0142-9612(03)00374-0

Martínez-Osorio, H., Juárez-Campo, M., Diebold, Y., Girotti, A., Alonso, M., Arias, F. J., Calonge, M. (2009). Genetically engineered elastin-like polymer as a substratum to culture cells from the ocular surface. *Curr Eye Res, 34*(1), 48-56. doi: 10.1080/02713680802542053

Maurice, D. M. (1957). The structure and transparency of the cornea. *The Journal of Physiology, 136*(2), 263-286.

McLaughlin, C. R., Osborne, R., Hyatt, A., Watsky, M. A., Dare, E. V., Jarrold, B. B., Griffith, M. (2009). Tissue engineered models for in vitro studies. In U. Meyer, J. Handschel, H. P. Wiesmann & T. Meyer (Eds.), *Fundamentals of tissue engineering and regenerative medicine* (1st ed.,). New York: Verlag Berlin Heidelberg.

McLaughlin, C. R., Acosta, M. C., Luna, C., Liu, W., Belmonte, C., Griffith, M., & Gallar, J. (2010). Regeneration of functional nerves within full thickness collagen–phosphorylcholine corneal substitute implants in guinea pigs. *Biomaterials, 31*(10), 2770-2778. doi: 10.1016/j.biomaterials.2009.12.031

Meek, K. M., & Leonard, D. W. (1993). Ultrastructure of the corneal stroma: A comparative study. *Biophysical Journal, 64*(1), 273-280. doi: 10.1016/S0006-3495(93)81364-X

Meek, K. M., & Fullwood, N. J. (2001). Corneal and scleral collagens—a microscopist's perspective. *Micron, 32*(3), 261-272. doi: 10.1016/S0968-4328(00)00041-X

Meek, K. M., Leonard, D. W., Connon, C. J., Dennis, S., & Khan, S. (2003). Transparency, swelling and scarring in the corneal stroma. *Eye (London, England), 17*(8), 927-936.

Meek, K. M., & Boote, C. (2004). The organization of collagen in the corneal stroma. *Experimental Eye Research, 78*(3), 503-512. doi: 10.1016/j.exer.2003.07.003

Meek, K. (2009). Corneal collagen-"its role in maintaining corneal shape and transparency". *Biophysical Reviews, 1*(2), 83-93. doi: 10.1007/s12551-009-0011-x

Menzies, K.,L., & Jones, L. (2010). The impact of contact angle on the biocompatibility of biomaterials. *Optometry and Vision Science,* , 1.

Merrett, K., Liu, W., Mitra, D., Camm, K. D., McLaughlin, C. R., Liu, Y., Fogg, D. E. (2009). Synthetic neoglycopolymer-recombinant human collagen hybrids as biomimetic crosslinking agents in corneal tissue engineering. *Biomaterials, 30*(29), 5403-5408. doi: 10.1016/j.biomaterials.2009.06.016

Muraine, M., Toubeau, D., Menguy, E., & Brasseur, G. (2002). Analysing the various obstacles to cornea postmortem procurement. *The British Journal of Ophthalmology, 86*(8), 864-868.

Murphy, C. M., Haugh, M. G., & O'Brien, F. J. (2010). The effect of mean pore size on cell attachment, proliferation and migration in collagen–glycosaminoglycan scaffolds for bone tissue engineering. *Biomaterials, 31*(3), 461-466. doi: 10.1016/j.biomaterials.2009.09.063

Muthusubramaniam, L., Peng, L., Zaitseva, T., Paukshto, M., Martin, G. R., & Desai, T. A. (2012). Collagen fibril diameter and alignment promote the quiescent keratocyte phenotype. *Journal of Biomedical Materials Research Part A, 100 A*(3), 613-621. doi: 10.1002/jbm.a.33284

Myung, D., Duhamel, P. E., Cochran, J. R., Noolandi, J., Ta, C. N., & Frank, C. W. (2008). Development of hydrogel-based keratoprostheses: A materials perspective. *Biotechnology Progress, 24*(3), 735-741. doi: 10.1021/bp070476n

Nair, L. S., & Laurencin, C. T. (2007). Biodegradable polymers as biomaterials. *Progress in Polymer Science, 32*(8–9), 762-798. doi: 10.1016/j.progpolymsci.2007.05.017

Negrel, A. D., & Thylefors, B. (1998). The global impact of eye injuries. *Ophthalmic Epidemiology, 5*(3), 143-169.

Nishida, T. (2005). Cornea. In J. H. Krachmer, M. J. Mannis & E. J. Holland (Eds.), *Cornea* (2nd ed.,). Philadelphia: Elsevier/Mosby.

Oliva, M. S., Schottman, T., & Gulati, M. (2012). Turning the tide of corneal blindness. *Indian Journal of Ophthalmology, 60*(5), 423-427. doi: 10.4103/0301-4738.100540; 10.4103/0301-4738.100540

Olsen, D., Yang, C., Bodo, M., Chang, R., Leigh, S., Baez, J., Polarek, J. (2003). Recombinant collagen and gelatin for drug delivery. *Advanced Drug Delivery Reviews, 55*(12), 1547-1567. doi: 10.1016/j.addr.2003.08.008

Ozturk, N., Girotti, A., Kose, G. T., Rodríguez-Cabello, J. C., & Hasirci, V. (2009). Dynamic cell culturing and its application to micropatterned, elastin-like protein-modified poly(N-isopropylacrylamide) scaffolds. *Biomaterials, 30*(29), 5417-5426. doi: 10.1016/j.biomaterials.2009.06.044

Pachence, J. M., Bohrer, M. P., & Kohn, J. (2007). Chapter twenty-three - biodegradable polymers. In Robert Lanza A2Robert Langer and Joseph VacantiA2 Robert Lanza,Robert Langer, & Joseph Vacanti (Eds.), *Principles of tissue engineering (third edition)* (pp. 323-339). Burlington: Academic Press. doi: 10.1016/B978-012370615-7/50027-5

Panda, A., Vanathi, M., Kumar, A., Dash, Y., & Priya, S. (2007). Corneal graft rejection. *Survey of Ophthalmology, 52*(4), 375-396. doi: 10.1016/j.survophthal.2007.04.008

Pang, Y., Wang, X., Ucuzian, A. A., Brey, E. M., Burgess, W. H., Jones, K. J., Greisler, H. P. (2010). Local delivery of a collagen-binding FGF-1 chimera to smooth muscle cells in collagen scaffolds for vascular tissue engineering. *Biomaterials, 31*(5), 878-885. doi: 10.1016/j.biomaterials.2009.10.007

Rafat, M., Li, F., Fagerholm, P., Lagali, N. S., Watsky, M. A., Munger, R., Griffith, M. (2008). PEG-stabilized carbodiimide crosslinked collagen–chitosan hydrogels for corneal tissue engineering. *Biomaterials, 29*(29), 3960-3972. doi: 10.1016/j.biomaterials.2008.06.017

Rajan, N., Habermehl, J., Cote, M., Doillon, C. J., & Mantovani, D. (2007). Preparation of ready-to-use, storable and reconstituted type I collagen from rat tail tendon for tissue engineering applications. *Nat.Protocols, 1*(6), 2753-2758.

Ribeiro, A., Arias, F. J., Reguera, J., Alonso, M., & Rodríguez-Cabello, J. C. (2009). Influence of the amino-acid sequence on the inverse temperature transition of elastin-like polymers. *Biophysical Journal, 97*(1), 312-320. doi: 10.1016/j.bpj.2009.03.030

Robert, M., & Harissi-Dagher, M. (2011). Boston type 1 keratoprosthesis: The CHUM experience. *Canadian Journal of Ophthalmology / Journal Canadien d'Ophtalmologie, 46*(2), 164-168. doi: 10.3129/i10-103

Rodríguez-Cabello, J. C., Martín, L., Alonso, M., Arias, F. J., & Testera, A. M. (2009). "Recombinamers" as advanced materials for the post-oil age. *Polymer, 50*(22), 5159-5169. doi: 10.1016/j.polymer.2009.08.032

Rossert, J., & de Crombrugghe, B. (2002). Chapter 12 - type I collagen: Structure, synthesis, and regulation. In John P. Bilezikian, Lawrence G. Raisz and Gideon A. Rodan (Eds.), *Principles of bone biology (second edition)* (pp. 189-XVIII). San Diego: Academic Press. doi: 10.1016/B978-012098652-1.50114-1

Ruberti, J. W., Zieske, J. D., & Trinkaus-Randall, V. (2007). Chapter sixty-eight - corneal-tissue replacement. In Robert Lanza, Robert Langer and Joseph Vacanti (Eds.), *Principles of tissue engineering (third edition)* (pp. 1025-1047). Burlington: Academic Press. doi: 10.1016/B978-012370615-7/50072-X

Ruberti, J. W., & Zieske, J. D. (2008). Prelude to corneal tissue engineering – gaining control of collagen organization. *Progress in Retinal and Eye Research, 27*(5), 549-577. doi: 10.1016/j.preteyeres.2008.08.001

Ruszczak, Z., & Friess, W. (2003). Collagen as a carrier for on-site delivery of antibacterial drugs. *Advanced Drug Delivery Reviews, 55*(12), 1679-1698. doi: 10.1016/j.addr.2003.08.007

Sawhney, A. S., & Drumheller, P. D. (1998). Chapter II.4 - polymer synthesis. In Charles W. Patrick, Jr., Antonios G. Mikos, Larry V. McIntire and R.S. Langer (Eds.), *Frontiers in tissue engineering* (pp. 83-106). Oxford: Pergamon. doi: 10.1016/B978-008042689-1/50007-8

Senaratne, L. S., Park, P., & Kim, S. (2006). Isolation and characterization of collagen from brown backed toadfish (lagocephalus gloveri) skin. *Bioresource Technology, 97*(2), 191-197. doi: 10.1016/j.biortech.2005.02.024

Shah, A., Brugnano, J., Sun, S., Vase, A., & Orwin, E. (2008). The development of a tissue-engineered cornea: Biomaterials and culture methods. *Pediatric Research, 63*(5), 535-544. doi: 10.1203/PDR.0b013e31816bdf54; 10.1203/PDR.0b013e31816bdf54

Strahlman, E., Elman, M., Daub, E., & Baker, S. (1990). Causes of pediatric eye injuries. A population-based study. *Arch Ophthalmol, 108*(4), 603-606.

Su, Y., Su, Q., Liu, W., Lim, M., Venugopal, J. R., Mo, X., El-Newehy, M. (2012). Controlled release of bone morphogenetic protein 2 and dexamethasone loaded in core–shell PLLACL–collagen fibers for use in bone tissue engineering. *Acta Biomaterialia, 8*(2), 763-771. doi: 10.1016/j.actbio.2011.11.002

Subramani, K. (2010). Chapter 11 - fabrication of hydrogel micropatterns by soft photolithography. In Waqar Ahmed, & Mark J. Jackson (Eds.), *Emerging nanotechnologies for manufacturing* (pp. 261-276). Boston: William Andrew Publishing. doi: 10.1016/B978-0-8155-1583-8.00011-9

Suzuki, K., Saito, J., Yanai, R., Yamada, N., Chikama, T., Seki, K., & Nishida, T. (2003). Cell–matrix and cell–cell interactions during corneal epithelial wound healing. *Progress in Retinal and Eye Research, 22*(2), 113-133. doi: 10.1016/S1350-9462(02)00042-3

Taraballi, F., Zanini, S., Lupo, C., Panseri, S., Cunha, C., Riccardi, C., Cipolla, L. (2012). Amino and carboxyl plasma functionalization of collagen films for tissue engineering applications. *Journal of Colloid and Interface Science,* doi: http://dx.doi.org/10.1016/j.jcis.2012.11.041

Teichmann, J., Valtink, M., Gramm, S., Nitschke, M., Werner, C., Funk, R. H. W., & Engelmann, K. (2013). Human corneal endothelial cell sheets for transplantation: Thermo-responsive cell culture

carriers to meet cell-specific requirements. *Acta Biomaterialia, 9*(2), 5031-5039. doi: 10.1016/j.actbio.2012.10.023

Tian, H., Tang, Z., Zhuang, X., Chen, X., & Jing, X. (2012). Biodegradable synthetic polymers: Preparation, functionalization and biomedical application. *Progress in Polymer Science, 37*(2), 237-280. doi: 10.1016/j.progpolymsci.2011.06.004

Torbet, J., Malbouyres, M., Builles, N., Justin, V., Roulet, M., Damour, O., Hulmes, D. J. S. (2007). Orthogonal scaffold of magnetically aligned collagen lamellae for corneal stroma reconstruction. *Biomaterials, 28*(29), 4268-4276. doi: 10.1016/j.biomaterials.2007.05.024

Trinkaus-Randall, V. (2000). Cornea. In R. P. Lanza, R. Langer & J. Vacanti (Eds.), *Principles of tissue engineering* (2nd ed.,). San Diego, CA: Academic Press.

Vacanti, J., & Vacanti, C. A. (2007). Chapter one - the history and scope of tissue engineering. In Robert Lanza, Robert Langer and Joseph Vacanti (Eds.), *Principles of tissue engineering (third edition)* (pp. 3-6). Burlington: Academic Press. doi: 10.1016/B978-012370615-7/50005-6

Vasantha, V., Sehgal, P. K., & Rao, K. P. (1988). Collagen ophthalmic inserts for pilocarpine drug delivery system. *International Journal of Pharmaceutics, 47*(1–3), 95-102. doi: 10.1016/0378-5173(88)90219-0

Viitala, R., Franklin, V., Green, D., Liu, C., Lloyd, A., & Tighe, B. (2009). Towards a synthetic osteo-odonto-keratoprosthesis. *Acta Biomaterialia, 5*(1), 438-452. doi: 10.1016/j.actbio.2008.07.008

Vrana, N. E., Builles, N., Kocak, H., Gulay, P., Justin, V., Malbouyres, M., Hasirci, V. (2007a). EDC/NHS cross-linked collagen foams as scaffolds for artificial corneal stroma. *Journal of Biomaterials Science.Polymer Edition, 18*(12), 1527-1545.

Vrana, N. E., Elsheikh, A., Builles, N., Damour, O., & Hasirci, V. (2007b). Effect of human corneal keratocytes and retinal pigment epithelial cells on the mechanical properties of micropatterned collagen films. *Biomaterials, 28*(29), 4303-4310. doi: 10.1016/j.biomaterials.2007.06.013

Vrana, E., Builles, N., Hindie, M., Damour, O., Aydinli, A., & Hasirci, V. (2008a). Contact guidance enhances the quality of a tissue engineered corneal stroma. *Journal of Biomedical Materials Research.Part A, 84*(2), 454-463. doi: 10.1002/jbm.a.31442

Vrana, N. E., Builles, N., Justin, V., Bednarz, J., Pellegrini, G., Ferrari, B., Hasirci, V. (2008b). Development of a reconstructed cornea from Collagen–Chondroitin sulfate foams and human cell cultures. *Investigative Ophthalmology & Visual Science, 49*(12), 5325-5331. doi: 10.1167/iovs.07-1599

Wang, S., Liu, W., Han, B., & Yang, L. (2009). Study on a hydroxypropyl chitosan–gelatin based scaffold for corneal stroma tissue engineering. *Applied Surface Science, 255*(20), 8701-8705. doi: 10.1016/j.apsusc.2009.04.206

Weadock, K. S., Miller, E. J., Bellincampi, L. D., Zawadsky, J. P., & Dunn, M. G. (1995). Physical crosslinking of collagen fibers: Comparison of ultraviolet irradiation and dehydrothermal treatment. *Journal of Biomedical Materials Research, 29*(11), 1373-1379. doi: 10.1002/jbm.820291108

Wess, T. J. (2005) Collagen fibril form and function. *Advances in protein chemistry* (pp. 341-374) Academic Press. doi: 10.1016/S0065-3233(05)70010-3

West-Mays, J. A., & Dwivedi, D. J. (2006). The keratocyte: Corneal stromal cell with variable repair phenotypes. *The International Journal of Biochemistry & Cell Biology, 38*(10), 1625-1631. doi: 10.1016/j.biocel.2006.03.010

Williams, S. F., Martin, D. P., Horowitz, D. M., & Peoples, O. P. (1999). PHA applications: Addressing the price performance issue: I. tissue engineering. *International Journal of Biological Macromolecules, 25*(1–3), 111-121. doi: 10.1016/S0141-8130(99)00022-7

Whitcher, J. P., Srinivasan, M., & Upadhyay, M. P. (2001). Corneal blindness: A global perspective. *Bulletin of the World Health Organization, 79*(3), 214-221.

Yucel, D., Kose, G. T., & Hasirci, V. (2010). Polyester based nerve guidance conduit design. *Biomaterials, 31*(7), 1596-1603. doi: 10.1016/j.biomaterials.2009.11.013

Zhang, N., Yan, H., & Wen, X. (2005). Tissue-engineering approaches for axonal guidance. *Brain Research Reviews, 49*(1), 48-64. doi: 10.1016/j.brainresrev.2004.11.002

Zorlutuna, P., Tezcaner, A., Kıyat, I., Aydınlı, A., & Hasırcı, V. (2006). Cornea engineering on polyester carriers. *Journal of Biomedical Materials Research Part A, 79A*(1), 104-113. doi: 10.1002/jbm.a.30772

Zorlutuna, P., Builles, N., Damour, O., Elsheikh, A., & Hasirci, V. (2007). Influence of keratocytes and retinal pigment epithelial cells on the mechanical properties of polyester-based tissue engineering micropatterned films. *Biomaterials, 28*(24), 3489-3496. doi: 10.1016/j.biomaterials.2007.04.013

Zorlutuna, P., Elsheikh, A., & Hasirci, V. (2009). Nanopatterning of collagen scaffolds improve the mechanical properties of tissue engineered vascular grafts. *Biomacromolecules, 10*(4), 814-821. doi: 10.1021/bm801307y

APPENDIX A

STRESS STRAIN CURVE OF A VISCOELASTIC MATERIAL

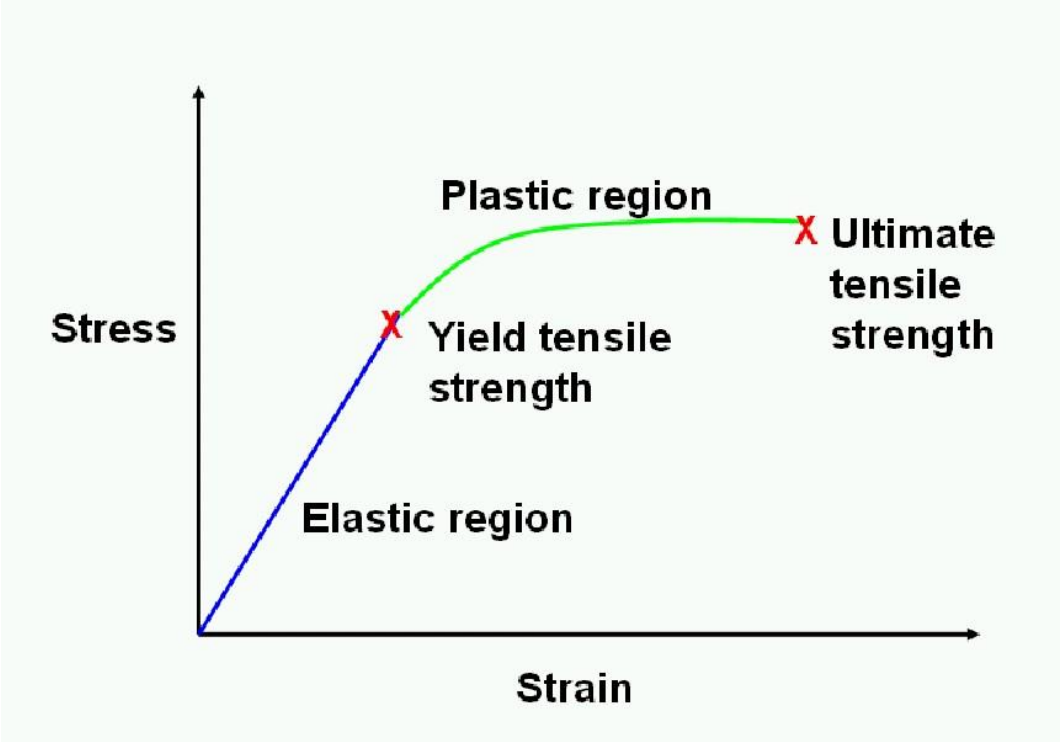

Figure A.1: A typical stress strain curve for viscoelastic materials. Slope of the curve gives Young's Modulus (E)

APPENDIX B

TENSILE TEST RESULTS

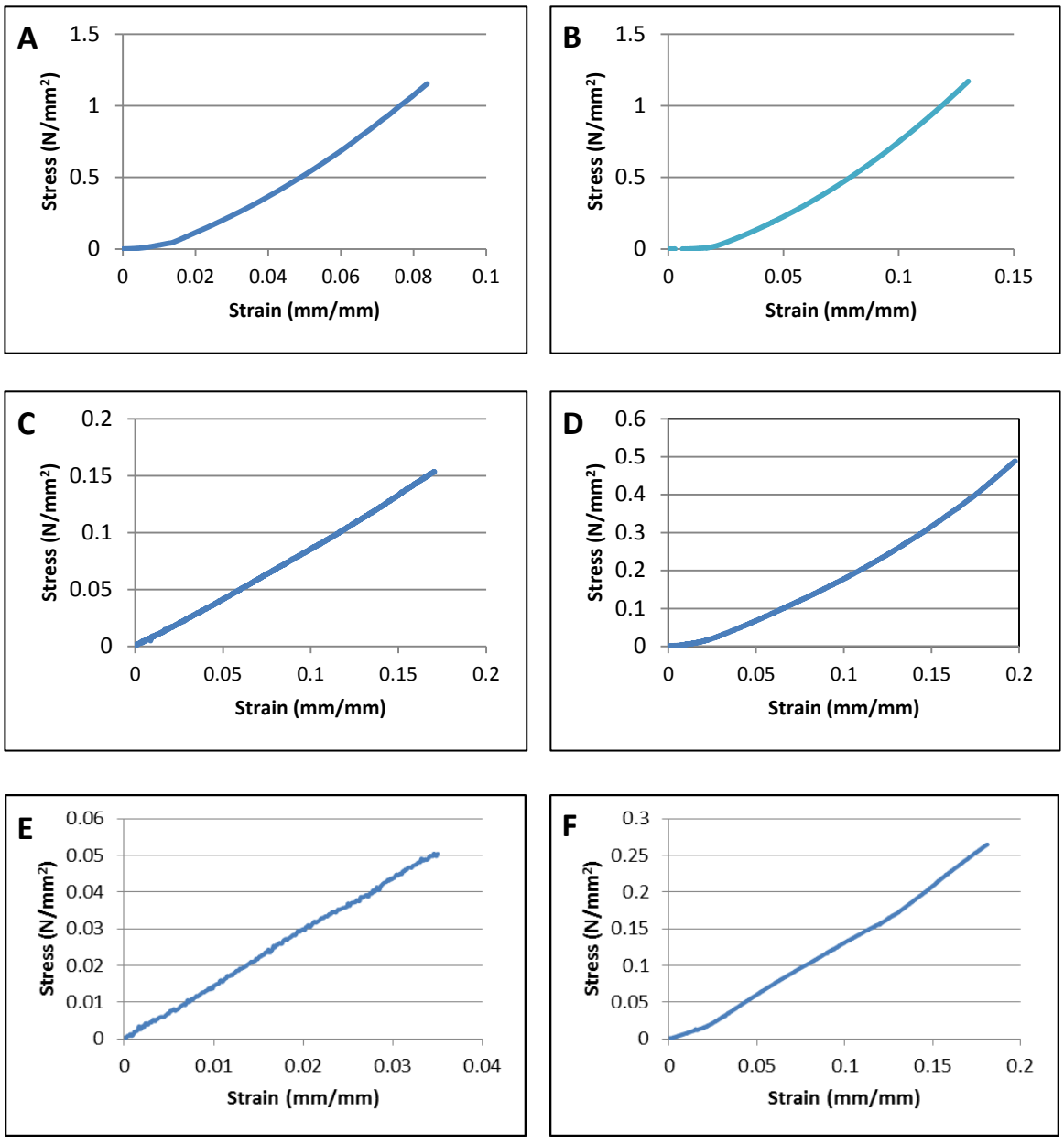

Figure A.2: Tensile test results of patterned Col and Col:ELR films. A) Day 1 Unseeded Col film, B) Day 1 Unseeded Col:ELR film, C) Day 30 Unseeded Col film, D) Day 30 Unseeded Col:ELR film, E) Day 30 Col film seeded w/ keratocytes, and F) Day 30 Col:ELR film seeded w/ keratocytes

APPENDIX C

ALAMAR BLUE CALIBRATION CURVE

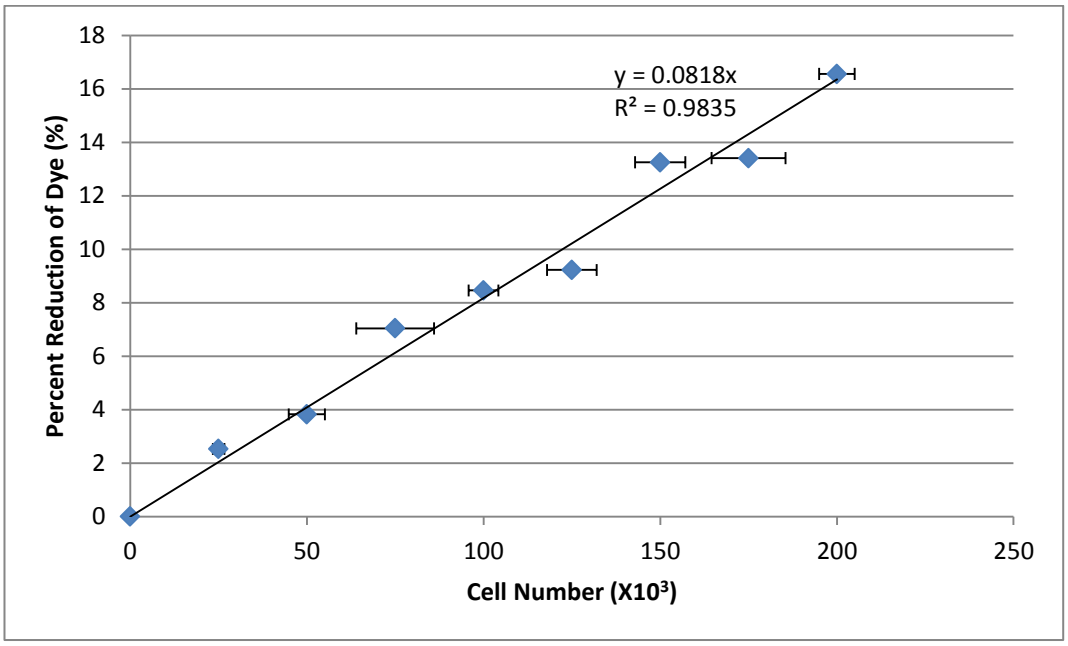

Figure A.3: Alamar blue assay calibration curve for human corneal keratocytes